CALIFORNIA INSTITUTE OF TECHNOLOGY

EARTHQUAKE ENGINEERING RESEARCH LABORATORY

EFFICIENT NONLINEAR SEISMIC ANALYSIS OF ARCH DAMS

USER'S MANUAL FOR SCADA

SMEARED
CRACK
ARCH
DAM
ANALYSIS

BY JOHN F. HALL

REPORT NO. EERL 96-01

PASADENA, CALIFORNIA
1996

MODIFIED JULY 1997

EFFICIENT NONLINEAR SEISMIC ANALYSIS OF ARCH DAMS

User's Manual for SCADA

Smeared
Crack
Arch
Dam
Analysis

John F. Hall
California Institute of Technology
April 1996
Modified July 1997

TABLE OF CONTENTS

1. INTRODUCTION

Linear earthquake analysis of a concrete arch dam, conducted either in the evaluation of an existing dam or in the design of a new one, typically shows large tensile stresses when the ground motion employed represents strong shaking. This result has spurred development of nonlinear analysis capabilities that attempt to model the opening and closing of contraction joints as well as cracks that are produced. Two recent computer programs (1a and 1b, 2) both treat joints and cracks as zero-width zones of nonlinear springs connecting adjacent finite elements, but differ in detail.

ADAP-88 (1a and 1b) uses a multi-element discretization of solid elements through the thickness of the dam so as to be able to represent states of partial contact in the joints and cracks. Standard joint elements are used in the joint and crack planes. The program of reference 2 uses a single shell element discretization in the thickness direction with specially calibrated nonlinear rotational and axial springs to represent states of partial contact. The disadvantage of ADAP-88 is the relatively high computational effort required, while disadvantages of the formulation of reference 2 are some loss of accuracy and an inability to be generalized to include sliding in the joints and cracks. However, while sliding is straightforward conceptionally when using the standard joint elements such as employed in ADAP-88, including friction may lead to severe convergence difficulties.

At present, nonlinear analysis methods have not gained acceptance in the dam engineering community. Reliance is still based on the inadequate linear methods and *ad hoc* procedures to assess the high tensile stresses that are computed. Part of the problem is the difficulty of validating the nonlinear analysis capabilities. Some progress is being made, however, by different researchers taking different approaches of nonlinear analysis and then comparing results. In this spirit and also with the goal of developing a practical nonlinear analysis technique that attempts to reach a compromise between computational effort and model complexity, while still giving useful results, this simplified nonlinear earthquake analysis procedure for concrete arch dams is offered together with fully documented computer program.

The procedure is based on the "smeared" approach to model joints and cracks whereby the contact nonlinearities are incorporated through conditions placed on the stresses at the

integration points of the (shell) finite elements of the dam. This approach sacrifices some accuracy for computational efficiency. The faster computation comes about by a reduction in the number of degrees of freedom and an improvement in convergence even to the point of being able to handle frictional sliding. A typical computer run for an earthquake analysis of an arch dam to strong ground motion takes about one hour on a DEC 3000 Model 400 computer with a 100 MIPS processor. This efficiency allows parameter studies to be undertaken which are an essential part of any evaluation process.

As with the linear analysis methods, engineering judgment is still a necessary and important element. However, it is hoped that the gap between mathematical model and real-world situation is reduced enough with the offered program so that the engineer can now be confident in spanning between them.

2. DESCRIPTION OF ANALYSIS PROCEDURE

2.1 Overview

The system analyzed (Figure 1) consists of an arch dam, foundation region and water reservoir where the global coordinates *x, y* and *z* are in the stream, vertical and cross-stream directions, respectively. Static analysis is performed first followed by earthquake analysis. Nonlinear behavior is confined to the dam in the form of opening, closing and sliding of contraction joints and cracks. Nonlinearities in concrete behavior associated with high compressive stresses are not considered.

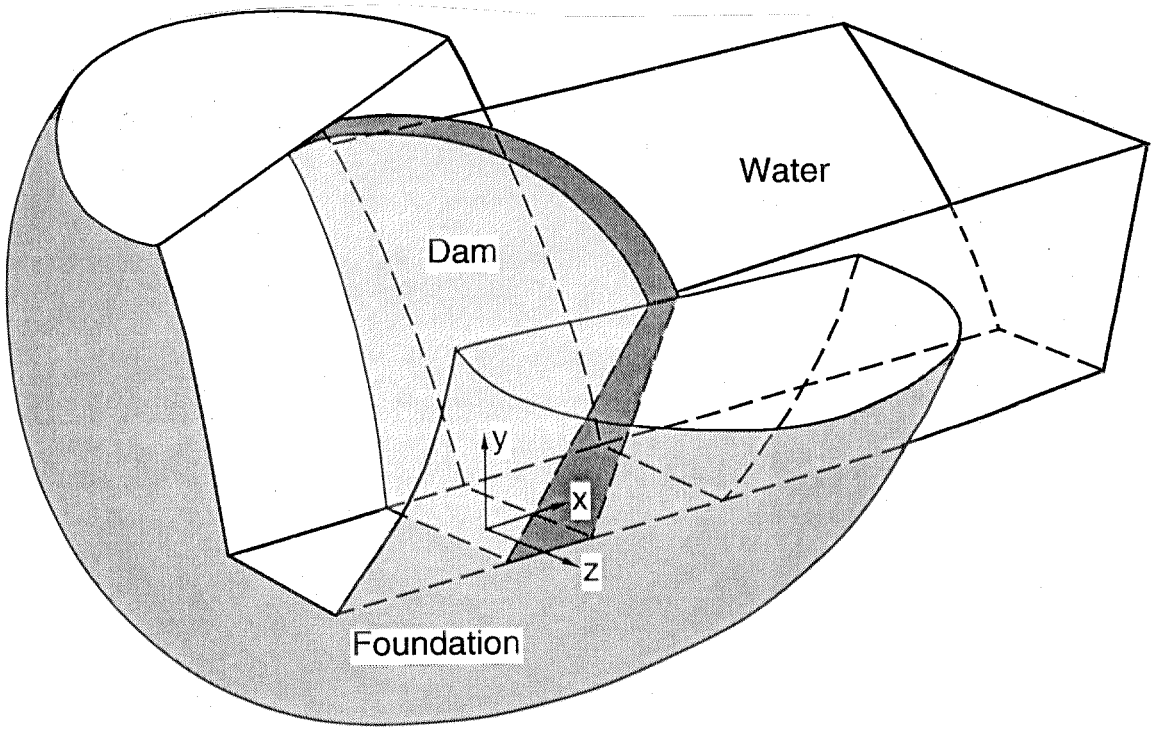

Figure 1. Arch dam with foundation and water showing coordinate system: x (stream direction), y (vertical) and z (cross-stream).

Static analysis simulates construction, temperature change, water level change and grouting. Each of these processes is divided into load steps. In a construction step, a specified set of elements with their gravity loads is assembled into the mesh. Each construction step can be followed by one or more temperature, water or grouting steps. In a temperature step, the elements present are subjected to a specified temperature which is assumed to vary linearly from

the upstream face of the dam to the downstream face. In a water step, the water level is raised or lowered, and the elements present are subjected to the altered hydrostatic pressure. If gaps develop because of joint or crack opening at any stage of the static loading, they can be closed by the filling in of material as simulated in a grouting step. The static analysis procedure does not model processes associated with young concrete such as evolution of material properties, *i.e.*, the same properties are used throughout the analysis.

In the static analysis, only finite element discretizations of the dam and foundation are needed since the water pressure is simple hydrostatic. The dam mesh is constructed of 4-node shell elements (the type with independent interpolation of translation and rotation; references 2, 3 and 4) that include shear deformations. A node is located on the mid-surface and contains five degrees of freedom: two rotations about local axes and translations in the x, y and z directions. Geometry of the shell element mesh is defined through locations of pairs of auxiliary nodes — one each on the upstream and downstream faces for each mid-surface node. No degrees of freedom are associated with the auxiliary nodes.

Contact nonlinearities associated with the dam's joints and cracks are included through conditions on the shell element stresses at the integration points. This technique is known as the smeared crack method. While the actual interface nature of joints and cracks can only be modelled with inter-element springs, the smeared crack approach is employed here because it is computationally more efficient and exhibits better convergence, while still giving useful results. Also, a single shell element discretization in the thickness direction of the dam is less able to represent states of partial contact than is a multi-element discretization, but it is felt to be a reasonable compromise between accuracy and computational requirements.

The foundation of the dam is elastic and is modelled with variable-node solid elements, each node containing three translational degrees of freedom. Locations of the nodes of the foundation mesh at the dam interface coincide with those of the auxiliary nodes of the dam. The foundation stiffness matrix is condensed down to the interface degrees of freedom, then transformed to the five degrees of freedom at each mid-surface node of the dam, and finally localized by zeroing all terms outside the coupling already present in the dam mesh (2).

Each load step of the static analysis involves the iterative solution of the matrix equation of equilibrium. Time is used as a load history parameter for notational convenience; t denotes the current configuration and $t + \Delta t$ denotes the configuration after application of the next load step. The equations solved in the ℓth iteration in going from t to $t + \Delta t$ are

$$\left[K^{\ell} + \overline{K}\right]\left\{\Delta a^{\ell}\right\} = \left\{f(t + \Delta t)\right\} - \left\{p^{\ell}(t + \Delta t)\right\} - \left[\overline{K}\right]\left\{a^{\ell}(t + \Delta t\right\} \tag{1a}$$

$$\left\{a^{\ell+1}(t + \Delta t)\right\} = \left\{a^{\ell}(t + \Delta t)\right\} + \left\{\Delta a^{\ell}\right\} \tag{1b}$$

where $[K^{\ell}]$ = stiffness matrix of the dam that is expressed as a combination of the linear stiffness matrix $[K_E]$ and the current tangent stiffness matrix $[K_T^{\ell}]$; $[\overline{K}]$ = condensed and localized stiffness matrix of the foundation; $\{f(t + \Delta t)\}$ = static load vector for state $t + \Delta t$ containing nodal forces from gravity and from water pressure acting on the upstream dam face; $\{a^{\ell+1}(t + \Delta t)\}$ = vector of dam displacement degrees of freedom obtained after ℓ iterations, where $\{a^{1}(t + \Delta t)\} = \{a(t)\}$; $\{\Delta a^{\ell}\}$ = increment of dam displacements computed in the ℓth iteration; and $\{p^{\ell}(t + \Delta t)\}$ = vector of dam forces corresponding to the stresses in state $^{\ell}(t + \Delta t)$. Temperature loads are included in $\{p^{\ell}(t + \Delta t)\}$ as discussed in the next section.

Earthquake ground motions are applied after the static analysis. Components in the x, y and z directions can be specified, and these are assumed to be spatially uniform. The ground motions are free-field motions that would occur at the dam-foundation interface without the dam present, and they are also applied to the floor and sides of the water reservoir. The dynamic solution is obtained from the system equation of motion which is a modification of equation (1) to include the mass of the dam, dam-water interaction (via a finite element discretization of the water), damping, and the earthquake excitation; foundation mass is omitted. Damping stresses in the dam are expressed as the product of a coefficient a_1 (the usual stiffness-matrix multiplier for stiffness-proportional damping) and the time rate of change of the stresses. This avoids damping stresses acting across an open joint or crack.

The system equation of motion is integrated using Bossak's extension (5) of Newmark's method except that a backward difference method is used for the terms representing damping

in the dam. The resulting equations for the ℓth iteration in going from time t to time $t + \Delta t$ (where t is now really time) are

$$\begin{bmatrix} \frac{(1-\alpha_B)}{\beta\Delta^2} M + \frac{1}{\Delta t} C_T^{\ell} + \frac{\gamma}{\beta\Delta t} \overline{C} + K^{\ell} + \overline{K} & K_p \\ \frac{(1-\alpha_B)}{\beta\Delta^2} M_p & K_{pp} \end{bmatrix} \begin{Bmatrix} \Delta a^{\ell} \\ \Delta p_d^{\ell} \end{Bmatrix} = \begin{Bmatrix} f(t+\Delta t) \\ f_p(t+\Delta t) \end{Bmatrix} - \left.\begin{array}{l} \begin{Bmatrix} p^{\ell}(t+\Delta t) \\ 0 \end{Bmatrix} - \begin{Bmatrix} q^{\ell}(t+\Delta t) \\ 0 \end{Bmatrix} - \begin{bmatrix} \frac{(1-\alpha_B)}{\beta\Delta^2} M + \frac{\gamma}{\beta\Delta t^2} \overline{C} + \overline{K} & K_p \\ \frac{(1-\alpha_B)}{\beta\Delta^2} M_p & K_{pp} \end{bmatrix} \begin{Bmatrix} a^{\ell}(t+\Delta t) \\ p_d^{\ell}(t+\Delta t) \end{Bmatrix} + \\ \begin{bmatrix} \frac{(1-\alpha_B)}{\beta\Delta t^2} M + \frac{\gamma}{\beta\Delta t} \overline{C} \\ \frac{(1-\alpha_B)}{\beta\Delta t^2} M_p \end{bmatrix} \{a(t)\} + \begin{bmatrix} \frac{(1-\alpha_B)}{\beta\Delta t} M + \left(\frac{\gamma}{\beta} - 1\right)\overline{C} \\ \frac{(1-\alpha_B)}{\beta\Delta t} M_p \end{bmatrix} \{\dot{a}(t)\} + \\ \begin{bmatrix} \left(\left(\frac{1}{2\beta} - 1\right)(1-\alpha_B) - \alpha_B\right) M + \left(\frac{\gamma}{2\beta} - 1\right)\Delta t \overline{C} \\ \left(\left(\frac{1}{2\beta} - 1\right)(1-\alpha_B) - \alpha_B\right) M_p \end{bmatrix} \{\ddot{a}(t)\} \end{array}\right\} \quad (2a)$$

$$\begin{Bmatrix} a^{\ell+1}(t+\Delta t) \\ p_d^{\ell+1}(t+\Delta t) \end{Bmatrix} = \begin{Bmatrix} a^{\ell}(t+\Delta t) \\ p_d^{\ell}(t+\Delta t) \end{Bmatrix} + \begin{Bmatrix} \Delta a^{\ell} \\ \Delta p_d^{\ell} \end{Bmatrix} \quad (2b)$$

which are written in partitioned form for the dam displacement degrees of freedom $\{a\}$ (relative to the free-field ground motions) and the dynamic water pressure degrees of freedom $\{p_d\}$. In equation 2, $[M]$ = mass matrix of the dam; $[C_T^{\ell}]$ = damping matrix of the dam = $a_1[K_T^{\ell}]$; $[\overline{C}]$ = damping matrix of the dam foundation = $a_1[\overline{K}]$; $\{q^{\ell}(t+\Delta t)\}$contains the nodal damping forces of the dam in state $^{\ell}(t+\Delta t)$; α_B = Bossak parameter which can be chosen to provide high-frequency algorithmic damping; γ and β are Newmark's parameters; and $\{f(t+\Delta t)\} = \{f_{st}\} - [M][r]\{\ddot{a}_g(t+\Delta t)\}$ where $\{f_{st}\}$ is the static load vector at the end of the static analysis, $\{\ddot{a}_g(t+\Delta t)\}$ contains the ground accelerations at time $t + \Delta t$ in the x, y and z directions, and $[r]$ = matrix of influence vectors (one for each component of ground motion). Mass-proportional damping in the dam can also be added by including in the term $a_0[M]$ in $[\overline{C}]$ in equation (2), where a_0 is the usual mass-matrix multiplier for mass-proportional damping.

Terms $[K_{pp}]$, $[K_p]$, $[M_p]$ and $\{f_p(t + \Delta t)\}$ in equation (2a) are computed from a finite element mesh of the water and associated boundary meshes (2). The equation representing the water is the LaPlace equation with the dynamic water pressure as the unknown. Water compressibility is neglected. $[K_{pp}]$ is a condensed and localized version of the water "stiffness" matrix which is constructed using 8-node water elements. The condensation is to the pressure degrees of freedom on the dam face, and the localization process is similar to that done for $[\overline{K}]$. Thus, the pressure unknowns in equation (2) are only for nodes of the water mesh on the dam face. The locations of these nodes must coincide with the locations of the auxiliary dam nodes on the upstream face. Since $\{f_{st}\}$ contains the static water pressures, the pressure unknowns in equation (2) correspond to the dynamic component of water pressure. In equation (2a), $[K_p]$ = transformation matrix from nodal dynamic water pressures to nodal forces on the dam; $[M_p]$ = transformation matrix from dam nodal accelerations to nodal "forces" on the water mesh; and $\{f_p(t + \Delta t)\}$ contains the nodal "forces" to the water mesh arising from rigid accelerations of the dam face and reservoir floor and sides at $\{\ddot{a}_g(t + \Delta t)\}$. No water-foundation interaction is included.

Vectors $\{\dot{a}(t)\}$ and $\{\ddot{a}(t)\}$ in equation (2a) are the velocity and acceleration vectors (relative to the free-field ground motions) for the dam degrees of freedom. When convergence to $\{a(t + \Delta t)\}$ is reached, $\{\dot{a}(t + \Delta t)\}$ and $\{\ddot{a}(t + \Delta t)\}$ for use in the next time step are found from the Newmark expressions

$$\left.\begin{aligned} \{\dot{a}(t + \Delta t)\} &= \{\dot{a}(t)\} + \{(1 - \gamma)\ddot{a}(t) + \gamma\ddot{a}(t + \Delta t)\}\Delta t \\ \{\ddot{a}(t + \Delta t)\} &= \frac{1}{\beta\Delta t^2}\{a(t + \Delta t) - a(t)\} - \frac{1}{\beta\Delta t}\{\dot{a}(t)\} - \left(\frac{1}{2\beta} - 1\right)\{\ddot{a}(t)\}\,. \end{aligned}\right\} \tag{3}$$

2.2 Details of Arch Dam Formulation

Each shell element of the dam is mapped from a 4-node parent element as shown in Figure 2. Local coordinates in the parent element are ξ, η, ζ; and the ξ-η plane maps to the mid-surface of the shell where the nodes are located. Each node has five displacement degrees of freedom: translations u, v, w in the x, y, z directions, respectively, and rotations θ and γ about axes $\hat{x}$ and $\hat{y}$, respectively, that are local to each node. The $\hat{x}$ and $\hat{y}$ axes at a node are

perpendicular to the mapped ζ direction which is the $\hat{z}$ axis. The $\hat{x}$ axis is in the $y \times \hat{z}$ direction, and so is in the horizontal plane; $\hat{y}$ is in the $\hat{z} \times \hat{x}$ direction. At each mid-surface node, the intersections of the $\hat{z}$ axis with the upstream and downstream faces of the dam are termed "auxiliary nodes" and are used to input the shell geometry. They contain no degrees of freedom.

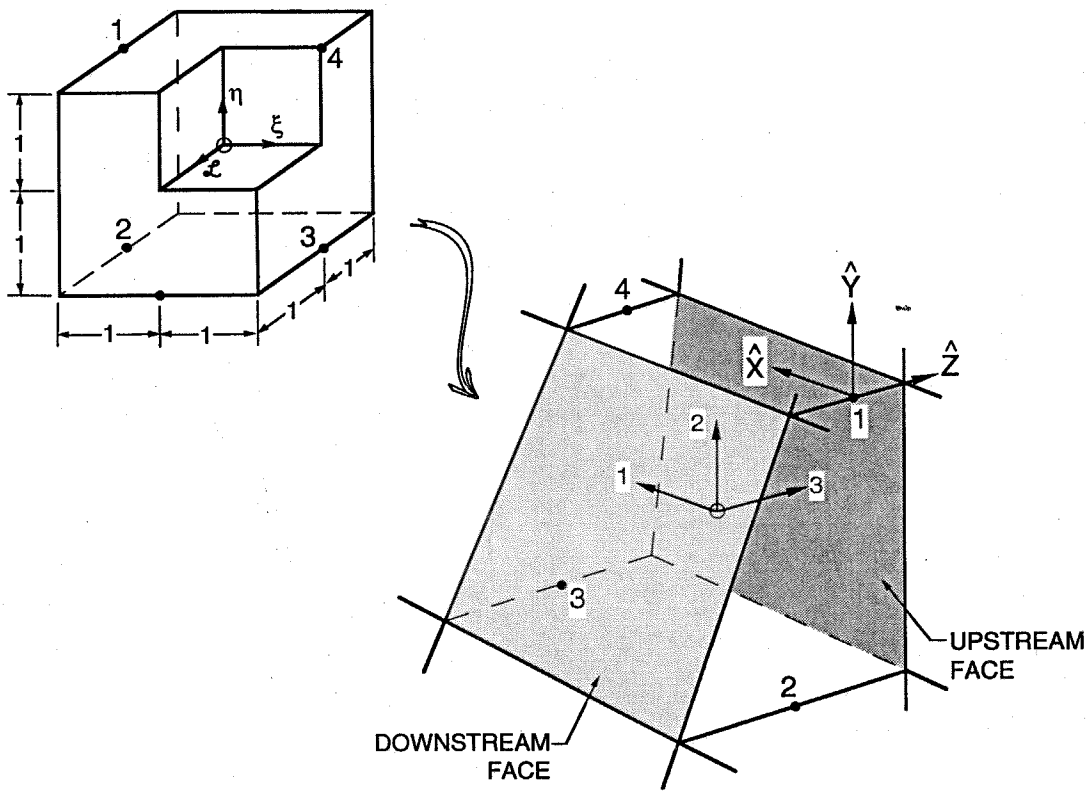

Figure 2. Shell element of an arch dam shown mapped from a parent element.

Stresses in a shell element are referenced to local 1,2,3 coordinates: 1 is horizontal in the mapped ξ-η plane and is oriented so that its z component is negative; 2 is in the same plane and perpendicular to 1; and 3 is in the 1×2 direction. Thus, the directions 1 and 2 can be associated with arch and cantilever actions, respectively. Normal stress components (tension positive) are σ_{11} (arch) and σ_{22} (cantilever); the through-thickness normal stress component σ_{33} is set to zero. Shear stress components are τ_{12} (in-plane shear), τ_{23} (out-of-plane cantilever shear) and τ_{13} (out-of-plane arch shear). A positive τ_{ij} stretches the bisector of the right angle formed by the positive i and j axes. Corresponding strain components are denoted

as ε_{11}, ε_{22}, ε_{33}, γ_{12}, γ_{23} and γ_{13}. Within each element a single set of 1,2,3 directions is used, and these directions are evaluated at the element center ($\xi = \eta = \zeta = 0$).

Nonlinear features of element behavior are associated with contact and sliding in the contraction joints and cracks. Actions at these locations are represented through conditions placed on the stresses at discrete points within the element used to evaluate element integrands. At each integration point, the orientation of the contraction joint is that of the 2-3 plane, while the orientation of the cracking plane is that of the 1-3 plane. The contraction joints are assumed to have zero tensile strength, and so

$$\left.\begin{array}{rll} \sigma_{11} &= 0 & \text{for joint open} \\ &< 0 & \text{for joint closed.} \end{array}\right\} \tag{4}$$

Crack formation on a cracking plane employs a simple strength criterion. Before cracking,

$$\sigma_{22} < \sigma_{ten} \tag{5}$$

where σ_{ten} is the tensile strength of the cracking plane. Cracking occurs when σ_{22} reaches σ_{ten}, upon which σ_{ten} is set to zero. After cracking,

$$\left.\begin{array}{rll} \sigma_{22} &= 0 & \text{for crack open} \\ &< 0 & \text{for crack closed.} \end{array}\right\} \tag{6}$$

Shear stresses in the contraction joints and cracks are limited by simple friction criteria according to

$$|\tau_{13}| \le f_1 |\sigma_{11}| \tag{7a}$$

$$|\tau_{23}| \le f_2 |\sigma_{22}| \text{ if crack is present} \tag{7b}$$

$$\left.\begin{array}{l} |\tau_{12}| \le \frac{1}{2}\left(f_1 |\sigma_{11}| + f_2 |\sigma_{22}| \right) \text{ if crack is present} \\ \left.\begin{array}{l} \tau_{12} \le \alpha_s \cdot G \cdot \gamma_{12} + f_1 |\sigma_{11}| \\ \tau_{12} \ge \alpha_s \cdot G \cdot \gamma_{12} - f_1 |\sigma_{11}| \end{array}\right\} \text{ if crack is not present} \end{array}\right\} \tag{7c}$$

where f_1 and f_2 are friction coefficients for contraction-joint and crack shear, respectively; α_s is a shear stiffness reduction factor; G = shear modulus; and < or > applies when sliding is not occurring, and = holds for sliding. These relations imply that there are three sliding

mechanisms, each one corresponding to one of the components of shear, and that all mechanisms are uncoupled. The $\alpha_s \cdot G \cdot \gamma_{12}$ term maintains some stiffness in the 12 component prior to cracking when the joint is open.

The current contact state is defined by the current tensile strength σ_{ten} of the cracking plane and by a contact descriptor LCON. The current value of σ_{ten} indicates whether a crack has formed (=0) or not (>0). Four contact states are possible as follows

$$\left.\begin{array}{lll} \text{LCON} = 1: & \text{both joint and cracking plane open} \\ = 2: & \text{joint closed, cracking plane open} \\ = 3: & \text{joint closed, no crack or cracking plane closed} \\ = 4: & \text{joint open, no crack or cracking plane closed.} \end{array}\right\} \tag{8}$$

Before cracking, only states LCON = 3 or 4 are possible.

The current sliding state is defined by LSLDij where *ij* take on values 12, 23 and 13 corresponding to the three shear components. In general, LSLDij = 0 if sliding is not occurring for shear component *ij*; $\neq 0$ if sliding is occurring, being < 0 if $\tau_{ij} < 0$ and > 0 if $\tau_{ij} \geq 0$.

In each element, the components of stress and strain as well as values of σ_{ten}, LCON, LSLD12, LSLD23, LSLD13 are kept track of at the integration points. These points are used in numerical integration over the element domain, and the particular integration scheme employed uses four points located at $\xi,\ \eta,\ \zeta = 0, 0, 1;\ 0, 0, \frac{1}{3};\ 0, 0, -\frac{1}{3};\ 0, 0, -1$. Weighting values are 1 for the two exterior points and 3 for the two interior points.

The four-point integration scheme is used to integrate the element tangent stiffness matrix $[K_T^\ell]^e$ (the linear matrix $[K_E]^e$ also) and the element right-side vectors $\{p^\ell(t + \Delta t)\}^e$ and $\{q^\ell(t + \Delta t)\}^e$, which get assembled into $[K_T^\ell]$, $\{p^\ell(t + \Delta t)\}$ and $\{q^\ell(t + \Delta t)\}$ of equations (1) and (2). Formulas for the element quantities are

$$\left[K_T^\ell\right]^e = \int_{v^e} \left[B^e\right]^T \left[D_T^\ell\right] \left[B^e\right] dv^e \tag{9}$$

$$\left\{p^\ell(t + \Delta t)\right\}^e = \int_{v^e} \left[B^e\right]^T \left\{\sigma^\ell(t + \Delta t)\right\}^e dv^e \tag{10}$$

$$\left\{q^{\ell}(t+\Delta t)\right\}^{e} = \int_{v^e} \left[B^e\right]^T \left\{\hat{\sigma}^{\ell}(t+\Delta t)\right\}^{e} dv^e \tag{11}$$

where v^e = element domain; $\{\sigma^{\ell}(t+\Delta t)\}^e$ lists the element stresses in the $^{\ell}(t+\Delta t)$ state; $[B^e]$ is the transformation matrix from element displacements $\{a\}^e$ to element strains $\{\varepsilon\}^e$; $[D_T^{\ell}]$ is the tangent material matrix which relates element strain increments $\{d\varepsilon^{\ell}\}^e$ to element stress increments $\{d\sigma^{\ell}\}^e$; ^ denotes damping stress; and the element stresses and strains are listed in the order 11, 22, 12, 23, 13. With E = Young's modulus, v = Poisson's ratio, and G = shear modulus, the nonzero values for $[D_T^{\ell}]$ are given by the following:

$$\left.\begin{aligned}
D_T^{\ell}(1,1) &= E \quad \text{if} \quad \text{LCON} = 2 \\
&= E \,/\, (1-v^2) \quad \text{if} \quad \text{LCON} = 3 \\
D_T^{\ell}(1,2) &= D_T^{\ell}(2,1) = Ev \,/\, (1-v^2) \quad \text{if} \quad \text{LCON} = 3 \\
D_T^{\ell}(2,2) &= E \quad \text{if} \quad \text{LCON} = 4 \\
&= E \,/\, (1-v^2) \quad \text{if} \quad \text{LCON} = 3 \\
D_T^{\ell}(3,1) &= \mp \tfrac{1}{2}\left(f_1 \cdot D_T^{\ell}(1,1) + f_2 \cdot D_T^{\ell}(2,1)\right) \quad \text{if} \quad \text{LCON} = 2 \text{ or } 3 \\
&\quad \text{and} \quad \text{LSLD12} \gtrless 0 \text{ and } \sigma_{\text{ten}} = 0 \\
&= \mp f_1 \cdot D_T^{\ell}(1,1) \quad \text{if} \quad \text{LCON} = 3 \quad \text{and} \quad \text{LSLD12} \gtrless 0 \text{ and } \sigma_{\text{ten}} > 0 \\
D_T^{\ell}(3,2) &= \mp \tfrac{1}{2}\left(f_1 \cdot D_T^{\ell}(1,2) + f_2 \cdot D_T^{\ell}(2,2)\right) \quad \text{if} \quad \text{LCON} = 3 \text{ or } 4 \\
&\quad \text{and} \quad \text{LSLD12} \gtrless 0 \text{ and } \sigma_{\text{ten}} = 0 \\
&= \mp f_1 \cdot D_T^{\ell}(1,2) \quad \text{if} \quad \text{LCON} = 3 \quad \text{and} \quad \text{LSLD12} \gtrless 0 \text{ and } \sigma_{\text{ten}} > 0 \\
D_T^{\ell}(3,3) &= G \quad \text{if} \quad \text{LCON} = 2,3 \text{ or } 4 \quad \text{and} \quad \text{LSLD12} = 0 \\
&= \alpha_s \cdot G \quad \text{if} \quad \text{LCON} = 3 \text{ or } 4 \quad \text{and} \quad \text{LSLD12} \neq 0 \quad \text{and} \quad \sigma_{\text{ten}} > 0 \\
D_T^{\ell}(4,1) &= \mp f_2 \cdot D_T^{\ell}(2,1) \quad \text{if} \quad \text{LCON} = 3 \quad \text{and} \quad \text{LSLD23} \gtrless 0 \\
D_T^{\ell}(4,2) &= \mp f_2 \cdot D_T^{\ell}(2,2) \quad \text{if} \quad \text{LCON} = 3 \text{ or } 4 \quad \text{and} \quad \text{LSLD23} \gtrless 0 \\
D_T^{\ell}(4,4) &= G' \quad \text{if} \quad \text{LCON} = 3 \text{ or } 4 \quad \text{and} \quad \text{LSLD23} = 0 \\
D_T^{\ell}(5,1) &= \mp f_1 \cdot D_T^{\ell}(1,1) \quad \text{if} \quad \text{LCON} = 2 \text{ or } 3 \quad \text{and} \quad \text{LSLD13} \gtrless 0 \\
D_T^{\ell}(5,2) &= \mp f_1 \cdot D_T^{\ell}(1,2) \quad \text{if} \quad \text{LCON} = 3 \quad \text{and} \quad \text{LSLD13} \gtrless 0 \\
D_T^{\ell}(5,5) &= G' \quad \text{if} \quad \text{LCON} = 2 \text{ or } 3 \quad \text{and} \quad \text{LSLD13} = 0 \,,
\end{aligned}\right\} \tag{12}$$

where $G' = \frac{5}{6} G$ (the usual correction for out-of-plane shear). The values that result from LCON = 3 and LSLD12 = LSLD23 = LSLD13 = 0 give the linear material matrix $[D_E]$ which leads to the linear stiffness matrix $[K_E]$.

Following solution of equation (1a) or (2a) for the incremental displacements $\{\Delta a^{\ell}\}$ of the dam, the state ${}^{\ell}(t + \Delta t)$ is updated to the state ${}^{\ell+1}(t + \Delta t)$ at each integration point. This process begins by determining the element strain increments from

$$\left\{\Delta\varepsilon^{\ell}\right\}^{e} = \left[B^{e}\right]\left\{\Delta a^{\ell}\right\}^{e} \tag{13}$$

and then updating the strains as

$$\left\{\varepsilon^{\ell+1}(t + \Delta t)\right\}^{e} = \left\{\varepsilon^{\ell}(t + \Delta t)\right\}^{e} + \left\{\Delta\varepsilon^{\ell}\right\}^{e} . \tag{14}$$

The normal stresses $\sigma_{11}^{\ell+1}(t + \Delta t)$ and $\sigma_{22}^{\ell+1}(t + \Delta t)$ depend only on the normal strains $\varepsilon_{11}^{\ell+1}(t + \Delta t)$ and $\varepsilon_{22}^{\ell+1}(t + \Delta t)$. For each of the four contact conditions:

$$\left.\begin{aligned} \sigma_{11}^{\ell+1}(t + \Delta t) &= 0 \quad \text{for LCON} = 1 \text{ or } 4 \\ &= E \cdot \varepsilon_{11}^{\ell+1}(t + \Delta t) \quad \text{for LCON} = 2 \\ &= \tfrac{E}{1-\upsilon^2} \cdot \left(\varepsilon_{11}^{\ell+1}(t + \Delta t) + \upsilon \cdot \varepsilon_{22}^{\ell+1}(t + \Delta t)\right) \quad \text{for LCON} = 3 \end{aligned}\right\} \tag{15a}$$

$$\left.\begin{aligned} \sigma_{22}^{\ell+1}(t + \Delta t) &= 0 \text{ for LCON} = 1 \text{ or } 2 \\ &= \tfrac{E}{1-\upsilon^2} \cdot \left(\upsilon \cdot \varepsilon_{11}^{\ell+1}(t + \Delta t) + \varepsilon_{22}^{\ell+1}(t + \Delta t)\right) \text{for LCON} = 3 \\ &= E \cdot \varepsilon_{22}^{\ell+1}(t + \Delta t) \quad \text{for LCON} = 4 . \end{aligned}\right\} \tag{15b}$$

Each of the four contact states occupies a sector in ε_{11}-ε_{22} space (numbered 1, 2, 3 or 4 to coincide with the value of LCON); the diagram differs according to whether a crack has not formed (Figure 3a) or has formed (Figure 3b). Should the strain location $\varepsilon_{11}^{\ell+1}(t + \Delta t)$, $\varepsilon_{22}^{\ell+1}(t + \Delta t)$ fall above the top line in Figure 3a, indicating crack formation, then σ_{ten} is set to zero and Figure 3b is used thereafter. LCON takes the number of the sector in which $\varepsilon_{11}^{\ell+1}(t + \Delta t)$, $\varepsilon_{22}^{\ell+1}(t + \Delta t)$ resides.

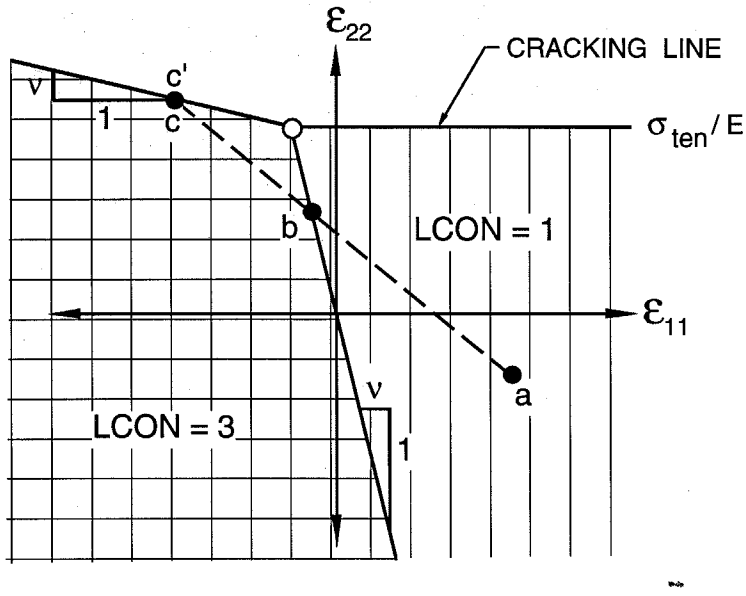

(a) Sector diagram before cracking

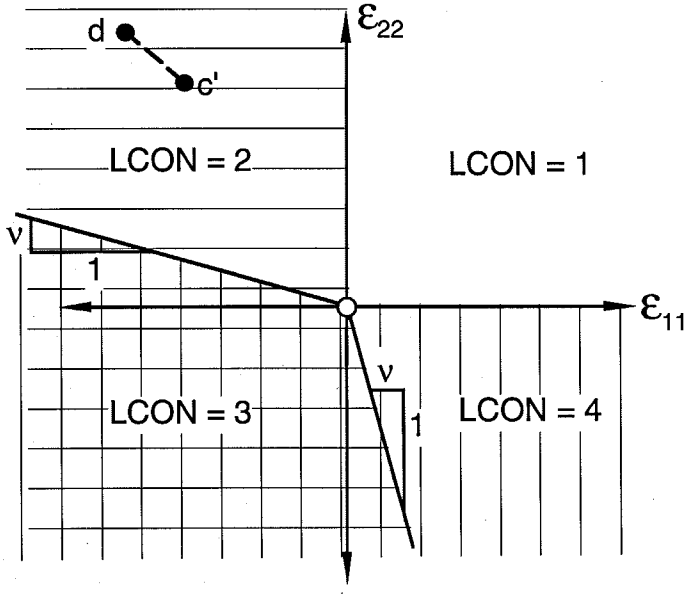

(b) Sector diagram after cracking

Figure 3. Division of ε_{11}-ε_{22} space into sectors corresponding to specific contact states when a contraction joint is present. The line from *a* to *d* represents a strain path.

Updating a shear stress requires integration over the strain increment path. A trial value of shear stress is obtained assuming linear behavior over the increment, and then the trial stress is scaled back if needed to satisfy equation (7). A shear stress that needs to be scaled back means that sliding is present. In the procedure, the strain increment is divided into segments in order to account for spanning multiple sectors and/or a cracking event. As an example, consider computation of $\tau_{12}^{\ell+1}(t + \Delta t)$ for a strain increment $\Delta\gamma_{12}^{\ell}$. The result also depends on the strain increments $\Delta\varepsilon_{11}^{\ell}$ and $\Delta\varepsilon_{22}^{\ell}$ which are shown in Figure 3 as the path from a to d. (Point a is $\varepsilon_{11}^{\ell}(t + \Delta t)$, $\varepsilon_{22}^{\ell}(t + \Delta t)$ and point d is $\varepsilon_{11}^{\ell+1}(t + \Delta t)$, $\varepsilon_{22}^{\ell+1}(t + \Delta t)$.) Four segments are necessary: ab, bc, cc' (cracking event) and $c'd$. The computation proceeds as follows.

$$\bar{\tau}_{12}^{b} = \tau_{12}^{\ell}(t + \Delta t) + G \cdot \Delta\gamma_{12}^{ab} \qquad \left(\Delta\gamma_{12}^{ab} = \Delta\gamma_{12}^{\ell} \cdot \frac{L_{ab}}{L_{ad}}\right)$$

$$\bar{\tau}_{12}^{b} \rightarrow \tau_{12}^{b}$$

$$\bar{\tau}_{12}^{c} = \tau_{12}^{b} + G \cdot \Delta\gamma_{12}^{bc} \qquad \left(\Delta\gamma_{12}^{bc} = \Delta\gamma_{12}^{\ell} \cdot \frac{L_{bc}}{L_{ad}}\right)$$

$$\bar{\tau}_{12}^{c} \rightarrow \tau_{12}^{c}$$

$$\tau_{12}^{c} \rightarrow \tau_{12}^{c'}$$

$$\bar{\tau}_{12}^{d} = \tau_{12}^{c'} + G \cdot \Delta\gamma_{12}^{c'd} \qquad \left(\Delta\gamma_{12}^{c'd} = \Delta\gamma_{12}^{\ell} \cdot \frac{L_{c'd}}{L_{ad}}\right)$$

$$\bar{\tau}_{12}^{d} \rightarrow \tau_{12}^{\ell+1}(t + \Delta t)$$

where $\bar{}$ denotes trial stress; $\rightarrow$ represents the scaling back operation; and L_{ab}, L_{bc}, $L_{c'd}$ and L_{ad} are the lengths of the segments shown in Figure 3. LSLD12 is updated according to the action taken in the last segment. Stresses $\tau_{23}^{\ell+1}(t + \Delta t)$ and $\tau_{13}^{\ell+1}(t + \Delta t)$, along with LSLD23 and LSLD13, are computed similarly but with G replaced by G'.

After the stresses are updated, the updated damping stresses are found from

$$\left\{\hat{\sigma}^{\ell+1}(t + \Delta t)\right\}^{e} = \frac{a_1}{\Delta t}\left\{\sigma^{\ell+1}(t + \Delta t) - \sigma(t)\right\}^{e} . \tag{16}$$

The mass matrix $[M]$ of the dam in equation (2a) is assembled from element mass matrices $[M]^e$ computed for mass lumped at the eight auxiliary node locations in each element. The amount of mass at each auxiliary node location is the product of the concrete density and the mapped volume of the corresponding octant of the parent element. This mass lumping removes coupling of inertial forces across the contraction joints and cracks.

The static loading from a temperature step is incorporated in equation (1a) through a modification of the stress calculation that affects $\{p^{\ell}(t + \Delta t)\}$ through equation (10). If a temperature change ΔT (positive for temperature increase) is specified for step t to $t+\Delta t$, the sector diagram (including the cracking line) is shifted relative to the strain axes by amounts $\alpha_1 \Delta T$ and $\alpha_2 \Delta T$ along the ε_{11} and ε_{22} axes, respectively, where α_1 and α_2 are coefficients of thermal expansion in the 1 and 2 directions. This is shown in Figure 4a which is based on Figure 3b. The initial strain state $\varepsilon^1_{11}(t + \Delta t)$, $\varepsilon^1_{22}(t + \Delta t)$ is not affected, although the sector in which the strain state resides might change. The stresses $\sigma^1_{11}(t + \Delta t)$ and $\sigma^1_{22}(t + \Delta t)$, which would be the converged values $\sigma_{11}(t)$ and $\sigma_{22}(t)$ from the previous load step, are recomputed using strains measured from the origin of the shifted sector diagram; i.e., the strains in equation (15) are replaced by $\varepsilon^1_{11}(t + \Delta t) - \alpha_1 \Delta T$ and $\varepsilon^1_{22}(t + \Delta t) - \alpha_2 \Delta T$. The shear stresses $\tau^1_{12}(t + \Delta t)$, $\tau^1_{23}(t + \Delta t)$ and $\tau^1_{13}(t + \Delta t)$ are taken as the previously converged values $\tau_{12}(t)$, $\tau_{23}(t)$ and $\tau_{13}(t)$, but subject to the scaling back operation if equation (7) is not satisfied with the recomputed $\sigma^1_{11}(t + \Delta t)$ and $\sigma^1_{22}(t + \Delta t)$. With these new stresses, $\{p^1(t + \Delta t)\}$ is computed from equation (10) and equation (1) is solved at ℓ=1; iterations continue until convergence. For each iteration and in subsequent load steps, stresses are computed using the shifted sector diagrams. Future temperature load steps cause additional shifts in the sector diagrams.

A grouting step in the static analysis to fill in gaps in the contraction joints and cracks also involves shifting the sector diagram, additive to those shifts resulting from temperature steps and previous grouting steps. If the current strain resides in sector 1 or 4, then the open contraction joint is "filled in" by shifting the sector diagram to the right an amount $\Delta\varepsilon^{op}_{11}$ until the right edge of sector 2 or 3 intersects the strain location (Figures 4b and d). If the current strain

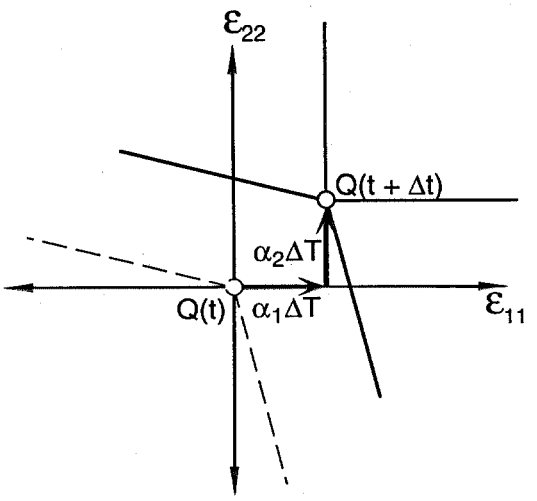

(a) Temperature shift of previously unshifted sector diagram.

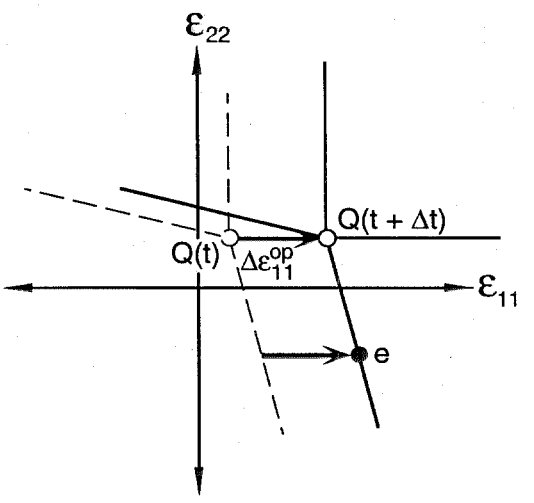

(b) Grouting shift of previously shifted sector diagram to close a joint.

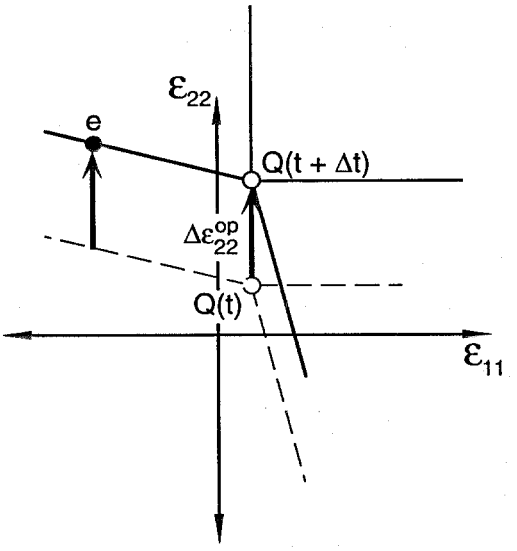

(c) Grouting shift of previously shifted sector diagram to close a crack.

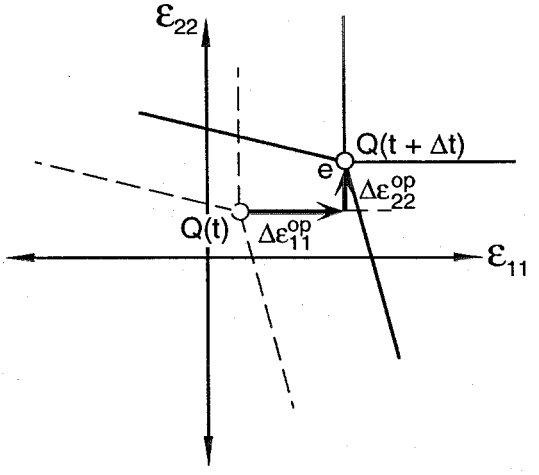

(d) Grouting shift of previously shifted sector diagram to close a joint and a crack.

Figure 4. Shifts in sector diagram caused by temperature change (Part a) or grouting (Parts b, c, d) from step t to $t + \Delta t$. Point Q marks the origin of the sector diagram. Point q represents a strain state containing an open joint and/or crack that is/are closed by grouting. The sector diagram shown is for both contraction joint and crack present.

resides in sector 1 or 2, then the open crack is "filled in" by shifting the sector diagram upward an amount $\Delta\varepsilon_{22}^{op}$ until the top edge of sector 3 or 4 intersects the strain location (Figures 4c and d). In neither case do the stresses change, and no solutions of equation (1a) are required. The shifted sector diagrams are used in all subsequent stress calculations.

2.3 Convergence Issues

Convergence in a load or time step is attained when the maximum force and moment residuals, absolute values denoted by $F_{\max}^{\ell}$ and $M_{\max}^{\ell}$ and taken from the residual vector for the ℓth iteration [the right side of equation (1a) or (2a)], are reduced below specified tolerances. A proper choice of the iterating stiffness matrix $[K^{\ell}]$ in equation (1a) or (2a) is necessary so that the iterations in each load or time step converge within a reasonable computational effort. This matrix is taken to be a combination of $[K_E]$, the linear stiffness matrix with the dam as an elastic monolithic structure, and $[K_T^{\ell}]$, the tangent stiffness matrix representing the contact and sliding nonlinearities in the ${}^{\ell}(t + \Delta t)$ state, as follows:

$$\left[K^{\ell}\right] = S^{\ell} \cdot \left[K_E\right] + \left(1 - S^{\ell}\right) \cdot \left[K_T^{\ell}\right] . \tag{17}$$

The parameter S^{ℓ} is selected according to an algorithm that makes use of $F_{\max}^{\ell}$ and $M_{\max}^{\ell}$:

For the first iteration (ℓ=1), set S^1 equal to a "safe" value $S_{\max} \leq 1$. The closer $S_{\max}$ is to one, the closer is $[K^{\ell}]$ to the "safe" matrix $[K_E]$.

For subsequent iterations (ℓ>1), set

$$\begin{aligned} S^{\ell} &= S_{\max} \quad \text{if} \quad F_{\max}^{\ell} > 1.1 \cdot F_{\max}^{\ell-1} \\ &= S^{\ell-1} \quad \text{if} \quad F_{\max}^{\ell} < 0.7 \cdot F_{\max}^{\ell-1} \quad \text{or} \quad M_{\max}^{\ell} < 0.7 \cdot M_{\max}^{\ell-1} \\ &= S^{\ell-1} / 2 \quad \text{otherwise, but with some lower limit } S_{\min}. \end{aligned}$$

Thus, as the iterations proceed, S^{ℓ} is reduced as convergence slows, bringing the iterating matrix close to the current tangent, but S^{ℓ} is returned to the "safe" value $S_{\max}$ should the residual jump up significantly.

Even with the above algorithm for selecting $[K^{\ell}]$, convergence still sometimes proceeds very slowly or even stops if the computations get stuck in a loop and repeat every so many

iterations. For situations in which convergence does not occur within a specified number of iterations, automatic division of the load or time step is employed. The substep lengths are from the set $\Delta t/4$, $\Delta t/16$, $\Delta t/64$. During step division, if a state between time t and time $t+\Delta t$ is accepted, either because convergence occurred or because the minimum substep was reached, then the next substep is attempted with the previous substep length unless the previous convergence was fast, in which case the state $t + \Delta t$ is again attempted.

Convergence difficulties are sometimes encountered during the static analysis, especially with the construction and temperature steps. In a dynamic analysis, the mass and damping terms on the left side of equation (2a) smooth out the nonlinearities associated with the stiffness, especially with a small time step, and convergence is usually easier to obtain.

2.4 Additional Features of Dam Model

An option is included to omit the contraction joint from an element. In the formulation, equations (4) and (7a) are ignored; equation (7c) is replaced by

$$\left.\begin{aligned} \tau_{12} &\le \alpha_s \cdot G \cdot \gamma_{12} + f_2 \left|\sigma_{22}\right| \\ \tau_{12} &\ge \alpha_s \cdot G \cdot \gamma_{12} - f_2 \left|\sigma_{22}\right| \end{aligned}\right\} \text{ if crack is present;} \qquad (7c')$$

equation (12) for the tangent material matrix is changed appropriately; and LSLD13 = 0. Applicable sector diagrams contain only sectors 2 and 3 and are shown in Figure 5. One use for this option is that its selection for every element, along with a high tensile strength for the cracking planes, produces linear behavior.

Another option is intended to simulate keying action such as produced by shear keys in the contraction joints and by rough surfaces of the cracking planes. A keyed condition that allows opening but no sliding (perfect shear keys) can be applied to each of the three shear components as desired. The appropriate parts of equation (7) are not enforced and the appropriate LSLDij stay at zero. Note that the keying is enforced even when a contraction joint or crack is completely open.

Once the first integration point of an element cracks, a third option facilitates crack extension through the dam by reducing the cracking strength at the other three integration points to some specified value σ_{ten}^{red}. Because of the linear stress distribution through the thickness of

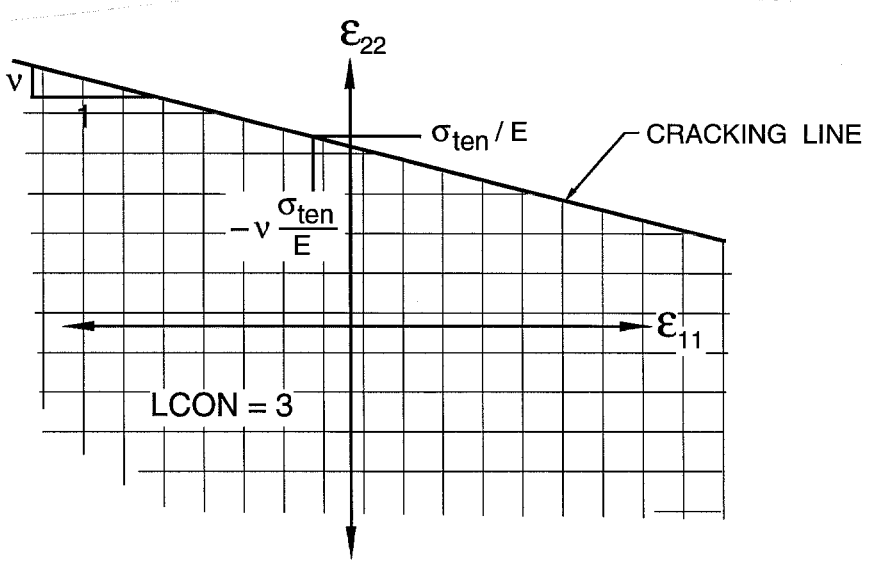

(a) Sector diagram before cracking

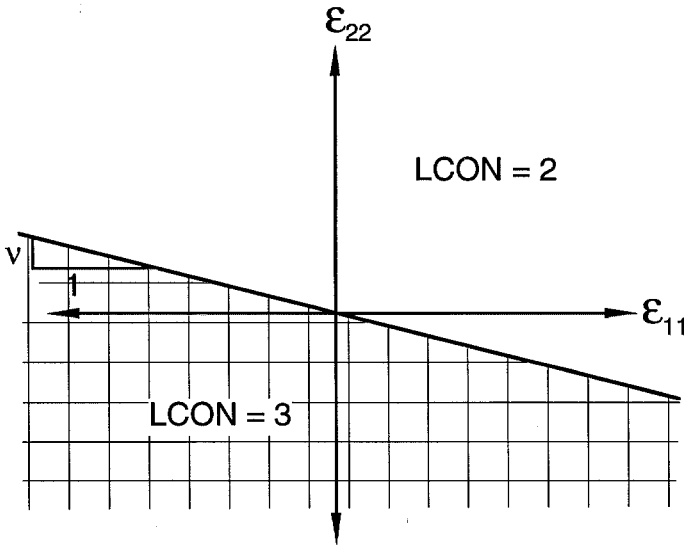

(b) Sector diagram after cracking

Figure 5. Division of ε_{11}-ε_{22} space into sectors corresponding to specific contact states when no contraction joint is present.

the dam, the first integration point of an element to crack will always be an exterior one, either on the upstream or downstream face. Once this crack forms, the use of the full tensile strength at the other integration points ahead of the crack tip would be too restrictive regarding crack propagation.

Another option related to cracking is to spread out the interval of time over which stresses are released once cracking occurs at an integration point. This may be more realistic and it also improves some aspects of the behavior of the numerical solution. When the cracking strength is reached at an integration point, say at time t_c, the stresses to be released (denoted by $\{\sigma_c\}^e$) are computed as discussed in Section 2.2 for a cracking event. To spread the stress release out over some finite time interval T_r, the stresses $\{\sigma^\ell(t + \Delta t)\}^e$ in equation (10), computed as before assuming instantaneous stress release, are augmented by the term $\{\sigma_c\}^e \cdot c(t)$, where $c(t)$ varies linearly from one at $t = t_c$ to zero at $t = t_c + T_r$ and remains at zero for $t > t_c + T_r$.

A final feature pertains to water pressure loads on the dam. The loading discussed in Section 2.1 is for water pressure acting on the upstream dam face, both static and dynamic components. Water pressure can also act internally in the pores of the concrete as well as on the faces of contraction joints and cracks if water penetration occurs. While the static problem is tractable, the dynamic one is very complicated and even approximate treatment is probably not feasible. The approach here is to make some simple calculations of the internal pressures $p_{11}^\ell(t + \Delta t)$ and $p_{22}^\ell(t + \Delta t)$ in the 1 and 2 directions at each integration point, and then to add these pressures (compression being negative) to the stresses $\sigma_{11}^\ell(t + \Delta t)$ and $\sigma_{22}^\ell(t + \Delta t)$ in equation (10). For the static case, whether or not contraction joints or cracks are present,

$$p_{11}^\ell(t + \Delta t) = p_{22}^\ell(t + \Delta t) = \frac{1+\zeta}{2} \left\langle \tfrac{1}{4} \ \tfrac{1}{4} \ \tfrac{1}{4} \ \tfrac{1}{4} \right\rangle \{p_s\}^e \tag{18}$$

which corresponds to a linear variation in pressure through the dam thickness from the static water pressure at the upstream face (nodal values in $\{p_s\}^e$) to zero at the downstream face. In the dynamic case, this expression is still used for $p_{11}^\ell(t + \Delta t)$ if a contraction joint is not present and for $p_{22}^\ell(t + \Delta t)$ if a crack is not present. In the dynamic case if a joint is present

$$p_{11}^{\ell}(t + \Delta t) = \frac{1+\zeta}{2} \left\langle \frac{1}{4} \; \frac{1}{4} \; \frac{1}{4} \; \frac{1}{4} \right\rangle \left\{ p_s + p_d^{\ell}(t + \Delta t) \right\}^e \tag{19a}$$

and if a crack is present

$$p_{22}^{\ell}(t + \Delta t) = \frac{1+\zeta}{2} \left\langle \frac{1}{4} \; \frac{1}{4} \; \frac{1}{4} \; \frac{1}{4} \right\rangle \left\{ p_s + p_d^{\ell}(t + \Delta t) \cdot (1 - c(t)) \right\}^e \; , \tag{19b}$$

which are written for the total water pressure (static and dynamic values in $\{p_s\}^e$ and $\{p_d^{\ell}(t + \Delta t)\}^e$, respectively).

When the internal dynamic pressure is included, a tangent contribution is added to $[K_p]$ in equation (2a) that is assembled from element matrices

$$\left[K_{ip}\right]^e = \int_{v^e} \left\{ b_1 + b_2 \cdot (1 - c(t)) \right\}^e \frac{1+\zeta}{2} \left\langle \frac{1}{4} \; \frac{1}{4} \; \frac{1}{4} \; \frac{1}{4} \right\rangle dv^e \tag{20}$$

integrated by the 4-point scheme. In equation (20), $\{b_1\}^e$ and $\{b_2\}^e$ are the first two columns of $[B^e]^T$; $\{b_1\}^e$ is included only if a contraction joint is present, and $\{b_2\}^e$ is included only if a crack is present.

Incorporating the internal water pressure as described above is designated as Option 1. Another scheme, Option 2, replaces the nodal dynamic pressures $\{p_d^{\ell}(t + \Delta t)\}^e$ with the average dynamic pressures $\{\overline{p}_d^{\ell}(t + \Delta t)\}^e$ over the previous time interval T_p:

$$\left\{ \overline{p}_d^{\ell} \; (t + \Delta t) \right\}^e = \frac{1}{T_p} \int_{t+\Delta t-T_p}^{\ell(t+\Delta t)} \min \left\{ p_d(t), 0 \right\}^e dt \quad , \tag{21}$$

where only compressive (negative) pressure are used in the averaging. Also, the tangent matrix [equation (20)] is not applicable and so is not used. Convergence for Option 2 tends to be slower than for Option 1, especially if T_p is small.

2.5 Accuracy

A dam-water-foundation system subjected to strong earthquake shaking is a complex situation, and numerous assumptions are necessary to replace the actual system with one that can be analyzed. In such a process, it is important to understand the severity of the

assumptions regarding accuracy of the computed results. Therefore, some discussion of the assumptions used in the computer program is presented below.

The treatment of the free-field ground motions along the dam and water boundaries as spatially uniform is far from reality as shown most recently by the accelerograms recorded at Pacoima Dam during the Northridge earthquake (6). Studies (7) show that nonuniformity in ground motion is an important parameter and that the assumption of uniformity can be either conservative or unconservative. The major difficulty is not so much in the formulation but in defining the nonuniformity itself, and this is an issue that needs more study. Therefore, in this first version of the computer program, the treatment of seismic input is limited to the simple case of uniform free-field motion.

An assumption associated with modelling the water is that of incompressibility. Including water compressibility would significantly increase the cost of the analysis, and while water compressibility effects are known to be important for some dams, this is probably not a major limitation of the program. One ongoing study of Morrow Point Dam (8), where water compressibility effects are thought to play an important role in the dynamic response, has not been successful in reproducing the results of carefully controlled force vibration tests. This study uses a finite element model that includes water compressibility, and the model overpredicts the amount of radiation damping associated with the water. Until such matters can be resolved, the use of water compressibility in analyses can be questioned.

The foundation of the dam is taken as a finite region of massless rock, and so only its flexibility is included. Omission of foundation mass precludes any radiation of energy through the foundation away from the dam. However, force vibration testing typically shows a small amount of damping for a concrete dam, and this should include all radiation damping mechanisms. Further, the use of modal damping in an analytical model of a dam with a massless foundation (or equivalently, the use of mass and stiffness-proportional damping based on modal damping values) works well in many cases (9), so this simpler and computationally less intensive approach is adopted here.

Approximations involved in the modelling of the opening and closing of contraction joints and cracks include a single shell element discretization in the thickness direction of the dam

and smeared cracking. A scheme using several elements in the thickness direction connected by contact springs at a joint or crack would be more accurate but is computationally much more expensive. To compare the two procedures, the two-dimensional plane-strain beam problem of Figure 6a containing a center joint and subjected to compressive force P and bending moment M is considered. Of interest are the contributions θ_J and U_J to the rotation and axial displacement, respectively, at a support caused by joint opening [See reference (2) for details.] for the case where the ratio of the beam half-length L to the depth h is high enough so that θ_J and U_J are independent of L/h. A ratio of L/h equal to two is sufficient for this purpose.

Results of the problem of Figure 6a are shown in normalized form in Figure 7: solid line by the finite element mesh of Figure 6b with contact springs in the joint, and dashed lines by the single beam element with smeared cracking shown in Figure 6c. This beam element is the plane-strain version of the shell element used in this report and is representative of the behavior of the shell element. The solid line in Figure 7 should be close to the actual solution of interest because the mesh of Figure 6b is relatively fine and because $L/h = 2$. For the beam element, the normalized joint displacements are proportional to L/h, as shown in Figures 7a and b for the two cases $L/h = 1$ and $L/h = 2$, which is fundamentally different from the actual behavior. Nevertheless, the agreement is reasonable in the range $1 \leq L/h \leq 2$ which is typical of L/h in the upper part of an arch dam where joint opening is most important. Also shown in Figure 7 is the stress σ_{top} across the top edge of the joint (Figure 7c) computed by the two procedures, and the agreement here is good except when the joint contact at the top reduces to a small value $\left(\frac{M}{Ph} \rightarrow 0.5\right)$. However, as $\frac{M}{Ph} \rightarrow 0.5$, the actual value of σ_{top} becomes unbounded, and so the stresses computed by the computer program at a joint edge ($\zeta = \pm 1$) should be interpreted as average values over the 1/8 depth tributary to a $\zeta = \pm 1$ integration point. Such stresses are probably more useful than large values resulting from a fine mesh in the vicinity of a stress singularity.

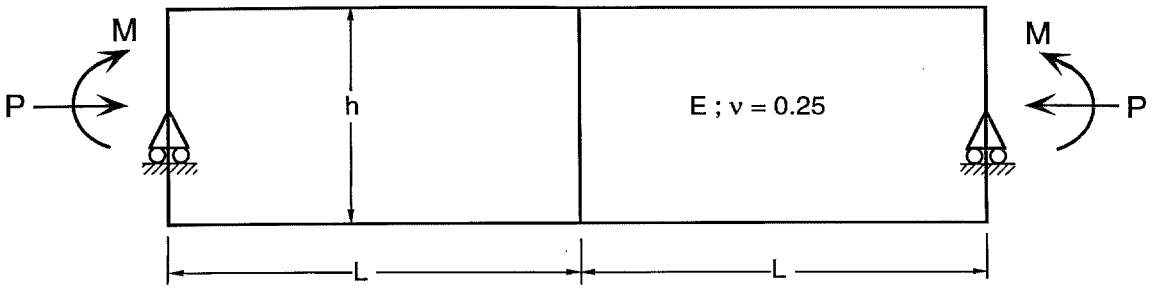

(a) Plane - strain beam with a center joint.

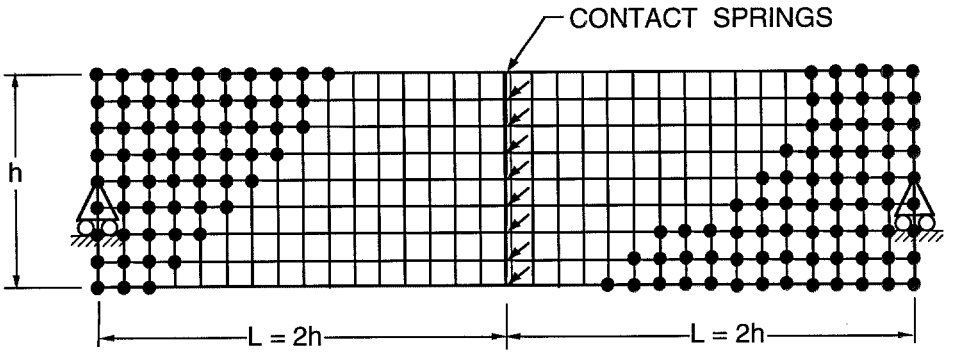

(b) Finite element mesh of 4 - node, plane - strain elements with contact springs in center joint.

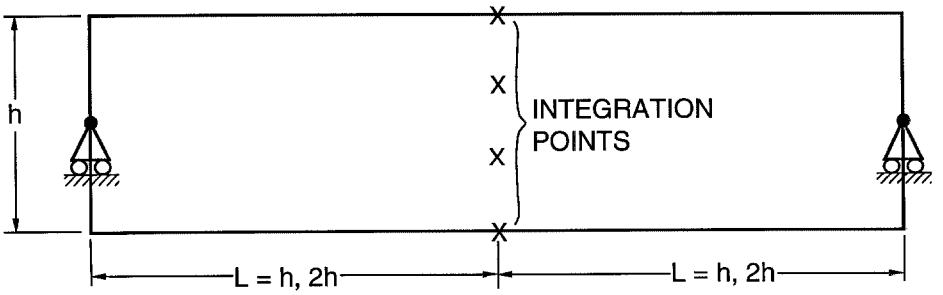

(c) Single plane - strain beam element with smeared cracking at integration points along (pre-cracked) center joint.

Figure 6. Problem of a plane-strain beam with center joint (a) and discrete versions by finite elements with contact springs (b) and by a single beam element with smeared cracking (c).

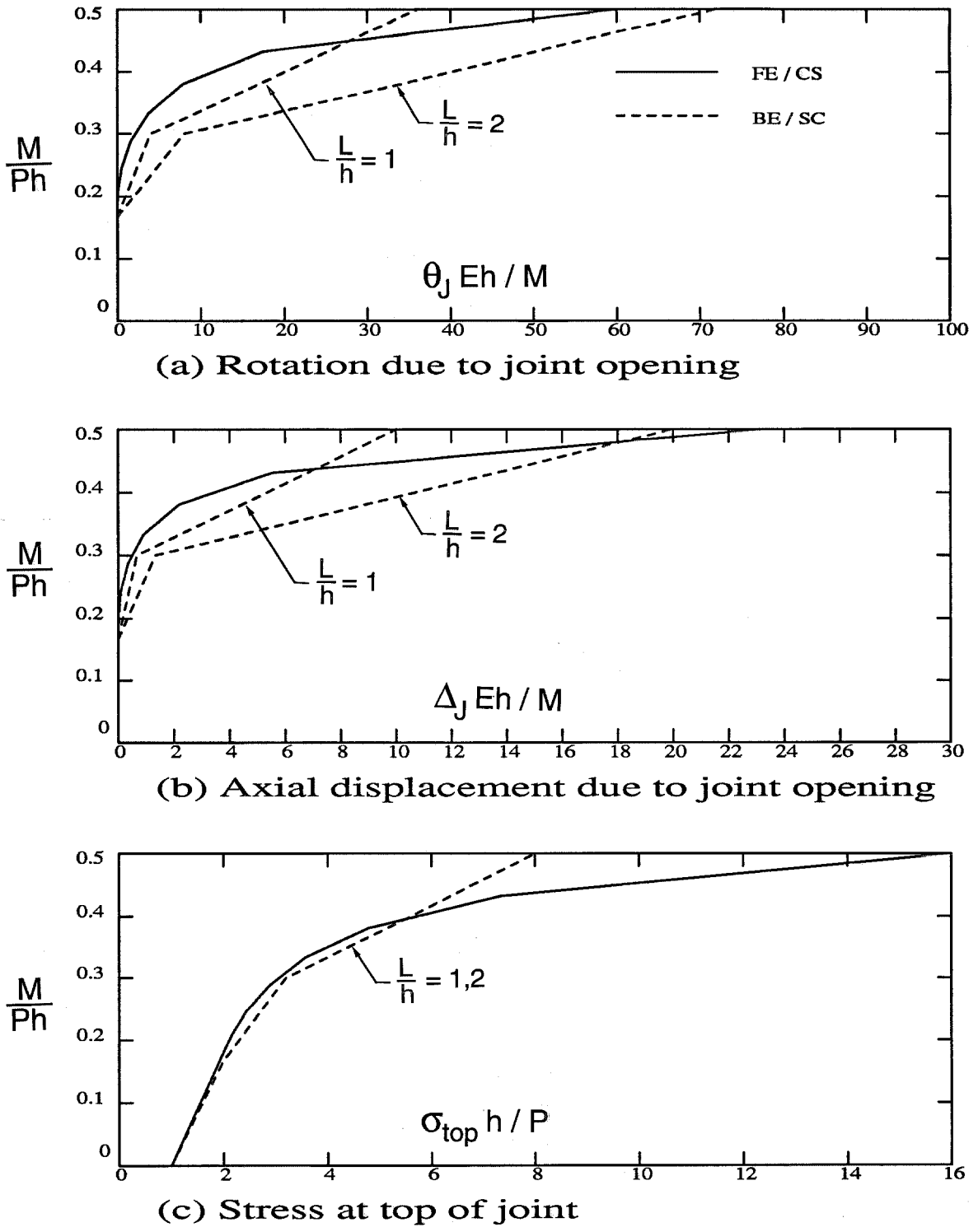

Figure 7. Results for the problem of Figure 6a using the finite element mesh with contact springs (FE/CS) shown in Figure 6b and the beam element with smeared cracking (BE/SC) shown in Figure 6c.

Orientation of the cracking planes is predetermined as the 1-3 plane in each element, which is close to being perpendicular to the cantilever bending stress. Although this seems reasonable, it should be noted that other orientations and patterns are possible, and the assumed one is not necessarily conservative.

Assumptions are also present in the sliding capability of the contraction joints and cracks. As mentioned previously, sliding can occur in the dam's joints and cracks and is associated with the three shear components. Sliding is assumed to be uncoupled for each component, and this is thought to be a reasonable approximation. The option to provide keys for one or more shear components precludes any tangential motion in these components (perfect keys). In reality, however, some tangential motion will accompany opening of a joint or crack (i.e., when the interlocking pieces have sloping sides such as do rough crack surfaces and beveled keys). This sliding-with-dilation action has not been included in this first version of the computer program.

Treatment of τ_{12} is somewhat *ad hoc* because contact conditions in both the joint and crack are relevant. Before cracking occurs, the term $\alpha_s \cdot G \cdot \gamma_{12}$ in equation (7c) prevents the stiffness of the 12 component from dropping to zero when the joint opens. Without this term, excessive sliding displacements can result. The $\alpha_s \cdot G \cdot \gamma_{12}$ term in equation (7c′) for the no-joint case plays a similar role after cracking takes place. Unfortunately, results are somewhat sensitive to the value of α_s; see Chapter 5.

The two options provided to include water pressure in the contraction joints and cracks, which are based on the pressure in the reservoir at the upstream face of the dam, are very crude for the dynamic analysis. When a joint or crack closes and the water is forced out, high pressures must be generated. However, no procedures to account for this action or to assess its importance are available.

The foundation is modelled as linearly elastic, and so no abutment instabilities can occur. Such considerations can be important, such as at Pacoima Dam during the 1971 San Fernando and 1994 Northridge earthquakes (10), and must be checked separately.

As is evident, many assumptions have been introduced for a variety of practical reasons, and not all can be justified on the basis of their effects being small. However, it is felt that as

experience is gained with the procedure, it will prove to be much more effective and realistic in the seismic assessment or design of a dam than the presently used linear analysis. Since the high artificial tensions of a linear analysis will not occur because of the joint opening and cantilever cracking capabilities, attention should focus on the magnitude of the compressive stresses, the amount of cracking, and the amplitude of sliding displacements.

Another aspect of accuracy is the precision retained in the numerical calculations. The nature of the terms in equations (1a) and (2a) is such that double precision is required in their formation and solution. In addition, the matrix solver monitors the diagonal terms in factoring the left-side matrix of equation (1a) or (2a) and prints a warning on the log file if the minimum diagonal encountered (DMIN) is below a tolerance set equal to 10^{-7} times the average original diagonal (AVOD) of the matrix. Both DMIN and AVOD are absolute-value quantities. Since parts of the left-side matrix in equation (2a) associated with the dam displacement and water pressure degrees of freedom differ in scale, the diagonals for these two types of degrees of freedom are handled separately. If a diagonal term is encountered below $10^{-9} \cdot$ AVOD, then execution is stopped. Serious problems with numerical precision are unlikely but could occur in static analysis if a temperature drop causes excessive cracking and contraction joint opening such that the left-side matrix of equation (1a) approaches a singular matrix.

Values of the tolerances used on $F^{\ell}_{\max}$ and $M^{\ell}_{\max}$ also affect accuracy. Reasonable choices for these tolerances are given in Section 3.2.3.

Errors in the time integration for dynamic analysis are controlled by the size of the time step Δt. Choosing Δt small enough to make such errors negligible may require some experimentation, especially if nonlinear response is important. The increase in computational effort from the greater number of time steps resulting from a smaller Δt is partially offset by a reduction in the number of iterations to convergence. Some data on the choice of Δt is given in Chapter 5.

3. USER'S GUIDE TO COMPUTER PROGRAM

3.1 General

The system consists of an arch dam, foundation region and water reservoir (Figure 1). A smeared crack approach is used to represent opening, closing and sliding of contraction joints and cracks in the dam. The foundation is linearly elastic, massless and finite, and it connects only to the dam. The water, assumed incompressible, is contained in a region bounded by the upstream face of the dam and a finite, rigid reservoir. No connection exists between the water and the foundation supporting the dam. Global coordinates are x, y, z in the stream, vertical and cross-stream directions, respectively. The x coordinate is positive upstream, y is positive upward, and z is positive as determined by the right hand rule.

Two kinds of analysis are performed: static and dynamic. The static analysis considers loads from gravity, temperature and water pressure and allows open contraction joints and cracks to be filled (grouted). Through load steps, construction of the dam can be simulated. The dynamic analysis follows the static solution and uses ground acceleration components in the x, y and z directions. These ground motions are spatially uniform and are applied to the dam as free-field motions and to the reservoir boundaries as rigid motions.

The dam, foundation and water are represented by separate meshes of shell, solid and water elements, respectively. The dam mesh is used to construct the matrix equations of equilibrium and motion of the dam [equations (1a) and (2a)]. Degrees of freedom are three translations and two rotations at each node of the dam; these nodes are located on the mid-surface of the shell. Terms representing stiffness of the foundation are computed from the foundation mesh and, after condensation to eliminate degrees of freedom off the dam-foundation interface, are transformed to the dam degrees of freedom along this interface and added into the dam equations. For dynamic analysis, damping in the dam and foundation is included by the usual mass and stiffness-proportional terms except that damping forces across open joints and cracks are automatically omitted. The water mesh is needed only in the dynamic analysis; in which case, terms representing the water and the reservoir boundary accelerations are computed and added into the dam equation of motion. Another condensation eliminates most of the degrees of freedom associated with the water mesh,

leaving only one additional degree of freedom at each dam node (a dynamic water pressure degree of freedom). Thus, only the mid-surface nodes of the dam are present in the final equations of equilibrium and motion, including along the foundation interface, and each node has the five dam degrees of freedom and, for the dynamic analysis, one additional dynamic water pressure degree of freedom.

The computer program uses 12 files for input and output that are referred to by unit numbers as follows:

Unit Number	File Type	Contents
2	output	response time histories
3	output	response pictures
4	input	problem description
7	output	problem setup information
9	input/output	restart information
12	input/output	scratch
14	input/output	scratch
15	input/output	scratch
17	input/output	scratch
20	input	x ground acceleration history
21	input	y ground acceleration history
22	input	z ground acceleration history
25	input/output	foundation matrix $[\overline{K}]$

In addition, progress information during execution (Unit * in the program) is output to the terminal screen for an interactive run or to a log file for a batch run. Before running the program, the input files have to be prepared and assigned to Units 4, 20, 21 and 22. Results of the computations that should be saved are written to files that are assigned to Units 2, 3 and 7. Using Unit 25, $[\overline{K}]$ can be computed and saved during a run and then read without recomputation in subsequent runs.

A restart option, using the file assigned to Unit 9, allows an analysis to be run in stages. A restart file is written to Unit 9 at the end of the static analysis and is overwritten periodically during the dynamic analysis. In a restarted run, Unit 9 is read at the beginning of the restart and then periodically overwritten. The output files assigned to Units 2 and 3 are augmented with the new output during a restarted run while the one on Unit 7 is overwritten.

All program arrays are stored in a master one-dimensional array A by dynamic storage allocation. Array A is dimensioned at 1.2 million, and this number can be increased or decreased by the user. If this is done the program variable MTOT should be reset to equal the new dimension of array A because MTOT is used in the program's check that available storage (MTOT) equals or exceeds needed storage. Computations for the foundation mesh will usually control the amount of storage needed.

If symmetry in the geometry of the problem exists about the x-y plane, then separate symmetric and antisymmetric analyses can be run using a half mesh that extends only on one side of the plane of symmetry. A symmetric analysis is for the static problem and for the x and y components of ground motion in the dynamic problem; an antisymmetric analysis is for the z ground motion component in the dynamic problem. The two analyses use the same mesh except for the fixity conditions on the plane of symmetry, as given in the following table. Any attempt to combine results from separate symmetric and antisymmetric analyses with nonlinearity included (opening and/or sliding of joints and cracks) should be done with caution since the principle of superposition does not hold. It is not recommended.

Degree of Freedom	Symmetric Analysis	Antisymmetric Analysis
u (dam or foundation*)	active	fixed*
v (dam or foundation*)	active	fixed*
w (dam or foundation*)	fixed*	active
θ (dam)	active	fixed
γ (dam)	fixed	active
water pressure	active	zero

*A fixed condition for foundation degrees of freedom on the plane of symmetry should only be applied at nodes off the dam-foundation interface.

3.2 Description of Input

Data to be supplied to the input files is shown below within brackets [.....]. All data can be freely spaced. Variables beginning with letters I through N are integer; others are real. The indicated default values are used by the program when zeroes are read. Units are stated in italics. Consistent units should be used for all united quantities. References in the right column are to notes contained in Section 3.2.3.

3.2.1 Input file assigned to Unit 4

	Notes
1. [Title] Single line of descriptive text.	
GENERAL PROGRAM VARIABLES	
2. [NSSTPS, NDSTPS, NITMAX]	
NSSTPS = number of load steps in the static analysis (>0).	A
NDSTPS = number of time steps at increment Δt in the dynamic analysis (≥0).	B,C,D
NITMAX = maximum number of iterations to reach convergence in a load step or time step before automatic step division occurs (default = 100).	B,C
3. [SMINS, SMAXS, SMIND, SMAXD]	E
SMINS = minimum value of S^{ℓ} for static analysis.	
SMAXS = maximum value of S^{ℓ} for static analysis (default = 1.0).	
SMIND = minimum value of S^{ℓ} for dynamic analysis.	B
SMAXD = maximum value of S^{ℓ} for dynamic analysis (default = 1.0).	B
4. [IRES, IRINT, IOINT]	
IRES = 0 then present run is the initial run of a problem; = 1 then present run is a restart.	B,F
IRINT = time step interval for which restart file is overwritten on Unit 9 (default = 1000).	B,C
IOINT = time step interval for which time history responses are written to unit 2 (default = 10).	C
5. [NWATER, NFOUND, (IKEY(I), I=1,3), IPRES]	
NWATER = 1 then water mesh is present; = 0 then absent.	A
NFOUND ≥ 1 then foundation mesh of dam is present; = 0 then absent; = 1 then Unit 25 is not used; = 2 then $[\overline{K}]$ is written to Unit 25; = 3 then $[\overline{K}]$ is read from Unit 25.	U
IKEY(1), IKEY(2), IKEY(3) = 1 then key present for shear components 12, 23, 13 in the dam, respectively; = 0 then no key. See Section 2.4.	
IPRES = 1,2 then internal water pressure included in the dam by Option 1 (IPRES=1) or Option 2 (IPRES=2); = 0 then not included. See Section 2.4.	
6. [WW, G, ALP1, ALP2, SFT, (COEF(I), I=1,3), ALPS, TRF, FTOL, ZTOL]	
WW = unit weight of water (*force/volume*).	
G = acceleration of gravity (*length/time*^{2}).	

	Notes
ALP1 = coefficient for thermal expansion for dam concrete in the arch direction, α_1 (*degrees/strain*).	G
ALP2 = coefficient for thermal expansion for dam concrete in the cantilever direction, α_2 (*degrees/strain*).	G
SFT = reference temperature for dam concrete at which the stresses and strains produced by temperature loading are zero.	A
COEF(1), COEF(2) = coefficients of friction for sliding in the dam on the contraction joints (f_1) and cracking planes (f_2), respectively. See Section 2.2.	
ALPS = shear stiffness reduction factor, α_s (recommended value = 0.25). See Sections 2.2 and 2.5.	
TRF = reduction factor for tensile strength at an integration point; thus $\sigma_{ten}^{red} = \text{TRF} \cdot \sigma_{ten}$ (recommended value = 0.10). See section 2.4.	
FTOL = convergence tolerance used for translational degrees of freedom of the dam (*force*).	B,F,H
ZTOL = convergence tolerance used for rotational degrees of freedom of the dam (*force · length*).	B,F,H
DAM MESH	
7. [NPD, NELD, NMATD] NPD = number of mid-surface nodes in the dam mesh. NELD = number of shell elements in the dam mesh. NMATD = number of material property sets for the dam elements.	
8. [XMULT, YMULT, ZMULT] XMULT, YMULT, ZMULT = multipliers for the input *x,y,z* coordinates, respectively, of the dam mesh nodes.	
9. [N, NE, NG, NRC, CXUN, CYUN, CZUN, CXUNE, CYUNE, CZUNE] [CXDN, CYDN, CZDN, CXDNE, CYDNE, CZDNE] ⋮ Dam mesh nodal coordinates. Equally spaced coordinates for upstream auxiliary dam nodes corresponding to mid-surface dam nodes N through NE at an increment of NG are generated, similar for the corresponding downstream auxiliary dam nodes. NE = 0 to input coordinates of auxiliary nodes at node N only. Repeat to input coordinates of NPD upstream and NPD downstream auxiliary nodes.	I
NRC = coordinate system specifier for the generated set of nodal coordinates.	J
CXUN, CYUN, CZUN = *x,y,z* coordinates of the upstream auxiliary node at mid-surface node N (*length*).	
CXUNE, CYUNE, CZUNE = *x,y,z* coordinates of the upstream auxiliary node at mid-surface node NE (*length*).	

Notes

CXDN, CYDN, CZDN = x,y,z coordinates of the downstream auxiliary node at mid-surface node N (*length*).
CXDNE, CYDNE, CZDNE = x,y,z coordinates of the downstream auxiliary node at mid-surface node NE (*length*).

10. [N, NE, NG, (ID(I), I=1,6)] K,L
⋮

Fixity conditions for mid-surface dam nodes. Nodes N through NE at an increment of NG are assigned the values of ID. Repeat as necessary; end with a line of 0's.

ID(1) = 1 if u degree of freedom is active; = 0 if fixed.
ID(2) = 1 if v degree of freedom is active; = 0 if fixed.
ID(3) = 1 if w degree of freedom is active; = 0 if fixed.
ID(4) = 1 if θ degree of freedom is active; = 0 if fixed.
ID(5) = 1 if γ degree of freedom is active; = 0 if fixed.
ID(6) = 1 if dynamic water pressure degree of freedom is active; = 0 for zero pressure. Input value of ID(6) is not used in static analysis.

[0 0 0 0 0 0 0 0 0]

11. [EE, PR, WT, TEN, IJON]
⋮

Material properties for the dam. Repeat NMATD times to input NMATD material sets. Ith line is Ith set.

EE = Young's modulus for dam concrete , E (*force/area*).
PR = Poisson's ratio for dam concrete, υ.
WT = Unit weight for dam concrete (*force/volume*).
TEN = tensile strength for dam concrete, σ_{ten} (*force/area*).
IJON = 1 then contraction joint is present; = 0 then no joint. See Section 2.4.

12. [N, NE, NG, MAT, H1, H2, (LM(I), I=1,4), LMG] M
⋮

Material set numbers, dimensions and mid-surface nodal arrays for the dam elements. Elements N through NE at an increment of NG are assigned the material set number MAT, dimensions H1 and H2, and a generated nodal array. Repeat to cover all NELD elements.

H1, H2 = approximate element dimensions in the arch and cantilever directions, respectively, H_1 and H_2 (*length*). See Section 3.3.
LM(I) = Ith node number of element N.
LMG = node number increment for generated nodal arrays.

	Notes
WATER MESH	V
Omit this section if NWATER = 0.	
13. [NPW, NELW, NPDW, NSWR, NSWD]	
NPW = number of nodes in the water mesh.	
NELW = number of elements in the water mesh.	
NPDW = number of water mesh nodes on the upstream face of the dam.	N
NSWR = number of sides of water elements on the reservoir floor and sides where ground accelerations will be applied.	O
NSWD = number of sides of water elements on the upstream face of the dam.	O
14. [XMULT, YMULT, ZMULT]	
XMULT, YMULT, ZMULT = multipliers for the input *x,y,z* coordinates, respectively, of the water mesh nodes.	
15. [N, NE, NG, NRC, CXN, CYN, CZN, CXNE, CYNE, CZNE]	P
⋮	
Water mesh nodal coordinates. Equally spaced coordinates of water mesh nodes N through NE at an increment of NG are generated. NE = 0 to input coordinates of node N only. Repeat to input coordinates of NPW water mesh nodes.	
NRC = coordinate system specifier for the generated set of nodal coordinates.	J
CXN, CYN, CZN = *x,y,z* coordinates of node N (*length*).	
CXNE, CYNE, CZNE = *x,y,z* coordinates of node NE (*length*).	
16. [N, NE, NG, ID]	K, V
⋮	
Fixity conditions for water mesh nodes. Nodes N through NE at an increment of NG are assigned the value ID. Repeat as necessary; end with a line of 0's.	
ID = 1 if dynamic water pressure degree of freedom is active; = 0 for zero pressure.	
[0 0 0 0]	
17. [N, NE, NG, (LM(I), I=1,8), LMG]	Q
⋮	
Nodal arrays for the water elements. Elements N through NE at an increment of NG are assigned a generated nodal array. Repeat to cover all NELW elements.	

	Notes
LM(I) = Ith node number of element N. LMG = node number increment for generated nodal arrays.	
18. [NODEW, NODED] ⋮ Dam and water connectivity. NODED is the number of the dam mid-surface node whose upstream auxiliary node connects to water mesh node number NODEW. Repeat NPDW times to input NPDW nodal pairs. Nodes at the free surface of the water should be included.	N
19. [N, NE, NG, ISIDE] ⋮ Side numbers of elements along the reservoir floor and sides. Elements N through NE at an increment of NG are assigned the value ISIDE. Repeat to cover all NSWR sides. ISIDE = side number (≥1, ≤8).	O
20. [N, NE, NG, ISIDE] ⋮ Side numbers of elements along the dam-water interface. Elements N through NE at an increment of NG are assigned the value ISIDE. Repeat to cover all NSWD sides. ISIDE = side number (≥1, ≤8).	O
FOUNDATION MESH	
Omit this section if NFOUND = 0.	U
21. [NPG, NELG, NMATG, NPDG, NINTG] NPG = number of nodes in the foundation mesh. NELG = number of elements in the foundation mesh. NMATG = number of material property sets for the foundation elements. NPDG = number of dam mid-surface nodes on the dam-foundation interface.	N
NINTG specifies the integration scheme for the foundation elements, = 1 for lowest order; = 2 for middle order; = 3 for highest order.	R
22. [XMULT, YMULT, ZMULT] XMULT, YMULT, ZMULT = multipliers for the input x,y,z coordinates, respectively, of the foundation mesh nodes.	
23. [N, NE, NG, NRC, CXN, CYN, CZN, CXNE, CYNE, CZNE] ⋮	P

Notes

Foundation mesh nodal coordinates. Equally spaced coordinates of foundation mesh nodes N through NE at an increment of NG are generated. NE = 0 to input coordinates of node N only. Repeat to input coordinates of NPG foundation mesh nodes.

NRC = coordinate system specifier for the generated set of nodal coordinates. — J

CXN, CYN, CZN = x,y,z coordinates of node N (*length*).
CXNE, CYNE, CZNE = x,y,z coordinates of node NE (*length*).

24. [N, NE, NG, (ID(I), I=1, 3] — K,L,N

⋮

Fixity conditions for foundation nodes. Nodes N through NE at an increment of NG are assigned the values of ID. Repeat as necessary; end with a line of 0's.

ID(1) = 1 if u degree of freedom is active; = 0 if fixed.
ID(2) = 1 if v degree of freedom is active; = 0 if fixed.
ID(3) = 1 if w degree of freedom is active; = 0 if fixed.

[0 0 0 0 0 0]

25. [EE, PR]

⋮

Material properties for the foundation. Repeat NMATG times to input NMATG material sets. Ith line is Ith set.

EE = Young's modulus for foundation (*force/area*).
PR = Poisson's ratio for foundation.

26. [N, NE, NG, MAT, NENI, (LM(I), I=1, NENI), LMG] — R

⋮

Material set numbers and nodal arrays for the foundation elements. Elements N through NE at an increment of NG are assigned the material set number MAT and a generated nodal array. Repeat to cover all NELG elements.

NENI = 15 for a triangular solid element;
= 20 for a rectangular solid element.
LM(I) = Ith node number of element N; or = 0 for an omitted mid-edge node.
LMG = node number increment for generated nodal arrays.

27. [NODEGU, NODEGD, NODED] — N

⋮

Notes

Dam and foundation connectivity. NODED is the number of the dam mid-surface node whose upstream and downstream auxiliary nodes connect to foundation node numbers NODEGU and NODEGD, respectively. Repeat NPDG times to input NPDG nodal trios.

STATIC ANALYSIS

The data in this section consists of NSSTPS groups of lines, each of which defines a load step.

28. [ISTPTYP, NSUB] — A

The first line in a group that defines a load step.

ISTPTYP = 1 for a construction step;
= 2 for a temperature step;
= 3 for a water level step;
= 4 for a grouting step.

NSUB = number of substeps. Input value is used for the temperature step only. — F

29. [N, NE, NG] — A

⋮

For a construction step, dam elements N through NE at an increment of NG are assembled into the mesh and loaded by gravity. Repeat to input all elements to be assembled in the current step; end with a line of 0's.

[0 0 0]

30. [N, NE, NG, UTEMP, DTEMP] — A

⋮

For a temperature step, dam elements N through NE at an increment of NG are assigned a new temperature that varies from UTEMP (*degrees*) at the upstream face to DTEMP (*degrees*) at the downstream face. Repeat to cover all elements receiving new temperatures in the current step; end with a line of 0's.

[0 0 0 0. 0.]

31. [SELEV] — A, V

For a water level step.

SELEV = y coordinate of new water free-surface elevation (*length*).

32. [KJOINT, KCRACK] — A

⋮

	Notes
For a grouting step, all dam elements have their contraction joints filled in, if open, if KJOINT = 1 (or left alone if KJOINT = 0) and have their cracks filled in, if open, if KCRACK = 1 (or left alone if KCRACK = 0).	
DYNAMIC ANALYSIS	
Only needed if NDSTPS > 0.	
33. [DT, NDTGM, BINT, PINT]	
DT = time step of computation, Δt (*time*).	C
NDTGM = length of time increment in the ground acceleration data as a multiple of Δt.	C,D
BINT = duration of crack rupture process, T_r (*time*, recommended value = 0.05 sec). See Section 2.4.	
PINT = duration, T_p, over which dynamic water pressures are averaged in the calculation of internal water pressure (*time*). Input value of PINT is used only if IPRES = 2. See Section 2.4.	
34. [ALPHA, GAMMA, BETA, A0, A1]	
ALPHA = Bossak time integration parameter, α_B (recommended value = –0.2). See Section 2.1.	S
GAMMA = Newmark time integration parameter, γ (recommended value = $0.5-\alpha_B$). See Section 2.1.	
BETA = Newmark time integration parameter, β (recommended value = $0.25\cdot(1-\alpha_B)^2$). See Section 2.1.	
A0 = mass-proportional damping coefficient a_0 used for the dam (*1/time*). See Section 2.1.	T
A1 = stiffness-proportional damping coefficient a_1 used for the dam and foundation (*time*). See Section 2.1.	T
35. [NPIC, NHIST]	
NPIC = number of response pictures to be written to Unit 3 at specified time steps during the dynamic analysis. See Section 3.3.	B
NHIST = number of time history quantities to be written to Unit 2. See Section 3.3.	
36. [(IDPIC(I), I=1, NPIC)]	B,C
IDPIC(I) = time step number of the Ith response picture. Values should be input in increasing order. Omit if NPIC = 0. See Section 3.3.	
37. [NODEL, NQ]	
⋮	

	Notes
NQ specifies the response type and NODEL the node or element number for the quantities whose time histories are written to Unit 2. Repeat NHIST times to input NHIST time history quantities; Ith line is Ith quantity. Omit if NHIST = 0. See Section 3.3.	
NODEL = dam mid-surface node number (for NQ = 1 to 5, 26) or dam element number (for NQ = 6 to 25).	
NQ = 1, 2, 3, 4, 5 for u, v, w, θ, γ nodal displacements, respectively;	L
= 6, 7, 8, 9, 10 for σ_{11}, σ_{22}, τ_{12}, τ_{23}, τ_{13} stresses on the upstream face, respectively;	L
= 11, 12, 13, 14, 15 for σ_{11}, σ_{22}, τ_{12}, τ_{23}, τ_{13} stresses on the downstream face, respectively;	L
= 16, 17, 18, 19, 20 for OD1, OD2, SD12, SD23, SD13 opening and sliding displacements on the upstream face, respectively;	L
= 21, 22, 23, 24, 25 for OD1, OD2, SD12, SD23, SD13 opening and sliding displacements on the downstream face, respectively;	L
= 26 for water pressure at the upstream face.	
38. [(AMULT(I), I=1,3)]	D
AMULT(1), AMULT(2), AMULT(3) = multipliers for the input x, y, z components, respectively, of the ground acceleration time histories.	

3.2.2 Input files assigned to Units 20, 21 and 22

	Notes
39. [(ACGX(I), I=1, NDSTPS, NDTGM)]	B,C,D
Ground acceleration values for x component of ground motion on Unit 20 (*length/time*^{2}).	
40. [ACGY(I), I=1, NDSTPS, NDTGM)]	B,C,D
Ground acceleration values for y component of ground motion on Unit 21 (*length/time*^{2}).	
41. [ACGZ(I), I=1, NDSTPS, NDTGM)]	B,C,D
Ground acceleration values for z component of ground motion on Unit 22 (*length/time*^{2}).	

3.2.3 Notes

A. Load steps in static analysis. There are no restrictions on the number of load steps or their order except practical considerations, for example: a temperature step can only involve elements that have already been assembled into the mesh by a previous construction step. In a construction step, a set of elements is assembled into the mesh and then gravity loads applied. A temperature step specifies a new temperature distribution that varies linearly from the upstream face to the downstream face. Elements are initially placed at temperature SFT, and the values of UTEMP and DTEMP are new temperatures, not temperature increments. An element not listed in a temperature step retains its current temperature for the step. A step to change the water free-surface elevation specifies a new water level which can be either higher or lower than the previous level. Initially, the reservoir is empty. If no dynamic analysis is to be run, then no water mesh is needed. A grouting step resets strains in the concrete to simulate the closing of open joints and cracks such as could be accomplished by filling with grout. No stress changes occur in a grouting step.

B. Restart run. The restart file is written to Unit 9 every IRINT timesteps during the dynamic analysis. The initial run of a problem (IRES = 0) starts with the static analysis and either stops at the end of the static analysis (NDSTPS = 0) or after NDSTPS of the dynamic analysis. A restarted run (IRES = 1) is a continuation of the previous run either

1. to start the dynamic analysis if the previous run was stopped after the end of the static analysis. NDSTPS is set to the desired number of timesteps.
2. or to continue the dynamic analysis. Increase NDSTPS to add time steps noting that NDSTPS is the total number of time steps, including those from the initial run, if any, and from any previous restarted runs, if any. If necessary, to accommodate the additional time steps, the ground motion files on Units 20, 21 and 22 can be lengthened, and additional response pictures can be specified by increasing NPIC and lengthening IDPIC. Changes are also allowed to NITMAX, SMIND, SMAXD, FTOL and ZTOL to alter the convergence conditions. Except as noted here, the input files should not be changed for a restarted run.

C. Time steps in dynamic analysis. The time step Δt is DT which may differ from the time increment of the ground motion data. The latter is NDTGM·DT where NDTGM ≥ 1. If NDTGM > 1, the program interpolates the ground motion data to the smaller time increment DT as the dynamic analysis is run. During a time step of the dynamic analysis, if convergence does not occur within NITMAX iterations, then automatic time step subdivision takes place during which the time step may be divided into substeps as short as DT/64. The input variables NDSTPS, IRINT, IOINT and IDPIC(I) refer to the full time steps of length DT and not to any substeps. DT should be chosen so that the equations of motion are integrated accurately, and some data on this is presented in Chapter 5.

D. Ground motions. All three ground motion components (input Units 20, 21 and 22) must be present for the dynamic analysis. Use zeros if one or more are unavailable. The first NDSTPS/NDTGM ground acceleration values on each unit are used. For a symmetric analysis, set AMULT(3) = 0. For an antisymmetric analysis, set AMULT(1) = AMULT(2) = 0.

E. Convergence parameter S^{ℓ}. The parameter S^{ℓ} and its upper and lower bounds are discussed in Section 2.3. An optimum choice of the bounds SMINS, SMAXS, SMIND and SMAXD depends on the problem being solved and on many factors such as the size of the load or time step. Using low values for the bounds may significantly reduce the computation time. Although low values also increase the risk that divergence will occur, especially in the static analysis, good results were achieved in Chapter 5 with SMINS = 0.0, SMAXS = 0.1, SMIND = 0.0 and SMAXD = 0.01.

F. Temperature step substeps. A temperature step can be divided into NSUB ≥ 1 substeps. This option is provided as a convenient way of applying the temperature loads in small increments. If the temperature is decreased in too large an increment, then severe convergence difficulties can result if frictional sliding (no keys) can occur. Some experimentation may be necessary to determine an appropriate temperature drop per substep; a value as low as 0.1°F per substep would not be unusual. For a static analysis where a temperature drop is present, it may also be necessary to use higher-than-normal values for

FTOL and ZTOL. These can be reduced again for the dynamic analysis if it is run as a restart. Convergence is much easier for temperature increases.

G. Thermal expansion coefficients for concrete. Different coefficients of thermal expansion can be specified for the arch and cantilever directions. In most situations, equal values are appropriate.

H. Convergence tolerances. Iterations in each load step of equation (1a) or in each time step of equation (2a) reach convergence when every term of the residual, i.e., the right-hand side expressed as a single vector, is below a specified tolerance: FTOL (units of force) for the translational degrees of freedom and ZTOL (units of moment) for the rotational degrees of freedom. FTOL and ZTOL should be chosen carefully to avoid excessive iterations if they are too small or inaccurate results if they are too high. Reasonable values are given by

$$\left.\begin{aligned} \text{FTOL} &= \tfrac{1}{2} \cdot \sigma \cdot W \cdot H \\ \text{ZTOL} &= \tfrac{1}{2} \cdot \text{FTOL} \cdot W \end{aligned}\right\} \tag{22}$$

where W = thickness of the dam at the crest, H = average height of the shell elements in the top row of the dam mesh, and $\sigma \approx 0.01$ psi converted to the user's system of units.

I. Dam nodes. The shell elements of the dam have mid-surface nodes where the degrees of freedom are defined. Associated with each mid-surface node are two auxiliary nodes: one on the upstream face and one on the downstream face. It is the coordinates of these auxiliary nodes that are input.

J. Coordinate systems. Nodal coordinates can be input using the x,y,z system or any of three cylindrical coordinate systems. These coordinate systems are shown in Figure 8. In the input, x,y,z are replaced by cylindrical coordinates as follows:

NRC	**Coordinates**		
0	x	y	z
1	x	R	θ_x
2	R	y	θ_y
3	R	θ_z	z

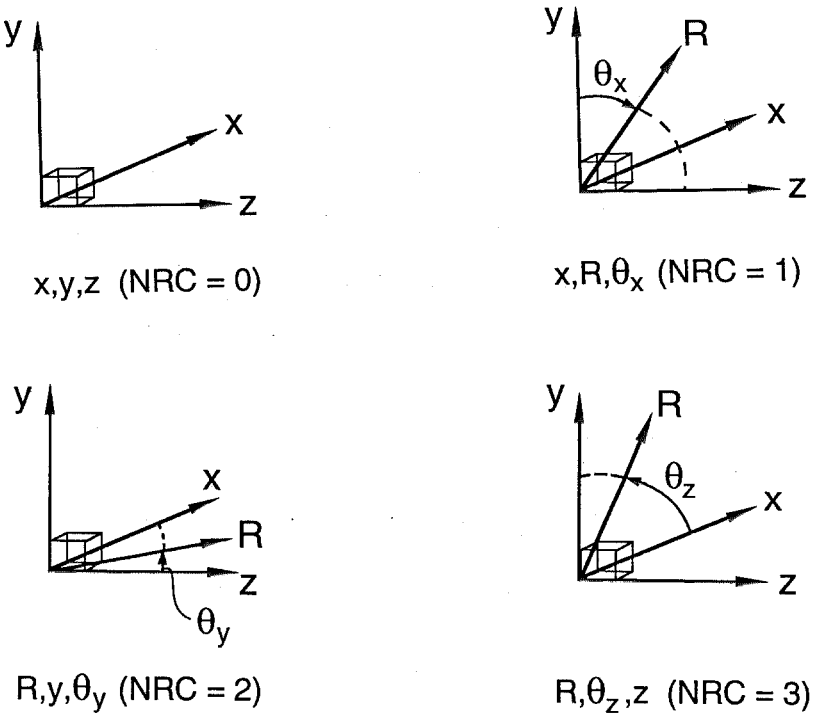

Figure 8. Selection of coordinate systems for input of nodal coordinates.

K. Fixity conditions. All displacement degrees of freedom in the dam and foundation meshes are initially assumed to be active, so only conditions at nodes where at least one degree of freedom is fixed need be input. Dam degrees of freedom on the dam-foundation interface should be left active when the foundation mesh is included, fixed otherwise. Degrees of freedom of the foundation on the far boundary of the foundation mesh should be fixed. The water pressure degrees of freedom in equation (2) (6th entry in the dam's ID) for dynamic analysis are initially assumed to be active, so those at the free surface of the water should be fixed to zero pressure. In the water mesh, all water pressure degrees of freedom are initially assumed to be active, so those at the free surface should be fixed to zero pressure. If it is desired to run the dynamic analysis with a water free surface below the top level of the water mesh, then both types of water pressure degrees of freedom should be fixed to zero pressure down to the desired water free-surface level. Additional fixity conditions for the dam, foundation and water meshes occur when a symmetric or antisymmetric analysis is performed;

see Section 3.1. If multiple entries for fixity conditions at a node are present, the last entry prevails.

L. Displacements and stresses. The u, v and w displacement degrees of freedom of the dam and foundation are in the x, y and z directions, respectively. Dam rotational degrees of freedom θ and γ are about local $\hat{x}$ and $\hat{y}$ axes, respectively, defined at the nodes; see Section 2.2. Stresses and strains in the dam are expressed with respect to a local set of 1, 2, 3 axes in each element which are the arch, cantilever and normal (to the mid-surface) directions, respectively; see Section 2.2. Opening and sliding displacements in the dam are referred to these 1, 2, 3 axes in each element.

M. Dam element. The dam element is a 4-node shell element (Figure 2) that can be mapped into an arbitrary orientation and shape in x,y,z space, including the superposition of two adjacent nodes to make a triangular element. The LM array must list the four dam mesh node numbers in the order shown. This numbering is counter-clockwise when viewed from upstream, and this ensures that the $\zeta = 1$ face is on the upstream face of the dam. Superimposed nodes have the same dam mesh node number, and this number will appear multiply in LM.

N. Dam-water-foundation connectivity. Figure 9 illustrates the connectivity between the dam and water meshes and between the dam and foundation meshes. The discretizations of the dam and water must match at the dam-water interface (which need not extend the full height of the dam) meaning that each water mesh node on the upstream face of the dam coincides with an upstream auxiliary dam mode. This connectivity is defined through the input nodal pairs NODED and NODEW (i and j in Figure 9). Along the dam-foundation interface, the dam and foundation discretizations must match. The face of a foundation element in contact with the dam should have mid-edge nodes omitted, and the four remaining nodes (corner nodes) should coincide with auxiliary dam nodes, two on the upstream face and two on the downstream face. This connectivity is established through the input nodal trios NODED, NODEGU and NODEGD (ℓ, m and k in Figure 9). All of the values NODED, NODEW, NODEGU and NODEGD must be actual node numbers; they cannot be zero. Furthermore, nodes NODEGU and NODEGD of the foundation mesh must have all three

degrees of freedom active, even in a symmetric or antisymmetric analysis for which the proper fixity conditions are established automatically by the program.

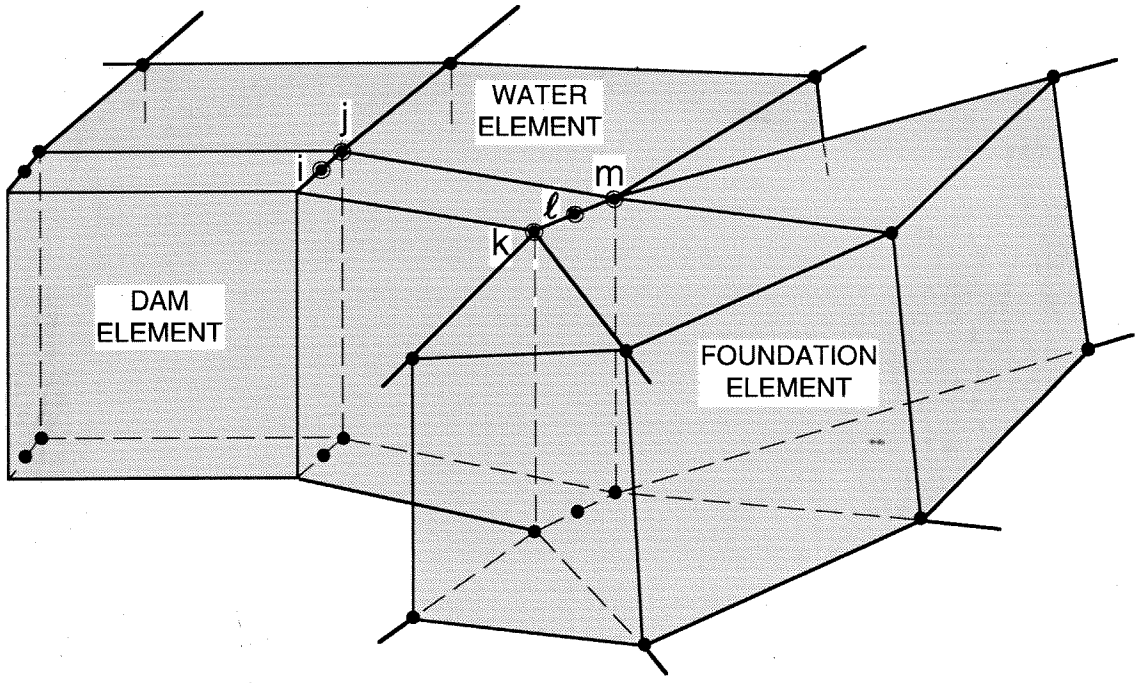

i, ℓ : dam mid - surface nodes
j : water node that connects to the upstream auxillary node at i
k : foundation node that connects to the downstream auxillary node at ℓ
m : foundation node that connects to the upstream auxillary node at ℓ

Figure 9. Portions of dam, foundation and water meshes showing dam-foundation and dam-water connectivity.

O. Reservoir boundary definition. The reservoir boundary needs to be defined since it accelerates during an earthquake and generates dynamic water pressures. The reservoir boundary is divided into the dam-water interface and the remaining floor and sides of the reservoir. The user can omit the earthquake acceleration on a portion of the reservoir floor and sides by leaving that part out of the boundary definition; i.e., the element sides of the water mesh along that part are not included in the input. All element sides on the dam-water interface should be identified as such. If an element has more than one side on the reservoir boundary, then multiple entries for that element are needed. For reference, element sides are numbered from 1 to 8 as shown in Figure 10.

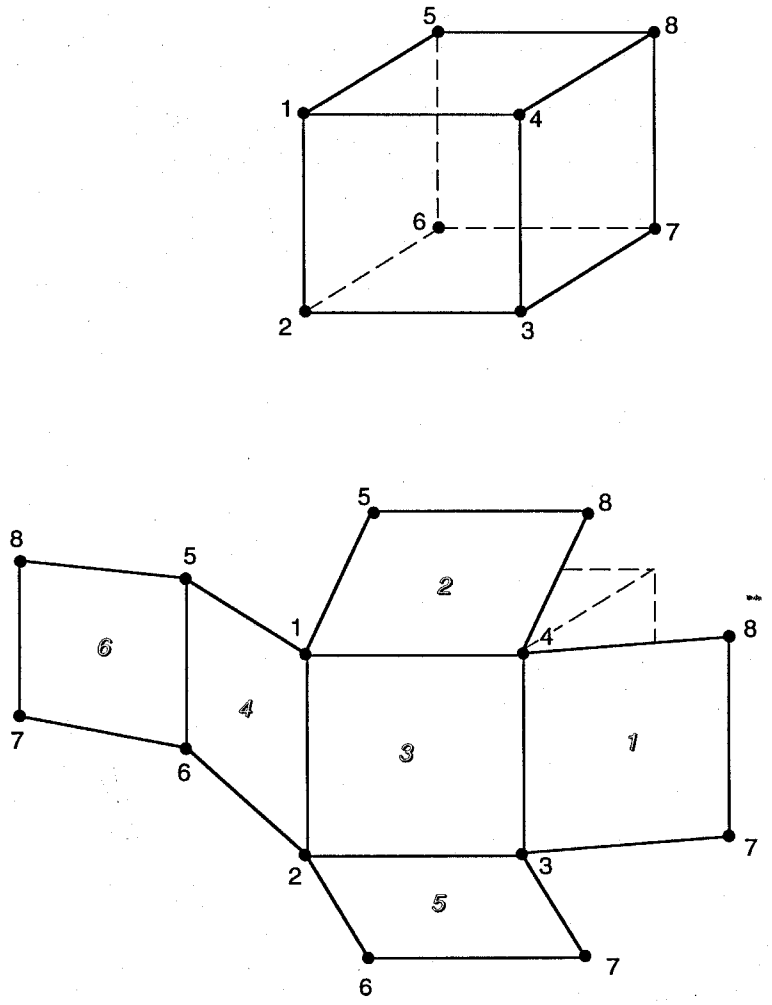

Figure 10. Node and side numbering for the water element.

P. Water and foundation mesh node numbering. The process of condensing out water and foundation degrees of freedom down to the set at nodes in contact with the dam expands the matrices and increases storage requirements. When the matrices are large, an effort may be necessary to reduce this effect. Toward this end, the nodes of the water and foundation meshes should be numbered, to the extent possible, to (1) make the bandwidth small, i.e., make the largest difference between the numbers of any two nodes connected by an element small, and (2) number the nodes not in contact with the dam before numbering those nodes in contact. A good node numbering scheme will be a compromise between these two criteria.

Q. Water element. The water element is an 8-node rectangular pressure element (Figure 10) that can be mapped into an arbitrary orientation and shape in x,y,z space, including the

superposition of two or more nodes. The LM array must list the eight water mesh node numbers in the order shown in Figure 10. Superimposed nodes have the same water mesh node number, and this number will appear multiply in LM. Element integration is by 2×2×2 Gauss quadrature.

R. Foundation element. The foundation element family consists of an 8 to 20-node rectangular solid element and a 6 to 15-node triangular version, as shown in Figure 11. Any of the mid-edge nodes 9 through 20 for the rectangular element and 7 through 15 for the triangular element can be omitted. The elements can be mapped into arbitrary orientation and shape in x,y,z space, including the superposition of two or more corner nodes after omitting the in-between mid-edge nodes. The LM array must list the foundation mesh node numbers in the order shown with zeros used to fill in spaces created by omitting mid-edge nodes. Superimposed corner nodes have the same foundation mesh node number, and this number will appear multiply in LM. Generated LM arrays only increment the nonzero terms; zeros remain zero.

Recommended integration schemes are NINTG = 1 or 2 for a linear element and NINTG = 2 or 3 for a quadratic element. For the rectangular solid, NINTG = 1 is 1-point Gauss quadrature; NINTG = 2 is 2×2×2 Gauss quadrature, and NINTG = 3 is 3×3×3 Gauss quadrature. For the triangular solid, integration schemes of similar order are used.

S. Numerical damping. The Bossak parameter α_B provides numerical dissipation to high-frequency spurious components of the solution. This can be quantified through an equivalent viscous damping $\overline{\xi}$ (as a fraction of critical) for a single-degree-of-freedom oscillator which turns out to be a function of the ratio of the time step Δt to the oscillator period T_n (Figure 12). A value $\alpha_B = -0.2$ is reasonable for many applications.

T. Damping. The constants a_0 and a_1 are mass and stiffness-proportional damping coefficients, respectively, used to provide damping to the dam-foundation system. Values can be selected according to linear theory from specified amounts of damping ξ_i, expressed as a fraction of critical, at two control frequencies ω_i (rad/sec) to satisfy

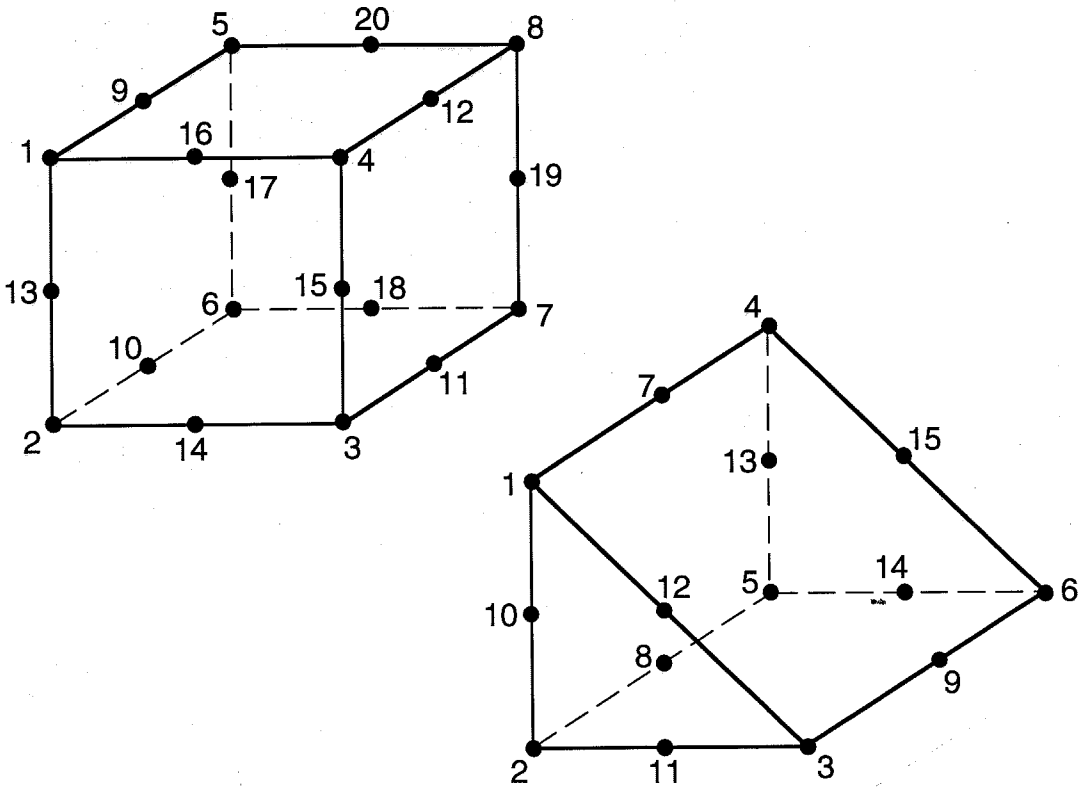

Figure 11. Node numbering for foundation elements: rectangular solid and triangular solid.

$$\xi_i = \frac{a_0}{2\omega_i} + \frac{a_1\omega_i}{2} \tag{23}$$

written for each of the two ξ_i, ω_i pairs. For mass-proportional damping only ($a_1 = 0$) or stiffness-proportional damping only ($a_0 = 0$), one equation for one ξ_i, ω_i pair suffices. Same data on selection of damping is presented in Chapter 5.

U. Foundation matrix. If the foundation mesh is large and to be used in a series of analyses without change, the computations can be reduced by saving $[\overline{K}]$ on Unit 25 during the first run (NFOUND = 2) and then reading it without recomputation from Unit 25 during subsequent runs (NFOUND = 3). The foundation mesh input on Unit 4 should still be present for a run in which NFOUND = 3.

V. Free surface of water. The same water mesh can be used to represent water bodies of different depth by changing the fixity conditions as described in Note K. Nothing else in the

water mesh input should be altered; however, SELEV in the static analysis should be reset accordingly.

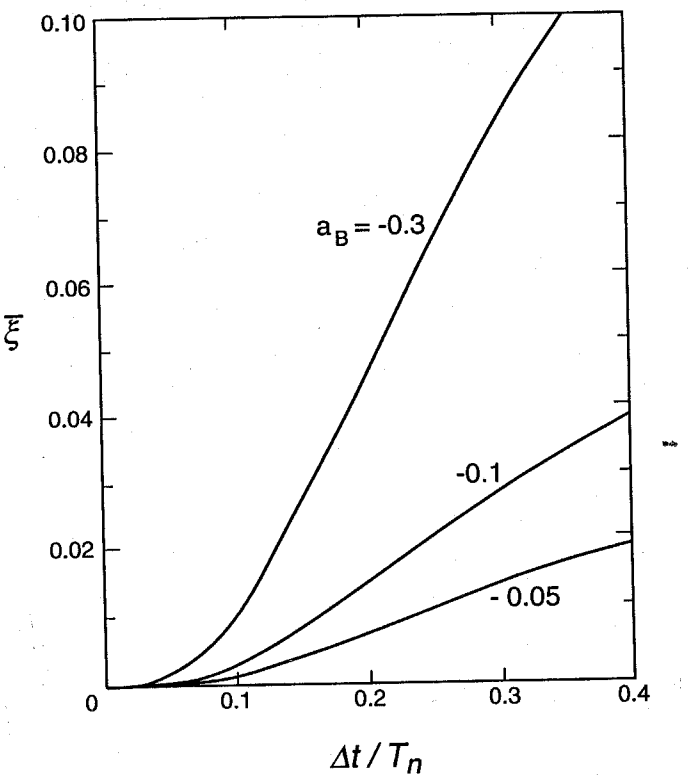

Figure 12. Algorithmic damping ratio $\bar{\xi}$ plotted against Δt / T_n for α_B = –0.30, –0.10 and –0.05, where T_n is the period of a single-degree-of-freedom oscillator (5).

3.3 Description of Output

An echo of the input data as well as results associated with constructing the meshes and setting up the problem are written to Unit 7 in ASCII. The echoed input data is designated by an "I" in column 2 of the output. The array A storage actually used in the static and dynamic analysis is printed. Should the dimension of array A be insufficient to run the problem, then the amount of storage required to complete the next task is printed. For the dam, water and foundation meshes, the volume of each element is printed as this information can sometimes be useful for detecting errors in nodal coordinates and in element nodal arrays. An example output file for Unit 7 appears in the next chapter for a sample problem.

A log file is written to Unit * in ASCII and contains convergence information for each load and time step. Printed are the number of iterations to convergence (NITER) and the maximum force residual $F^{\ell}_{\max}$ (FMAX) and moment residual $M^{\ell}_{\max}$ (ZMAX) remaining from the final iteration. When convergence does not occur within NITMAX iterations and automatic step division takes place, then this information is printed for each fractional step in which convergence is obtained or for the minimum fractional steps if the step division is unable to produce convergence. The minimum fractional step is 1/64 of the original step. The parameter NPOS, with an integer value from 1 to 64, indicates how much of the original step has been completed, with NPOS = 64 indicating completion. The convergence information on the log file is discussed further in the next chapter for the sample problem.

Unit 3 receives the response "pictures" (ASCII) which consist of tables of displacements and water pressure at every node, stresses in every element on the upstream and downstream faces of the dam (at the mapped locations $\xi = \eta = 0$, $\zeta = \pm 1$), and opening and sliding displacements in every element at the same locations. Response pictures are output at the end of the static analysis and at time steps IDPIC(I): I=1, NPIC during the dynamic analysis. Also, at the end of the dynamic analysis, pictures of the maximum and minimum values for the stresses and for the opening and sliding displacements are printed. For a restarted run in which a dynamic analysis is being continued, the maximum and minimum pictures from the previous run are overwritten with new pictures at time steps designated in IDPIC, and updated maximum and minimum pictures are printed at the end of the restarted dynamic analysis.

In the output on Unit 3, the stresses are referred to as follows:

SIG1 = σ_{11}
SIG2 = σ_{22}
TAU12 = τ_{12}
TAU23 = τ_{23}
TAU13 = τ_{13}.

The opening and sliding displacements are

OD1 = $\varepsilon_1^{op} \cdot H_1$ = opening displacement of contraction joint
OD2 = $\varepsilon_2^{op} \cdot H_2$ = opening displacement of crack
SD12 = $(\gamma_{12} - \tau_{12} / G) \cdot (H_1 + H_2) / 2$ = sliding displacement

corresponding to shear component 12 (in-plane sliding)

SD23 = $(\gamma_{23} - \tau_{23} / G') \cdot H_2$ = sliding displacement corresponding to shear component 23 (crack sliding)

SD13 = $(\gamma_{13} - \tau_{13} / G') \cdot H_1$ = sliding displacement corresponding to shear component 13 (contraction-joint sliding).

Like the stresses, the opening and sliding displacements are computed for each element at the upstream and downstream faces of the dam. H_1 and H_2 above are the element width (arch direction) and height (cantilever direction), respectively. The strains $\varepsilon_1^{op} \cdots \gamma_{13}$ and stresses τ_{12}, τ_{23}, τ_{13} above are from the integration points at $\xi = \eta = 0$, $\zeta = \pm 1$. Strains ε_{11}^{op} and ε_{22}^{op} are distances to the sector diagrams, similar to what is shown in Figures 4b, c and d for the Δ strains. An example output file from Unit 3 appears in the next chapter.

The time histories of NHIST quantities as defined through NODEL and NQ are written to Unit 2 as a binary file. The output statement is

WRITE(2) N, (TH(I), I=1, NHIST)

where TH contains the values of the time history quantities at the end of time step N. The output occurs at the end of the static analysis (N=0) and after every IOINT time steps during the dynamic analysis.

All values output on Units 2 and 3 during the dynamic analysis are total; that is, they include both the static and dynamic contributions. The displacements are relative to a ground reference moving at the free-field motions.

4. SAMPLE PROBLEM

The sample problem is a symmetric arch dam-water-foundation system subjected to static loads and ground motions in the upstream and vertical directions. For this symmetric analysis, half meshes of the dam, water and foundation are employed (Figure 13). Figures 14 through 16 show sketches of the meshes with the nodes and elements numbered. The meshes are coarse because the sample problem is meant only to document the input and output files. Listings are included here of four files in the following order: Unit 4, Unit 7, Unit 3 and the log file. Omitted are the ground acceleration data on Units 20, 21 and 22 and the output file on Unit 2. The problem is defined using feet, pounds and seconds.

The dam is 180 feet high with a cylindrical upstream face of radius 300 feet. The arch to one side of the plane of symmetry spans an angle of 30° at the crest and 10° at the base. Thickness of the dam varies linearly with height from 10 feet at the crest to 40 feet at the base. The dam is modeled with joints present, without any keying action in the joints and cracks, and with internal water pressure included by Option 1. Damping in the dam-foundation system is stiffness-proportional only to give $\xi = 3\%$ at a frequency of 4 Hz.

In the static analysis, the dam is constructed in three load steps followed by three load steps to fill the reservoir. Dynamic analysis consists of 1000 time steps at $\Delta t = 0.005$ seconds and uses ground acceleration data spaced at 0.01 seconds. No ground accelerations are applied to the upstream end of the reservoir. Desired output includes a response picture at time step 800 on Unit 3 and 23 time history quantities on Unit 2. A restart file is to be written at time steps 500 and 1000.

Following are listings of four files: the input file on Unit 4, output files on Units 7 and 3, and the log file.

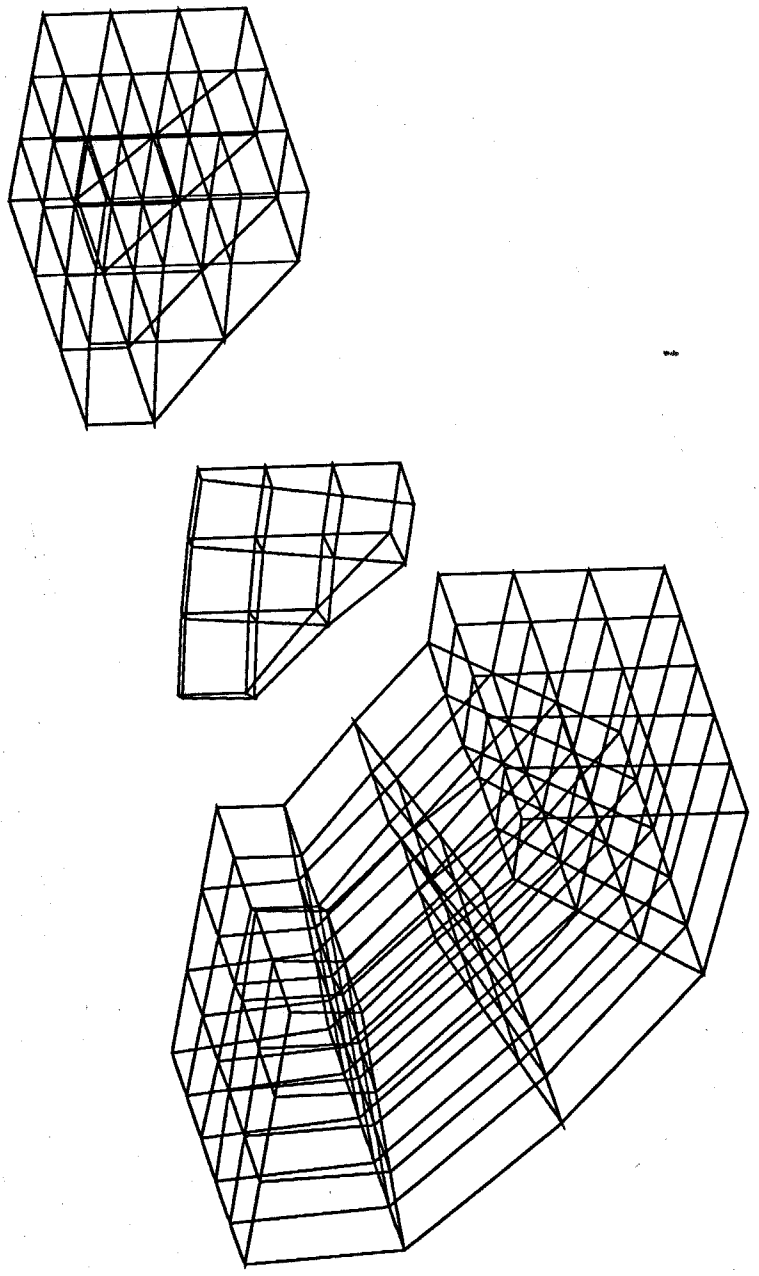

Figure 13. Foundation, dam and water half-meshes for the sample problem.

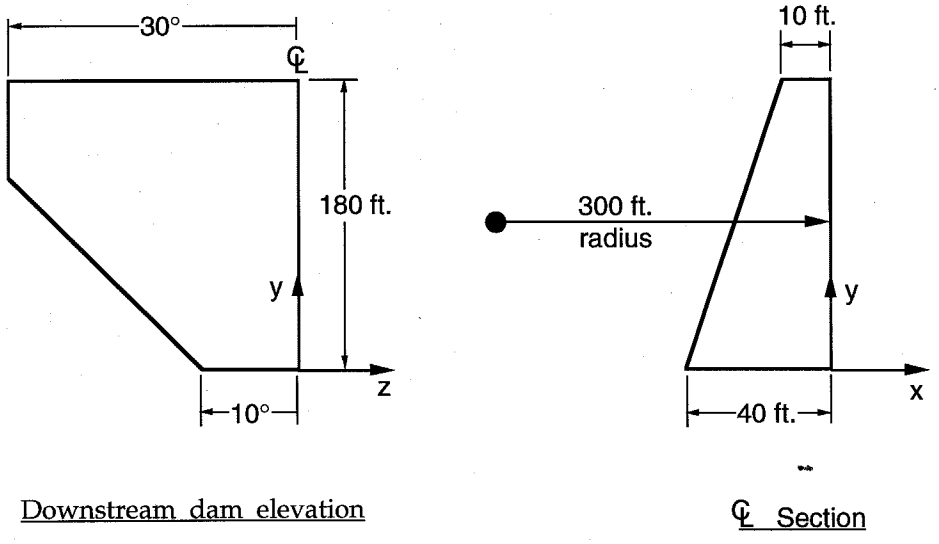

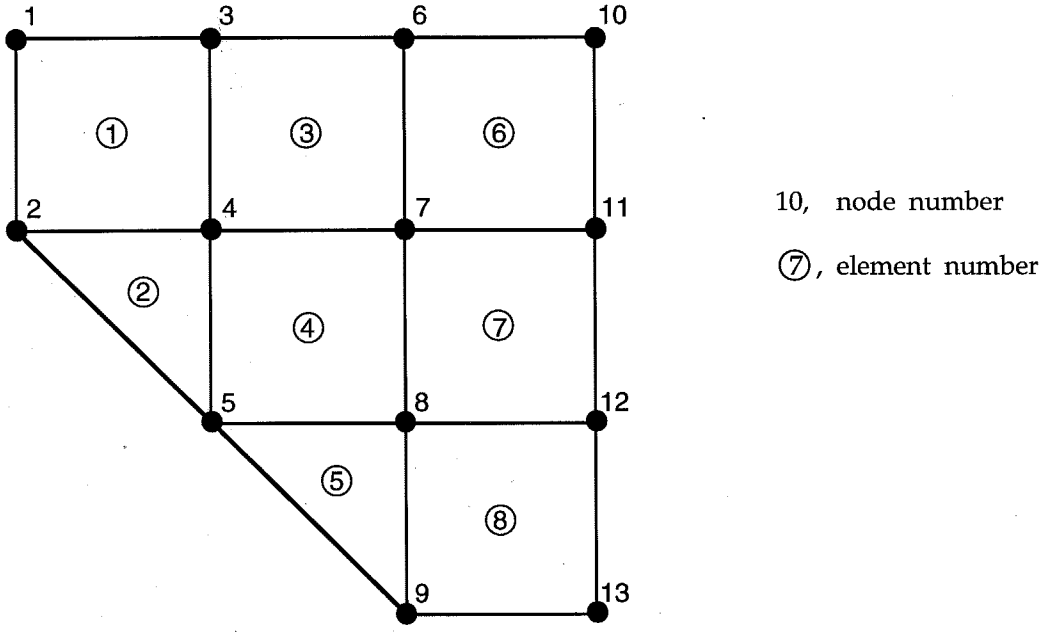

Figure 14. Sketch of dam mesh for sample problem showing dimensions and node and element numbering. Nodes shown are mid-surface nodes.

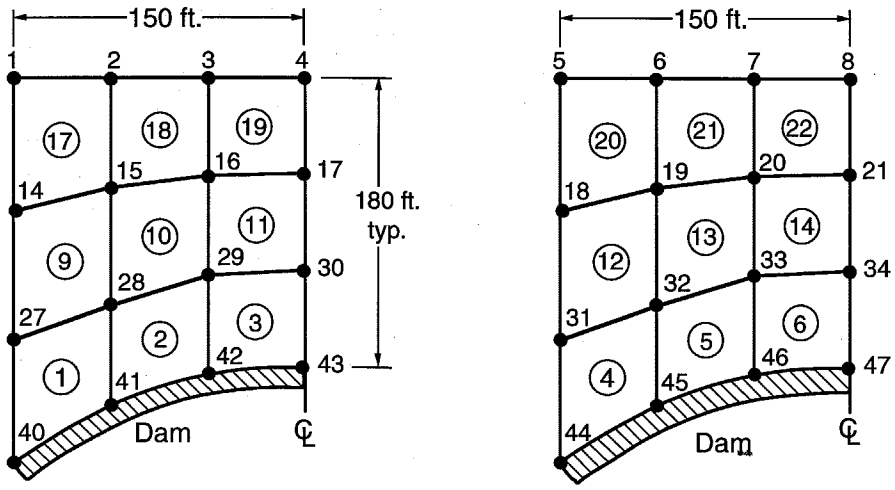

Plan at y = 180 ft.

Plan at y = 120 ft.

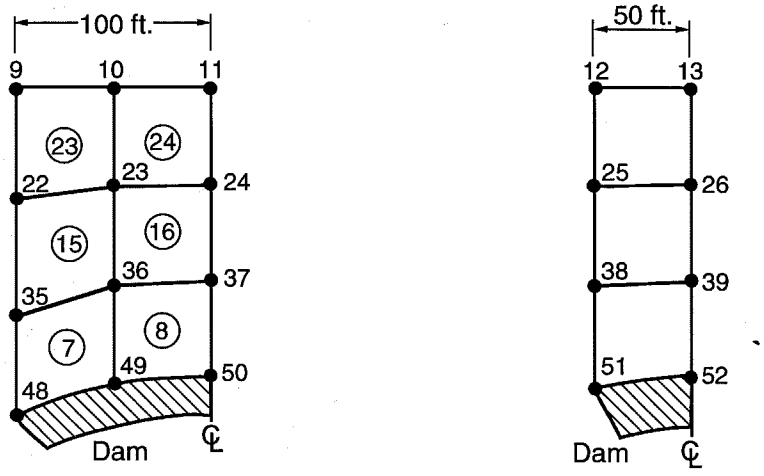

Plan at y = 60 ft.

Plan at y = 0 ft.

Figure 15. Sketch of water mesh for sample problem showing dimensions and node and element numbering. Example: element 5 connects nodes 32, 33, 45, 46 at y = 120 feet and nodes 35, 36, 48, 49 at y = 60 feet.

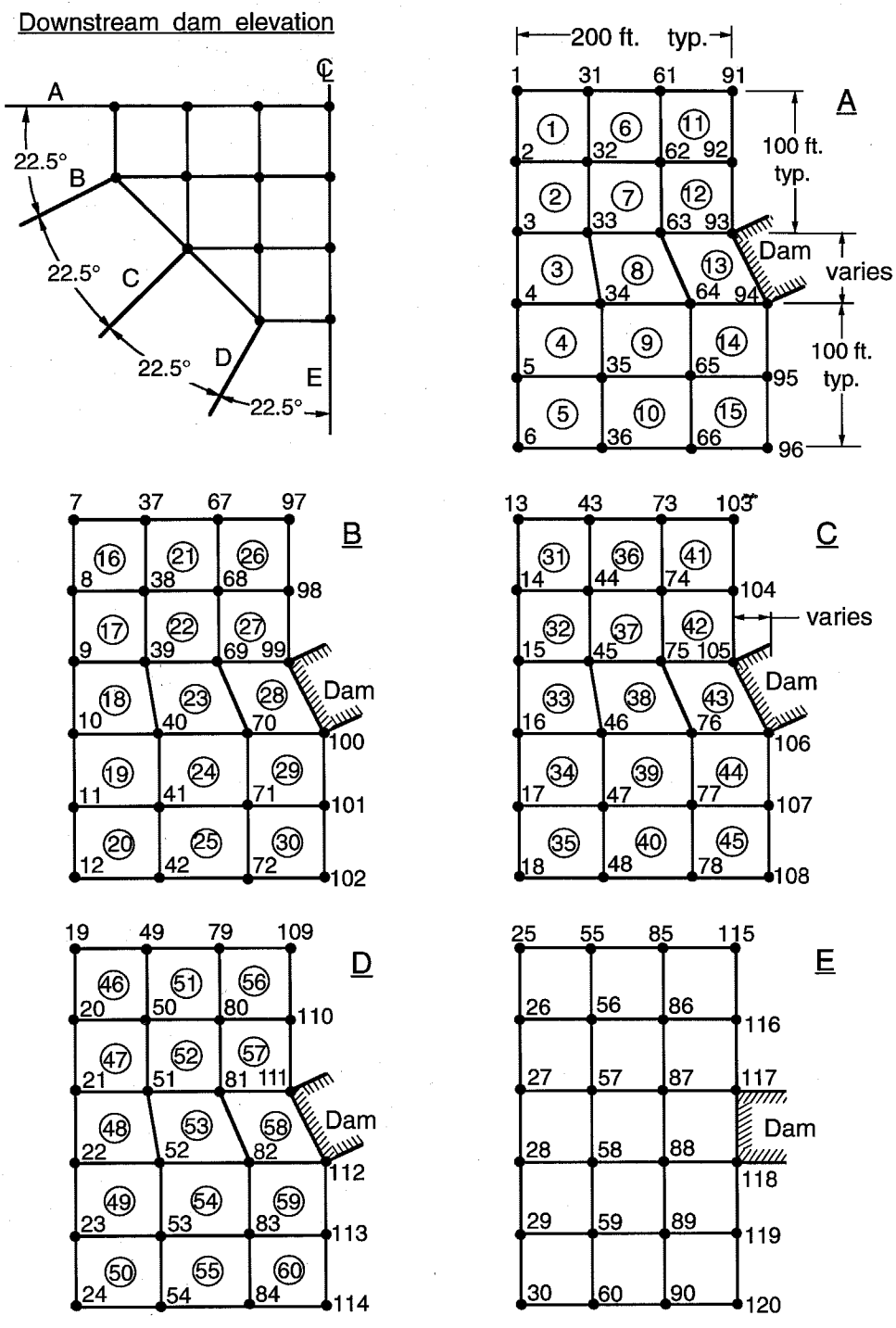

Figure 16. Sketch of foundation mesh for sample problem showing dimensions and node and element numbering. Example: element 44 connects nodes 76, 77, 106, 107 on plane C and nodes 82, 83, 112, 113 on plane D.

Input File on Unit 4

This file has been augmented with numbers in parentheses in the right margin that correspond to the numbered input groups in Section 3.2. This information is provided for reference only and would not be needed in the actual input file.

```
   SAMPLE PROBLEM                                                                  | ( 1)

 6 1000  100                                                                       | ( 2)

.0  .1  .0  .01                                                                    | ( 3)

 0 500  10                                                                         | ( 4)

 1   1   0   0   0   1                                                            | ( 5)

 62.4  32.2  0.0  0.0  0.0  .50  .50  0.25  0.1  4.D2  2.D3                        | ( 6)

13   8   1                                                                        | ( 7)

       1.      1.      1.                                                        | ( 8)

 1   2   1   0  259.81  180.00  -150.00  259.81  120.00  -150.00                 | ( 9)
                251.15  180.00  -145.00  242.49  120.00  -140.00                 | ( 9)
 3   5   1   0  281.91  180.00  -102.61  281.91   60.00  -102.61                 | ( 9)
                272.51  180.00   -99.19  253.72   60.00   -92.35                 | ( 9)
 6   9   1   0  295.44  180.00   -52.09  295.44    0.00   -52.09                 | ( 9)
                285.59  180.00   -50.36  256.05    0.00   -45.15                 | ( 9)
10  13   1   0  300.00  180.00     0.00  300.00    0.00     0.00                 | ( 9)
                290.00  180.00     0.00  260.00    0.00     0.00                 | ( 9)

 1   0   0   1   1   1   1   1   0                                               | (10)
 3   0   0   1   1   1   1   1   0                                               | (10)
 6   0   0   1   1   1   1   1   0                                               | (10)
10   0   0   1   1   0   1   0   0                                               | (10)
11  13   1   1   1   0   1   0   1                                               | (10)
 0   0   0   0   0   0   0   0   0                                               | (10)

4.32E+08  0.2  150.0   6.422E+04    1                                           | (11)

 1   0   0   1   50.  60.   3   4   2   1   0                                   | (12)
 2   0   0   1   50.  60.   4   5   5   2   0                                   | (12)
 3   4   1   1   50.  60.   6   7   4   3   1                                   | (12)
 5   0   0   1   50.  60.   8   9   9   5   0                                   | (12)
 6   8   1   1   50.  60.  10  11   7   6   1                                   | (12)

52  24  13  12   8                                                             | (13)

       1.      1.      1.                                                        | (14)

40   1  -13   0  259.81  180.00  -150.00  480.00  180.00  -150.00              | (15)
41   2  -13   0  281.91  180.00  -102.61  480.00  180.00  -100.00              | (15)
42   3  -13   0  295.44  180.00   -52.09  480.00  180.00   -50.00              | (15)
43   4  -13   0  300.00  180.00     0.00  480.00  180.00     0.00              | (15)
44   5  -13   0  259.81  120.00  -150.00  480.00  120.00  -150.00              | (15)
45   6  -13   0  281.91  120.00  -102.61  480.00  120.00  -100.00              | (15)
46   7  -13   0  295.44  120.00   -52.09  480.00  120.00   -50.00              | (15)
47   8  -13   0  300.00  120.00     0.00  480.00  120.00     0.00              | (15)
48   9  -13   0  281.91   60.00  -102.61  480.00   60.00  -100.00              | (15)
49  10  -13   0  295.44   60.00   -52.09  480.00   60.00   -50.00              | (15)
50  11  -13   0  300.00   60.00     0.00  480.00   60.00     0.00              | (15)
51  12  -13   0  295.44    0.00   -52.09  480.00    0.00   -50.00              | (15)
```

```
 52  13  -13    0  300.00     0.00      0.00  480.00     0.00      0.00       | (15)

  1  27   13    0                                                            | (16)
  2  28   13    0                                                            | (16)
  3  29   13    0                                                            | (16)
  4  30   13    0                                                            | (16)
  0   0    0    0                                                            | (16)

  1  17    8   27   40   41   28   31   44   45   32  -13                    | (17)
  2  18    8   28   41   42   29   32   45   46   33  -13                    | (17)
  3  19    8   29   42   43   30   33   46   47   34  -13                    | (17)
  4  20    8   31   44   45   32   35   48   48   35  -13                    | (17)
  5  21    8   32   45   46   33   35   48   49   36  -13                    | (17)
  6  22    8   33   46   47   34   36   49   50   37  -13                    | (17)
  7  23    8   35   48   49   36   38   51   51   38  -13                    | (17)
  8  24    8   36   49   50   37   38   51   52   39  -13                    | (17)

 40   1                                                                      | (18)
 41   3                                                                      | (18)
 42   6                                                                      | (18)
 43  10                                                                      | (18)
 44   2                                                                      | (18)
 45   4                                                                      | (18)
 46   7                                                                      | (18)
 47  11                                                                      | (18)
 48   5                                                                      | (18)
 49   8                                                                      | (18)
 50  12                                                                      | (18)
 51   9                                                                      | (18)
 52  13                                                                      | (18)

  1  17    8    4                                                           | (19)
  4  20    8    4                                                           | (19)
  7  23    8    4                                                           | (19)
  8  24    8    6                                                           | (19)

  1   8    1    5                                                           | (20)

120  60    1    5    2                                                      | (21)

    1.      1.     1.                                                       | (22)

 91   1  -30    0  359.81  180.00  -150.00  359.81  180.00  -350.00        | (23)
 92   2  -30    0  309.81  180.00  -150.00  318.08  180.00  -350.00        | (23)
 93   3  -30    0  259.81  180.00  -150.00  276.35  180.00  -350.00        | (23)
 94   4  -30    0  251.15  180.00  -145.00  234.61  180.00  -350.00        | (23)
 95   5  -30    0  201.15  180.00  -145.00  192.88  180.00  -350.00        | (23)
 96   6  -30    0  151.15  180.00  -145.00  151.15  180.00  -350.00        | (23)
 97   7  -30    0  359.81  120.00  -150.00  359.81   43.46  -334.78        | (23)
 98   8  -30    0  309.81  120.00  -150.00  316.35   43.46  -334.78        | (23)
 99   9  -30    0  259.81  120.00  -150.00  272.88   43.46  -334.78        | (23)
100  10  -30    0  242.49  120.00  -140.00  229.42   43.46  -334.78        | (23)
101  11  -30    0  192.49  120.00  -140.00  185.95   43.46  -334.78        | (23)
102  12  -30    0  142.49  120.00  -140.00  142.49   43.46  -334.78        | (23)
103  13  -30    0  381.91   60.00  -102.61  381.91  -81.42  -244.03        | (23)
104  14  -30    0  331.91   60.00  -102.61  336.27  -81.42  -244.03        | (23)
```

```
105  15  -30   0  281.91   60.00  -102.61  290.63   -81.42  -244.03     | (23)
106  16  -30   0  253.72   60.00   -92.35  245.90   -81.42  -244.03     | (23)
107  17  -30   0  203.72   60.00   -92.35  199.36   -81.42  -244.03     | (23)
108  18  -30   0  153.72   60.00   -92.35  153.72   -81.42  -244.03     | (23)
109  19  -30   0  395.44    0.00   -52.09  395.44  -184.78  -128.63     | (23)
110  20  -30   0  345.44    0.00   -52.09  347.56  -184.78  -128.63     | (23)
111  21  -30   0  295.44    0.00   -52.09  299.69  -184.78  -128.63     | (23)
112  22  -30   0  256.05    0.00   -45.15  251.81  -184.78  -128.63     | (23)
113  23  -30   0  206.05    0.00   -45.15  203.93  -184.78  -128.63     | (23)
114  24  -30   0  156.05    0.00   -45.15  156.05  -184.78  -128.63     | (23)
115  25  -30   0  400.00    0.00     0.00  400.00  -200.00     0.00     | (23)
116  26  -30   0  350.00    0.00     0.00  352.00  -200.00     0.00     | (23)
117  27  -30   0  300.00    0.00     0.00  304.00  -200.00     0.00     | (23)
118  28  -30   0  260.00    0.00     0.00  256.00  -200.00     0.00     | (23)
119  29  -30   0  210.00    0.00     0.00  208.00  -200.00     0.00     | (23)
120  30  -30   0  160.00    0.00     0.00  160.00  -200.00     0.00     | (23)

  1  30   1   0   0   0                                                | (24)
 55  60   1   1   1   0                                                | (24)
 85  90   1   1   1   0                                                | (24)
115 116   1   1   1   0                                                | (24)
119 120   1   1   1   0                                                | (24)
  0   0   0   0   0   0                                                | (24)

 4.32E+08   0.25                                                       | (25)

 1  5 1 1  20  1  2  32  31   7   8  38  37 0 0 0 0 0 0 0 0 0 0 0 0  1  | (26)
 6 10 1 1  20 31 32  62  61  37  38  68  67 0 0 0 0 0 0 0 0 0 0 0 0  1  | (26)
11 15 1 1  20 61 62  92  91  67  68  98  97 0 0 0 0 0 0 0 0 0 0 0 0  1  | (26)
16 20 1 1  20  7  8  38  37  13  14  44  43 0 0 0 0 0 0 0 0 0 0 0 0  1  | (26)
21 25 1 1  20 37 38  68  67  43  44  74  73 0 0 0 0 0 0 0 0 0 0 0 0  1  | (26)
26 30 1 1  20 67 68  98  97  73  74 104 103 0 0 0 0 0 0 0 0 0 0 0 0  1  | (26)
31 35 1 1  20 13 14  44  43  19  20  50  49 0 0 0 0 0 0 0 0 0 0 0 0  1  | (26)
36 40 1 1  20 43 44  74  73  49  50  80  79 0 0 0 0 0 0 0 0 0 0 0 0  1  | (26)
41 45 1 1  20 73 74 104 103  79  80 110 109 0 0 0 0 0 0 0 0 0 0 0 0  1  | (26)
46 50 1 1  20 19 20  50  49  25  26  56  55 0 0 0 0 0 0 0 0 0 0 0 0  1  | (26)
51 55 1 1  20 49 50  80  79  55  56  86  85 0 0 0 0 0 0 0 0 0 0 0 0  1  | (26)
56 60 1 1  20 79 80 110 109  85  86 116 115 0 0 0 0 0 0 0 0 0 0 0 0  1  | (26)

 93  94   1                                                           | (27)
 99 100   2                                                           | (27)
105 106   5                                                           | (27)
111 112   9                                                           | (27)
117 118  13                                                           | (27)

  1   0                                                               | (28)
  5   8   3                                                           | (29)
  0   0   0                                                           | (29)
  1   0                                                               | (28)
  2   0   0                                                           | (29)
  4   7   3                                                           | (29)
  0   0   0                                                           | (29)
  1   0                                                               | (28)
  1   0   0                                                           | (29)
  3   6   3                                                           | (29)
  0   0   0                                                           | (29)
```

```
  3    0                                                          | (28)
    60.                                                          | (31)
  3    0                                                          | (28)
   120.                                                          | (31)
  3    0                                                          | (28)
   180.                                                          | (31)

 .005  2   .05   .5                                              | (33)

  -0.2    0.70    0.36    0.0    0.00239                         | (34)

  1  23                                                          | (35)

800                                                              | (36)

 10   1                                                          | (37)
 10   2                                                          | (37)
  6   6                                                          | (37)
  6   7                                                          | (37)
  6   8                                                          | (37)
  6   9                                                          | (37)
  6  10                                                          | (37)
  6  11                                                          | (37)
  6  12                                                          | (37)
  6  13                                                          | (37)
  6  14                                                          | (37)
  6  15                                                          | (37)
  6  16                                                          | (37)
  6  17                                                          | (37)
  6  18                                                          | (37)
  6  19                                                          | (37)
  6  20                                                          | (37)
  6  21                                                          | (37)
  6  22                                                          | (37)
  6  23                                                          | (37)
  6  24                                                          | (37)
  6  25                                                          | (37)
 11  26                                                          | (37)

  24.74   24.74    0.00                                           | (38)
```

Output File on Unit 7

Output accompanied by an 'I' in the left margin is an echo of the input data. Other output pertains to tasks performed during problem setup as described in Section 3.3.

```
I              SAMPLE PROBLEM


    DIMENSION OF ARRAY A IS SET TO 1200000


         PROGRAM PARAMETERS
I   NSSTPS =    6
I   NDSTPS =  1000
I   NITMAX =  100
I   SMINS =  0.0000E+00
I   SMAXS =  0.1000E+00
I   SMIND =  0.0000E+00
I   SMAXD =  0.1000E-01
I   IRES =    0
I   IRINT =  500
I   IOINT =  10
I   NWATER =    1
I   NFOUND =    1
I   IKEY(1) =  0   IKEY(2) =  0   IKEY(3) =  0
I   IPRES =  1
I   WW =  0.6240E+02
I   G =  0.3220E+02
I   ALP1 =  0.0000E+00   ALP2 =  0.0000E+00
I   SFT =  0.0000E+00
I   COEF(1) =  0.5000E+00   COEF(2) =  0.5000E+00
I   ALPS =  0.2500E+00
I   TRF =  0.1000E+00
I   FTOL =  0.4000E+03
I   ZTOL =  0.2000E+04


    ******************************** DAM COMPUTATIONS ********************************


         DAM MESH PARAMETERS
I   NPD =   13
I   NELD =    8
I   NMATD =  1


         MULTIPLIERS FOR NODAL COORDINATES
I   CXMULT =  0.1000E+01   CYMULT =  0.1000E+01   CZMULT =  0.1000E+01


         NODAL COORDINATE DATA (AUXILLARY NODES)
I       N  NE  NG  NRC        CXUN        CYUN        CZUN        CXUNE       CYUNE       CZUNE
I                             CXDN        CYDN        CZDN        CXDNE       CYDNE       CZDNE
I       1   2   1   0    0.2598E+03  0.1800E+03 -0.1500E+03    0.2598E+03  0.1200E+03 -0.1500E+03
```

I					0.2512E+03	0.1800E+03	-0.1450E+03	0.2425E+03	0.1200E+03	-0.1400E+03
I	3	5	1	0	0.2819E+03	0.1800E+03	-0.1026E+03	0.2819E+03	0.6000E+02	-0.1026E+03
I					0.2725E+03	0.1800E+03	-0.9919E+02	0.2537E+03	0.6000E+02	-0.9235E+02
I	6	9	1	0	0.2954E+03	0.1800E+03	-0.5209E+02	0.2954E+03	0.0000E+00	-0.5209E+02
I					0.2856E+03	0.1800E+03	-0.5036E+02	0.2561E+03	0.0000E+00	-0.4515E+02
I	10	13	1	0	0.3000E+03	0.1800E+03	0.0000E+00	0.3000E+03	0.0000E+00	0.0000E+00
I					0.2900E+03	0.1800E+03	0.0000E+00	0.2600E+03	0.0000E+00	0.0000E+00

NODAL FIXITY DATA

I	N	NE	NG	ID(I),I=1,6					
I	1	0	0	1	1	1	1	1	0
I	3	0	0	1	1	1	1	1	0
I	6	0	0	1	1	1	1	1	0
I	10	0	0	1	1	0	1	0	0
I	11	13	1	1	1	0	1	0	1

AUXILLARY NODAL COORDINATES (AS SCALED) AND FIXITY CONDITIONS

NODE	LOC	XCOOR	YCOOR	ZCOOR	IDU	IDV	IDW	IDT	IDG	IDP
1	UPSF	0.2598E+03	0.1800E+03	-0.1500E+03	1	1	1	1	1	0
	DNSF	0.2512E+03	0.1800E+03	-0.1450E+03						
2	UPSF	0.2598E+03	0.1200E+03	-0.1500E+03	1	1	1	1	1	1
	DNSF	0.2425E+03	0.1200E+03	-0.1400E+03						
3	UPSF	0.2819E+03	0.1800E+03	-0.1026E+03	1	1	1	1	1	0
	DNSF	0.2725E+03	0.1800E+03	-0.9919E+02						
4	UPSF	0.2819E+03	0.1200E+03	-0.1026E+03	1	1	1	1	1	1
	DNSF	0.2631E+03	0.1200E+03	-0.9577E+02						
5	UPSF	0.2819E+03	0.6000E+02	-0.1026E+03	1	1	1	1	1	1
	DNSF	0.2537E+03	0.6000E+02	-0.9235E+02						
6	UPSF	0.2954E+03	0.1800E+03	-0.5209E+02	1	1	1	1	1	0
	DNSF	0.2856E+03	0.1800E+03	-0.5036E+02						
7	UPSF	0.2954E+03	0.1200E+03	-0.5209E+02	1	1	1	1	1	1
	DNSF	0.2757E+03	0.1200E+03	-0.4862E+02						
8	UPSF	0.2954E+03	0.6000E+02	-0.5209E+02	1	1	1	1	1	1
	DNSF	0.2659E+03	0.6000E+02	-0.4689E+02						
9	UPSF	0.2954E+03	0.0000E+00	-0.5209E+02	1	1	1	1	1	1
	DNSF	0.2561E+03	0.0000E+00	-0.4515E+02						
10	UPSF	0.3000E+03	0.1800E+03	0.0000E+00	1	1	0	1	0	0
	DNSF	0.2900E+03	0.1800E+03	0.0000E+00						
11	UPSF	0.3000E+03	0.1200E+03	0.0000E+00	1	1	0	1	0	1
	DNSF	0.2800E+03	0.1200E+03	0.0000E+00						
12	UPSF	0.3000E+03	0.6000E+02	0.0000E+00	1	1	0	1	0	1
	DNSF	0.2700E+03	0.6000E+02	0.0000E+00						
13	UPSF	0.3000E+03	0.0000E+00	0.0000E+00	1	1	0	1	0	1
	DNSF	0.2600E+03	0.0000E+00	0.0000E+00						

TOTAL NUMBER OF EQUATIONS IN DAM MESH = 66

MATERIAL PROPERTY DATA

I	(SET)	EE	PR	WT	TEN	IJON
I	(1)	0.4320E+09	0.2000E+00	0.1500E+03	0.6422E+05	1

ELEMENT MATERIAL SET, DIMENSION AND NODAL VECTOR DATA

I	N	NE	NG	MAT	H1	H2	LM(I),I=1,4				LMG
I	1	0	0	1	0.5000E+02	0.6000E+02	3	4	2	1	0
I	2	0	0	1	0.5000E+02	0.6000E+02	4	5	5	2	0
I	3	4	1	1	0.5000E+02	0.6000E+02	6	7	4	3	1
I	5	0	0	1	0.5000E+02	0.6000E+02	8	9	9	5	0
I	6	8	1	1	0.5000E+02	0.6000E+02	10	11	7	6	1

ELENENT MATERIAL SET NUMBERS, DIMENSIONS AND NODAL VECTORS

ELEM	SET	H1	H2	NODE NUMBERS			
1	1	0.5000E+02	0.6000E+02	3	4	2	1
2	1	0.5000E+02	0.6000E+02	4	5	5	2
3	1	0.5000E+02	0.6000E+02	6	7	4	3
4	1	0.5000E+02	0.6000E+02	7	8	5	4
5	1	0.5000E+02	0.6000E+02	8	9	9	5
6	1	0.5000E+02	0.6000E+02	10	11	7	6
7	1	0.5000E+02	0.6000E+02	11	12	8	7
8	1	0.5000E+02	0.6000E+02	12	13	9	8

ELEMENT VOLUMES

ELEMENT NUMBER 1 VOLUME = 0.4568E+05
ELEMENT NUMBER 2 VOLUME = 0.3588E+05
ELEMENT NUMBER 3 VOLUME = 0.4569E+05
ELEMENT NUMBER 4 VOLUME = 0.7486E+05
ELEMENT NUMBER 5 VOLUME = 0.5011E+05
ELEMENT NUMBER 6 VOLUME = 0.4568E+05
ELEMENT NUMBER 7 VOLUME = 0.7485E+05
ELEMENT NUMBER 8 VOLUME = 0.1030E+06

********** WATER COMPUTATIONS **********

WATER MESH PARAMETERS

I NPW = 52
I NELW = 24
I NPDW = 13
I NSWR = 12
I NSWD = 8

MULTIPLIERS FOR NODAL COORDINATES

I CXMULT = 0.1000E+01 CYMULT = 0.1000E+01 CZMULT = 0.1000E+01

NODAL COORDINATE DATA

I	N	NE	NG	NRC	CXN	CYN	CZN	CXNE	CYNE	CZNE
I	40	1	-13	0	0.2598E+03	0.1800E+03	-0.1500E+03	0.4800E+03	0.1800E+03	-0.1500E+03
I	41	2	-13	0	0.2819E+03	0.1800E+03	-0.1026E+03	0.4800E+03	0.1800E+03	-0.1000E+03
I	42	3	-13	0	0.2954E+03	0.1800E+03	-0.5209E+02	0.4800E+03	0.1800E+03	-0.5000E+02
I	43	4	-13	0	0.3000E+03	0.1800E+03	0.0000E+00	0.4800E+03	0.1800E+03	0.0000E+00
I	44	5	-13	0	0.2598E+03	0.1200E+03	-0.1500E+03	0.4800E+03	0.1200E+03	-0.1500E+03
I	45	6	-13	0	0.2819E+03	0.1200E+03	-0.1026E+03	0.4800E+03	0.1200E+03	-0.1000E+03

```
I   46   7 -13   0    0.2954E+03  0.1200E+03 -0.5209E+02   0.4800E+03  0.1200E+03 -0.5000E+02
I   47   8 -13   0    0.3000E+03  0.1200E+03  0.0000E+00   0.4800E+03  0.1200E+03  0.0000E+00
I   48   9 -13   0    0.2819E+03  0.6000E+02 -0.1026E+03   0.4800E+03  0.6000E+02 -0.1000E+03
I   49  10 -13   0    0.2954E+03  0.6000E+02 -0.5209E+02   0.4800E+03  0.6000E+02 -0.5000E+02
I   50  11 -13   0    0.3000E+03  0.6000E+02  0.0000E+00   0.4800E+03  0.6000E+02  0.0000E+00
I   51  12 -13   0    0.2954E+03  0.0000E+00 -0.5209E+02   0.4800E+03  0.0000E+00 -0.5000E+02
I   52  13 -13   0    0.3000E+03  0.0000E+00  0.0000E+00   0.4800E+03  0.0000E+00  0.0000E+00

      NODAL FIXITY DATA
I   N  NE  NG    ID
I   1  27  13     0
I   2  28  13     0
I   3  29  13     0
I   4  30  13     0

      NODAL COORDINATES (AS SCALED) AND FIXITY CONDITIONS
  NODE       XCOOR       YCOOR       ZCOOR   IDP
     1  0.4800E+03  0.1800E+03 -0.1500E+03     0
     2  0.4800E+03  0.1800E+03 -0.1000E+03     0
     3  0.4800E+03  0.1800E+03 -0.5000E+02     0
     4  0.4800E+03  0.1800E+03  0.0000E+00     0
     5  0.4800E+03  0.1200E+03 -0.1500E+03     1
     6  0.4800E+03  0.1200E+03 -0.1000E+03     1
     7  0.4800E+03  0.1200E+03 -0.5000E+02     1
     8  0.4800E+03  0.1200E+03  0.0000E+00     1
     9  0.4800E+03  0.6000E+02 -0.1000E+03     1
    10  0.4800E+03  0.6000E+02 -0.5000E+02     1
    11  0.4800E+03  0.6000E+02  0.0000E+00     1
    12  0.4800E+03  0.0000E+00 -0.5000E+02     1
    13  0.4800E+03  0.0000E+00  0.0000E+00     1
    14  0.4066E+03  0.1800E+03 -0.1500E+03     0
    15  0.4140E+03  0.1800E+03 -0.1009E+03     0
    16  0.4185E+03  0.1800E+03 -0.5070E+02     0
    17  0.4200E+03  0.1800E+03  0.0000E+00     0
    18  0.4066E+03  0.1200E+03 -0.1500E+03     1
    19  0.4140E+03  0.1200E+03 -0.1009E+03     1
    20  0.4185E+03  0.1200E+03 -0.5070E+02     1
    21  0.4200E+03  0.1200E+03  0.0000E+00     1
    22  0.4140E+03  0.6000E+02 -0.1009E+03     1
    23  0.4185E+03  0.6000E+02 -0.5070E+02     1
    24  0.4200E+03  0.6000E+02  0.0000E+00     1
    25  0.4185E+03  0.0000E+00 -0.5070E+02     1
    26  0.4200E+03  0.0000E+00  0.0000E+00     1
    27  0.3332E+03  0.1800E+03 -0.1500E+03     0
    28  0.3479E+03  0.1800E+03 -0.1017E+03     0
    29  0.3570E+03  0.1800E+03 -0.5139E+02     0
    30  0.3600E+03  0.1800E+03  0.0000E+00     0
    31  0.3332E+03  0.1200E+03 -0.1500E+03     1
    32  0.3479E+03  0.1200E+03 -0.1017E+03     1
    33  0.3570E+03  0.1200E+03 -0.5139E+02     1
    34  0.3600E+03  0.1200E+03  0.0000E+00     1
    35  0.3479E+03  0.6000E+02 -0.1017E+03     1
    36  0.3570E+03  0.6000E+02 -0.5139E+02     1
    37  0.3600E+03  0.6000E+02  0.0000E+00     1
```

38	0.3570E+03	0.0000E+00	-0.5139E+02	1
39	0.3600E+03	0.0000E+00	0.0000E+00	1
40	0.2598E+03	0.1800E+03	-0.1500E+03	1
41	0.2819E+03	0.1800E+03	-0.1026E+03	1
42	0.2954E+03	0.1800E+03	-0.5209E+02	1
43	0.3000E+03	0.1800E+03	0.0000E+00	1
44	0.2598E+03	0.1200E+03	-0.1500E+03	1
45	0.2819E+03	0.1200E+03	-0.1026E+03	1
46	0.2954E+03	0.1200E+03	-0.5209E+02	1
47	0.3000E+03	0.1200E+03	0.0000E+00	1
48	0.2819E+03	0.6000E+02	-0.1026E+03	1
49	0.2954E+03	0.6000E+02	-0.5209E+02	1
50	0.3000E+03	0.6000E+02	0.0000E+00	1
51	0.2954E+03	0.0000E+00	-0.5209E+02	1
52	0.3000E+03	0.0000E+00	0.0000E+00	1

TOTAL NUMBER OF EQUATIONS IN WATER MESH = 40

ELEMENT NODAL VECTOR DATA

I	N	NE	NG	LM(I),I=1,8								LMG
I	1	17	8	27	40	41	28	31	44	45	32	-13
I	2	18	8	28	41	42	29	32	45	46	33	-13
I	3	19	8	29	42	43	30	33	46	47	34	-13
I	4	20	8	31	44	45	32	35	48	48	35	-13
I	5	21	8	32	45	46	33	35	48	49	36	-13
I	6	22	8	33	46	47	34	36	49	50	37	-13
I	7	23	8	35	48	49	36	38	51	51	38	-13
I	8	24	8	36	49	50	37	38	51	52	39	-13

ELENENT NODAL VECTORS

ELEM	NODE NUMBERS							
1	27	40	41	28	31	44	45	32
2	28	41	42	29	32	45	46	33
3	29	42	43	30	33	46	47	34
4	31	44	45	32	35	48	48	35
5	32	45	46	33	35	48	49	36
6	33	46	47	34	36	49	50	37
7	35	48	49	36	38	51	51	38
8	36	49	50	37	38	51	52	39
9	14	27	28	15	18	31	32	19
10	15	28	29	16	19	32	33	20
11	16	29	30	17	20	33	34	21
12	18	31	32	19	22	35	35	22
13	19	32	33	20	22	35	36	23
14	20	33	34	21	23	36	37	24
15	22	35	36	23	25	38	38	25
16	23	36	37	24	25	38	39	26
17	1	14	15	2	5	18	19	6
18	2	15	16	3	6	19	20	7
19	3	16	17	4	7	20	21	8
20	5	18	19	6	9	22	22	9
21	6	19	20	7	9	22	23	10
22	7	20	21	8	10	23	24	11

23	9	22	23	10	12	25	25	12
24	10	23	24	11	12	25	26	13

DAM AND WATER NODAL CONNECTIVITY

I	NODEW	NODED
I	40	1
I	41	3
I	42	6
I	43	10
I	44	2
I	45	4
I	46	7
I	47	11
I	48	5
I	49	8
I	50	12
I	51	9
I	52	13

ELEMENT AND SIDE DATA FOR RESERVOIR FLOOR AND SIDES

I	N	NE	NG	ISIDE
I	1	17	8	4
I	4	20	8	4
I	7	23	8	4
I	8	24	8	6

ELEMENTS AND SIDE NODAL VECTORS ON RESERVOIR FLOOR AND SIDES

ELEM	NODE NUMBERS			
1	31	44	40	27
9	18	31	27	14
17	5	18	14	1
4	35	48	44	31
12	22	35	31	18
20	9	22	18	5
7	38	51	48	35
15	25	38	35	22
23	12	25	22	9
8	39	52	51	38
16	26	39	38	25
24	13	26	25	12

ELEMENT AND SIDE DATA FOR DAM-WATER INTERFACE

I	N	NE	NG	ISIDE
I	1	8	1	5

ELEMENTS AND SIDE NODAL VECTORS ON DAM-WATER INTERFACE

ELEM	NODE NUMBERS			
1	45	41	40	44
2	46	42	41	45
3	47	43	42	46
4	48	45	44	48

```
        5      49    46    45    48
        6      50    47    46    49
        7      51    49    48    51
        8      52    50    49    51


             ELEMENT VOLUMES
      ELEMENT NUMBER     1      VOLUME = 0.1996E+06
      ELEMENT NUMBER     2      VOLUME = 0.1925E+06
      ELEMENT NUMBER     3      VOLUME = 0.1886E+06
      ELEMENT NUMBER     4      VOLUME = 0.9794E+05
      ELEMENT NUMBER     5      VOLUME = 0.1925E+06
      ELEMENT NUMBER     6      VOLUME = 0.1886E+06
      ELEMENT NUMBER     7      VOLUME = 0.9510E+05
      ELEMENT NUMBER     8      VOLUME = 0.1886E+06
      ELEMENT NUMBER     9      VOLUME = 0.2034E+06
      ELEMENT NUMBER    10      VOLUME = 0.1920E+06
      ELEMENT NUMBER    11      VOLUME = 0.1860E+06
      ELEMENT NUMBER    12      VOLUME = 0.9985E+05
      ELEMENT NUMBER    13      VOLUME = 0.1920E+06
      ELEMENT NUMBER    14      VOLUME = 0.1860E+06
      ELEMENT NUMBER    15      VOLUME = 0.9487E+05
      ELEMENT NUMBER    16      VOLUME = 0.1860E+06
      ELEMENT NUMBER    17      VOLUME = 0.2072E+06
      ELEMENT NUMBER    18      VOLUME = 0.1916E+06
      ELEMENT NUMBER    19      VOLUME = 0.1835E+06
      ELEMENT NUMBER    20      VOLUME = 0.1018E+06
      ELEMENT NUMBER    21      VOLUME = 0.1916E+06
      ELEMENT NUMBER    22      VOLUME = 0.1835E+06
      ELEMENT NUMBER    23      VOLUME = 0.9465E+05
      ELEMENT NUMBER    24      VOLUME = 0.1835E+06


      ***************************** FOUNDATION COMPUTATIONS ******************************


             FOUNDATION MESH PARAMETERS
I     NPG =  120
I     NELG =   60
I     NMATG =  1
I     NPDG =    5
I     NINTG =  2


             MULTIPLIERS FOR NODAL COORDINATES
I     CXMULT =  0.1000E+01   CYMULT =  0.1000E+01   CZMULT =  0.1000E+01


             NODAL COORDINATE DATA
I       N   NE  NG  NRC        CXN         CYN         CZN         CXNE        CYNE        CZNE
I      91    1 -30   0    0.3598E+03  0.1800E+03 -0.1500E+03    0.3598E+03  0.1800E+03 -0.3500E+03
I      92    2 -30   0    0.3098E+03  0.1800E+03 -0.1500E+03    0.3181E+03  0.1800E+03 -0.3500E+03
I      93    3 -30   0    0.2598E+03  0.1800E+03 -0.1500E+03    0.2764E+03  0.1800E+03 -0.3500E+03
I      94    4 -30   0    0.2512E+03  0.1800E+03 -0.1450E+03    0.2346E+03  0.1800E+03 -0.3500E+03
I      95    5 -30   0    0.2012E+03  0.1800E+03 -0.1450E+03    0.1929E+03  0.1800E+03 -0.3500E+03
```

```
I    96    6 -30    0    0.1512E+03  0.1800E+03 -0.1450E+03  0.1512E+03  0.1800E+03 -0.3500E+03
I    97    7 -30    0    0.3598E+03  0.1200E+03 -0.1500E+03  0.3598E+03  0.4346E+02 -0.3348E+03
I    98    8 -30    0    0.3098E+03  0.1200E+03 -0.1500E+03  0.3164E+03  0.4346E+02 -0.3348E+03
I    99    9 -30    0    0.2598E+03  0.1200E+03 -0.1500E+03  0.2729E+03  0.4346E+02 -0.3348E+03
I   100   10 -30    0    0.2425E+03  0.1200E+03 -0.1400E+03  0.2294E+03  0.4346E+02 -0.3348E+03
I   101   11 -30    0    0.1925E+03  0.1200E+03 -0.1400E+03  0.1859E+03  0.4346E+02 -0.3348E+03
I   102   12 -30    0    0.1425E+03  0.1200E+03 -0.1400E+03  0.1425E+03  0.4346E+02 -0.3348E+03
I   103   13 -30    0    0.3819E+03  0.6000E+02 -0.1026E+03  0.3819E+03 -0.8142E+02 -0.2440E+03
I   104   14 -30    0    0.3319E+03  0.6000E+02 -0.1026E+03  0.3363E+03 -0.8142E+02 -0.2440E+03
I   105   15 -30    0    0.2819E+03  0.6000E+02 -0.1026E+03  0.2906E+03 -0.8142E+02 -0.2440E+03
I   106   16 -30    0    0.2537E+03  0.6000E+02 -0.9235E+02  0.2459E+03 -0.8142E+02 -0.2440E+03
I   107   17 -30    0    0.2037E+03  0.6000E+02 -0.9235E+02  0.1994E+03 -0.8142E+02 -0.2440E+03
I   108   18 -30    0    0.1537E+03  0.6000E+02 -0.9235E+02  0.1537E+03 -0.8142E+02 -0.2440E+03
I   109   19 -30    0    0.3954E+03  0.0000E+00 -0.5209E+02  0.3954E+03 -0.1848E+03 -0.1286E+03
I   110   20 -30    0    0.3454E+03  0.0000E+00 -0.5209E+02  0.3476E+03 -0.1848E+03 -0.1286E+03
I   111   21 -30    0    0.2954E+03  0.0000E+00 -0.5209E+02  0.2997E+03 -0.1848E+03 -0.1286E+03
I   112   22 -30    0    0.2561E+03  0.0000E+00 -0.4515E+02  0.2518E+03 -0.1848E+03 -0.1286E+03
I   113   23 -30    0    0.2061E+03  0.0000E+00 -0.4515E+02  0.2039E+03 -0.1848E+03 -0.1286E+03
I   114   24 -30    0    0.1561E+03  0.0000E+00 -0.4515E+02  0.1561E+03 -0.1848E+03 -0.1286E+03
I   115   25 -30    0    0.4000E+03  0.0000E+00  0.0000E+00  0.4000E+03 -0.2000E+03  0.0000E+00
I   116   26 -30    0    0.3500E+03  0.0000E+00  0.0000E+00  0.3520E+03 -0.2000E+03  0.0000E+00
I   117   27 -30    0    0.3000E+03  0.0000E+00  0.0000E+00  0.3040E+03 -0.2000E+03  0.0000E+00
I   118   28 -30    0    0.2600E+03  0.0000E+00  0.0000E+00  0.2560E+03 -0.2000E+03  0.0000E+00
I   119   29 -30    0    0.2100E+03  0.0000E+00  0.0000E+00  0.2080E+03 -0.2000E+03  0.0000E+00
I   120   30 -30    0    0.1600E+03  0.0000E+00  0.0000E+00  0.1600E+03 -0.2000E+03  0.0000E+00

      NODAL FIXITY DATA
I     N  NE  NG    ID(I),I=1,3
I     1  30   1    0   0   0
I    55  60   1    1   1   0
I    85  90   1    1   1   0
I   115 116   1    1   1   0
I   119 120   1    1   1   0

      NODAL COORDINATES (AS SCALED) AND FIXITY CONDITIONS
NODE       XCOOR       YCOOR       ZCOOR     IDU IDV IDW
   1  0.3598E+03  0.1800E+03 -0.3500E+03    0   0   0
   2  0.3181E+03  0.1800E+03 -0.3500E+03    0   0   0
   3  0.2764E+03  0.1800E+03 -0.3500E+03    0   0   0
   4  0.2346E+03  0.1800E+03 -0.3500E+03    0   0   0
   5  0.1929E+03  0.1800E+03 -0.3500E+03    0   0   0
   6  0.1512E+03  0.1800E+03 -0.3500E+03    0   0   0
   7  0.3598E+03  0.4346E+02 -0.3348E+03    0   0   0
   8  0.3164E+03  0.4346E+02 -0.3348E+03    0   0   0
   9  0.2729E+03  0.4346E+02 -0.3348E+03    0   0   0
  10  0.2294E+03  0.4346E+02 -0.3348E+03    0   0   0
  11  0.1859E+03  0.4346E+02 -0.3348E+03    0   0   0
  12  0.1425E+03  0.4346E+02 -0.3348E+03    0   0   0
  13  0.3819E+03 -0.8142E+02 -0.2440E+03    0   0   0
  14  0.3363E+03 -0.8142E+02 -0.2440E+03    0   0   0
  15  0.2906E+03 -0.8142E+02 -0.2440E+03    0   0   0
  16  0.2459E+03 -0.8142E+02 -0.2440E+03    0   0   0
  17  0.1994E+03 -0.8142E+02 -0.2440E+03    0   0   0
  18  0.1537E+03 -0.8142E+02 -0.2440E+03    0   0   0
```

19	0.3954E+03	-0.1848E+03	-0.1286E+03	0	0	0
20	0.3476E+03	-0.1848E+03	-0.1286E+03	0	0	0
21	0.2997E+03	-0.1848E+03	-0.1286E+03	0	0	0
22	0.2518E+03	-0.1848E+03	-0.1286E+03	0	0	0
23	0.2039E+03	-0.1848E+03	-0.1286E+03	0	0	0
24	0.1561E+03	-0.1848E+03	-0.1286E+03	0	0	0
25	0.4000E+03	-0.2000E+03	0.0000E+00	0	0	0
26	0.3520E+03	-0.2000E+03	0.0000E+00	0	0	0
27	0.3040E+03	-0.2000E+03	0.0000E+00	0	0	0
28	0.2560E+03	-0.2000E+03	0.0000E+00	0	0	0
29	0.2080E+03	-0.2000E+03	0.0000E+00	0	0	0
30	0.1600E+03	-0.2000E+03	0.0000E+00	0	0	0
31	0.3598E+03	0.1800E+03	-0.2833E+03	1	1	1
32	0.3153E+03	0.1800E+03	-0.2833E+03	1	1	1
33	0.2708E+03	0.1800E+03	-0.2833E+03	1	1	1
34	0.2401E+03	0.1800E+03	-0.2817E+03	1	1	1
35	0.1956E+03	0.1800E+03	-0.2817E+03	1	1	1
36	0.1512E+03	0.1800E+03	-0.2817E+03	1	1	1
37	0.3598E+03	0.6897E+02	-0.2732E+03	1	1	1
38	0.3142E+03	0.6897E+02	-0.2732E+03	1	1	1
39	0.2685E+03	0.6897E+02	-0.2732E+03	1	1	1
40	0.2338E+03	0.6897E+02	-0.2699E+03	1	1	1
41	0.1881E+03	0.6897E+02	-0.2699E+03	1	1	1
42	0.1425E+03	0.6897E+02	-0.2699E+03	1	1	1
43	0.3819E+03	-0.3428E+02	-0.1969E+03	1	1	1
44	0.3348E+03	-0.3428E+02	-0.1969E+03	1	1	1
45	0.2877E+03	-0.3428E+02	-0.1969E+03	1	1	1
46	0.2485E+03	-0.3428E+02	-0.1935E+03	1	1	1
47	0.2008E+03	-0.3428E+02	-0.1935E+03	1	1	1
48	0.1537E+03	-0.3428E+02	-0.1935E+03	1	1	1
49	0.3954E+03	-0.1232E+03	-0.1031E+03	1	1	1
50	0.3469E+03	-0.1232E+03	-0.1031E+03	1	1	1
51	0.2983E+03	-0.1232E+03	-0.1031E+03	1	1	1
52	0.2532E+03	-0.1232E+03	-0.1008E+03	1	1	1
53	0.2046E+03	-0.1232E+03	-0.1008E+03	1	1	1
54	0.1561E+03	-0.1232E+03	-0.1008E+03	1	1	1
55	0.4000E+03	-0.1333E+03	0.0000E+00	1	1	0
56	0.3513E+03	-0.1333E+03	0.0000E+00	1	1	0
57	0.3027E+03	-0.1333E+03	0.0000E+00	1	1	0
58	0.2573E+03	-0.1333E+03	0.0000E+00	1	1	0
59	0.2087E+03	-0.1333E+03	0.0000E+00	1	1	0
60	0.1600E+03	-0.1333E+03	0.0000E+00	1	1	0
61	0.3598E+03	0.1800E+03	-0.2167E+03	1	1	1
62	0.3126E+03	0.1800E+03	-0.2167E+03	1	1	1
63	0.2653E+03	0.1800E+03	-0.2167E+03	1	1	1
64	0.2456E+03	0.1800E+03	-0.2133E+03	1	1	1
65	0.1984E+03	0.1800E+03	-0.2133E+03	1	1	1
66	0.1512E+03	0.1800E+03	-0.2133E+03	1	1	1
67	0.3598E+03	0.9449E+02	-0.2116E+03	1	1	1
68	0.3120E+03	0.9449E+02	-0.2116E+03	1	1	1
69	0.2642E+03	0.9449E+02	-0.2116E+03	1	1	1
70	0.2381E+03	0.9449E+02	-0.2049E+03	1	1	1
71	0.1903E+03	0.9449E+02	-0.2049E+03	1	1	1
72	0.1425E+03	0.9449E+02	-0.2049E+03	1	1	1
73	0.3819E+03	0.1286E+02	-0.1498E+03	1	1	1
74	0.3334E+03	0.1286E+02	-0.1498E+03	1	1	1

75	0.2848E+03	0.1286E+02	-0.1498E+03	1	1	1
76	0.2511E+03	0.1286E+02	-0.1429E+03	1	1	1
77	0.2023E+03	0.1286E+02	-0.1429E+03	1	1	1
78	0.1537E+03	0.1286E+02	-0.1429E+03	1	1	1
79	0.3954E+03	-0.6159E+02	-0.7760E+02	1	1	1
80	0.3461E+03	-0.6159E+02	-0.7760E+02	1	1	1
81	0.2969E+03	-0.6159E+02	-0.7760E+02	1	1	1
82	0.2546E+03	-0.6159E+02	-0.7298E+02	1	1	1
83	0.2053E+03	-0.6159E+02	-0.7298E+02	1	1	1
84	0.1561E+03	-0.6159E+02	-0.7298E+02	1	1	1
85	0.4000E+03	-0.6667E+02	0.0000E+00	1	1	0
86	0.3507E+03	-0.6667E+02	0.0000E+00	1	1	0
87	0.3013E+03	-0.6667E+02	0.0000E+00	1	1	0
88	0.2587E+03	-0.6667E+02	0.0000E+00	1	1	0
89	0.2093E+03	-0.6667E+02	0.0000E+00	1	1	0
90	0.1600E+03	-0.6667E+02	0.0000E+00	1	1	0
91	0.3598E+03	0.1800E+03	-0.1500E+03	1	1	1
92	0.3098E+03	0.1800E+03	-0.1500E+03	1	1	1
93	0.2598E+03	0.1800E+03	-0.1500E+03	1	1	1
94	0.2512E+03	0.1800E+03	-0.1450E+03	1	1	1
95	0.2012E+03	0.1800E+03	-0.1450E+03	1	1	1
96	0.1512E+03	0.1800E+03	-0.1450E+03	1	1	1
97	0.3598E+03	0.1200E+03	-0.1500E+03	1	1	1
98	0.3098E+03	0.1200E+03	-0.1500E+03	1	1	1
99	0.2598E+03	0.1200E+03	-0.1500E+03	1	1	1
100	0.2425E+03	0.1200E+03	-0.1400E+03	1	1	1
101	0.1925E+03	0.1200E+03	-0.1400E+03	1	1	1
102	0.1425E+03	0.1200E+03	-0.1400E+03	1	1	1
103	0.3819E+03	0.6000E+02	-0.1026E+03	1	1	1
104	0.3319E+03	0.6000E+02	-0.1026E+03	1	1	1
105	0.2819E+03	0.6000E+02	-0.1026E+03	1	1	1
106	0.2537E+03	0.6000E+02	-0.9235E+02	1	1	1
107	0.2037E+03	0.6000E+02	-0.9235E+02	1	1	1
108	0.1537E+03	0.6000E+02	-0.9235E+02	1	1	1
109	0.3954E+03	0.0000E+00	-0.5209E+02	1	1	1
110	0.3454E+03	0.0000E+00	-0.5209E+02	1	1	1
111	0.2954E+03	0.0000E+00	-0.5209E+02	1	1	1
112	0.2561E+03	0.0000E+00	-0.4515E+02	1	1	1
113	0.2061E+03	0.0000E+00	-0.4515E+02	1	1	1
114	0.1561E+03	0.0000E+00	-0.4515E+02	1	1	1
115	0.4000E+03	0.0000E+00	0.0000E+00	1	1	0
116	0.3500E+03	0.0000E+00	0.0000E+00	1	1	0
117	0.3000E+03	0.0000E+00	0.0000E+00	1	1	1
118	0.2600E+03	0.0000E+00	0.0000E+00	1	1	1
119	0.2100E+03	0.0000E+00	0.0000E+00	1	1	0
120	0.1600E+03	0.0000E+00	0.0000E+00	1	1	0

TOTAL NUMBER OF EQUATIONS IN FOUNDATION MESH = 254

MATERIAL PROPERTY DATA

I	(SET)	EE	PR
I	(1)	0.4320E+09	0.2500E+00

ELEMENT MATERIAL SET AND NODAL VECTOR DATA

I	N	NE	NG	MAT	NENI	LM(I),I=1,NENI																		LMG
I	1	5	1	1	20	1	2	32	31	7	8	38	37	0	0	0	0	0	0	0	0	0	0	1
I	6	10	1	1	20	31	32	62	61	37	38	68	67	0	0	0	0	0	0	0	0	0	0	1
I	11	15	1	1	20	61	62	92	91	67	68	98	97	0	0	0	0	0	0	0	0	0	0	1
I	16	20	1	1	20	7	8	38	37	13	14	44	43	0	0	0	0	0	0	0	0	0	0	1
I	21	25	1	1	20	37	38	68	67	43	44	74	73	0	0	0	0	0	0	0	0	0	0	1
I	26	30	1	1	20	67	68	98	97	73	74	104	103	0	0	0	0	0	0	0	0	0	0	1
I	31	35	1	1	20	13	14	44	43	19	20	50	49	0	0	0	0	0	0	0	0	0	0	1
I	36	40	1	1	20	43	44	74	73	49	50	80	79	0	0	0	0	0	0	0	0	0	0	1
I	41	45	1	1	20	73	74	104	103	79	80	110	109	0	0	0	0	0	0	0	0	0	0	1
I	46	50	1	1	20	19	20	50	49	25	26	56	55	0	0	0	0	0	0	0	0	0	0	1
I	51	55	1	1	20	49	50	80	79	55	56	86	85	0	0	0	0	0	0	0	0	0	0	1
I	56	60	1	1	20	79	80	110	109	85	86	116	115	0	0	0	0	0	0	0	0	0	0	1

ELENENT MATERIAL SET NUMBERS AND NODAL VECTORS

ELEM	SET	NODE NUMBERS																			
1	1	1	2	32	31	7	8	38	37	0	0	0	0	0	0	0	0	0	0	0	0
2	1	2	3	33	32	8	9	39	38	0	0	0	0	0	0	0	0	0	0	0	0
3	1	3	4	34	33	9	10	40	39	0	0	0	0	0	0	0	0	0	0	0	0
4	1	4	5	35	34	10	11	41	40	0	0	0	0	0	0	0	0	0	0	0	0
5	1	5	6	36	35	11	12	42	41	0	0	0	0	0	0	0	0	0	0	0	0
6	1	31	32	62	61	37	38	68	67	0	0	0	0	0	0	0	0	0	0	0	0
7	1	32	33	63	62	38	39	69	68	0	0	0	0	0	0	0	0	0	0	0	0
8	1	33	34	64	63	39	40	70	69	0	0	0	0	0	0	0	0	0	0	0	0
9	1	34	35	65	64	40	41	71	70	0	0	0	0	0	0	0	0	0	0	0	0
10	1	35	36	66	65	41	42	72	71	0	0	0	0	0	0	0	0	0	0	0	0
11	1	61	62	92	91	67	68	98	97	0	0	0	0	0	0	0	0	0	0	0	0
12	1	62	63	93	92	68	69	99	98	0	0	0	0	0	0	0	0	0	0	0	0
13	1	63	64	94	93	69	70	100	99	0	0	0	0	0	0	0	0	0	0	0	0
14	1	64	65	95	94	70	71	101	100	0	0	0	0	0	0	0	0	0	0	0	0
15	1	65	66	96	95	71	72	102	101	0	0	0	0	0	0	0	0	0	0	0	0
16	1	7	8	38	37	13	14	44	43	0	0	0	0	0	0	0	0	0	0	0	0
17	1	8	9	39	38	14	15	45	44	0	0	0	0	0	0	0	0	0	0	0	0
18	1	9	10	40	39	15	16	46	45	0	0	0	0	0	0	0	0	0	0	0	0
19	1	10	11	41	40	16	17	47	46	0	0	0	0	0	0	0	0	0	0	0	0
20	1	11	12	42	41	17	18	48	47	0	0	0	0	0	0	0	0	0	0	0	0
21	1	37	38	68	67	43	44	74	73	0	0	0	0	0	0	0	0	0	0	0	0
22	1	38	39	69	68	44	45	75	74	0	0	0	0	0	0	0	0	0	0	0	0
23	1	39	40	70	69	45	46	76	75	0	0	0	0	0	0	0	0	0	0	0	0
24	1	40	41	71	70	46	47	77	76	0	0	0	0	0	0	0	0	0	0	0	0
25	1	41	42	72	71	47	48	78	77	0	0	0	0	0	0	0	0	0	0	0	0
26	1	67	68	98	97	73	74	104	103	0	0	0	0	0	0	0	0	0	0	0	0
27	1	68	69	99	98	74	75	105	104	0	0	0	0	0	0	0	0	0	0	0	0
28	1	69	70	100	99	75	76	106	105	0	0	0	0	0	0	0	0	0	0	0	0
29	1	70	71	101	100	76	77	107	106	0	0	0	0	0	0	0	0	0	0	0	0
30	1	71	72	102	101	77	78	108	107	0	0	0	0	0	0	0	0	0	0	0	0
31	1	13	14	44	43	19	20	50	49	0	0	0	0	0	0	0	0	0	0	0	0
32	1	14	15	45	44	20	21	51	50	0	0	0	0	0	0	0	0	0	0	0	0
33	1	15	16	46	45	21	22	52	51	0	0	0	0	0	0	0	0	0	0	0	0
34	1	16	17	47	46	22	23	53	52	0	0	0	0	0	0	0	0	0	0	0	0
35	1	17	18	48	47	23	24	54	53	0	0	0	0	0	0	0	0	0	0	0	0
36	1	43	44	74	73	49	50	80	79	0	0	0	0	0	0	0	0	0	0	0	0
37	1	44	45	75	74	50	51	81	80	0	0	0	0	0	0	0	0	0	0	0	0
38	1	45	46	76	75	51	52	82	81	0	0	0	0	0	0	0	0	0	0	0	0

```
 39   1   46   47   77   76   52   53   83   82    0    0    0    0    0    0    0    0    0    0    0    0    0    0
 40   1   47   48   78   77   53   54   84   83    0    0    0    0    0    0    0    0    0    0    0    0    0    0
 41   1   73   74  104  103   79   80  110  109    0    0    0    0    0    0    0    0    0    0    0    0    0    0
 42   1   74   75  105  104   80   81  111  110    0    0    0    0    0    0    0    0    0    0    0    0    0    0
 43   1   75   76  106  105   81   82  112  111    0    0    0    0    0    0    0    0    0    0    0    0    0    0
 44   1   76   77  107  106   82   83  113  112    0    0    0    0    0    0    0    0    0    0    0    0    0    0
 45   1   77   78  108  107   83   84  114  113    0    0    0    0    0    0    0    0    0    0    0    0    0    0
 46   1   19   20   50   49   25   26   56   55    0    0    0    0    0    0    0    0    0    0    0    0    0    0
 47   1   20   21   51   50   26   27   57   56    0    0    0    0    0    0    0    0    0    0    0    0    0    0
 48   1   21   22   52   51   27   28   58   57    0    0    0    0    0    0    0    0    0    0    0    0    0    0
 49   1   22   23   53   52   28   29   59   58    0    0    0    0    0    0    0    0    0    0    0    0    0    0
 50   1   23   24   54   53   29   30   60   59    0    0    0    0    0    0    0    0    0    0    0    0    0    0
 51   1   49   50   80   79   55   56   86   85    0    0    0    0    0    0    0    0    0    0    0    0    0    0
 52   1   50   51   81   80   56   57   87   86    0    0    0    0    0    0    0    0    0    0    0    0    0    0
 53   1   51   52   82   81   57   58   88   87    0    0    0    0    0    0    0    0    0    0    0    0    0    0
 54   1   52   53   83   82   58   59   89   88    0    0    0    0    0    0    0    0    0    0    0    0    0    0
 55   1   53   54   84   83   59   60   90   89    0    0    0    0    0    0    0    0    0    0    0    0    0    0
 56   1   79   80  110  109   85   86  116  115    0    0    0    0    0    0    0    0    0    0    0    0    0    0
 57   1   80   81  111  110   86   87  117  116    0    0    0    0    0    0    0    0    0    0    0    0    0    0
 58   1   81   82  112  111   87   88  118  117    0    0    0    0    0    0    0    0    0    0    0    0    0    0
 59   1   82   83  113  112   88   89  119  118    0    0    0    0    0    0    0    0    0    0    0    0    0    0
 60   1   83   84  114  113   89   90  120  119    0    0    0    0    0    0    0    0    0    0    0    0    0    0

     DAM AND FOUNDATION NODAL CONNECTIVITY
I  NODEGU  NODEGD  NODED
I     93     94      1
I     99    100      2
I    105    106      5
I    111    112      9
I    117    118     13

     ELEMENT VOLUMES
 ELEMENT NUMBER    1   VOLUME = 0.3546E+06
 ELEMENT NUMBER    2   VOLUME = 0.3547E+06
 ELEMENT NUMBER    3   VOLUME = 0.3124E+06
 ELEMENT NUMBER    4   VOLUME = 0.3687E+06
 ELEMENT NUMBER    5   VOLUME = 0.3687E+06
 ELEMENT NUMBER    6   VOLUME = 0.2959E+06
 ELEMENT NUMBER    7   VOLUME = 0.2959E+06
 ELEMENT NUMBER    8   VOLUME = 0.1828E+06
 ELEMENT NUMBER    9   VOLUME = 0.3088E+06
 ELEMENT NUMBER   10   VOLUME = 0.3088E+06
 ELEMENT NUMBER   11   VOLUME = 0.2288E+06
 ELEMENT NUMBER   12   VOLUME = 0.2288E+06
 ELEMENT NUMBER   13   VOLUME = 0.8724E+05
 ELEMENT NUMBER   14   VOLUME = 0.2402E+06
 ELEMENT NUMBER   15   VOLUME = 0.2402E+06
 ELEMENT NUMBER   16   VOLUME = 0.4196E+06
 ELEMENT NUMBER   17   VOLUME = 0.4196E+06
 ELEMENT NUMBER   18   VOLUME = 0.3843E+06
 ELEMENT NUMBER   19   VOLUME = 0.4409E+06
 ELEMENT NUMBER   20   VOLUME = 0.4372E+06
 ELEMENT NUMBER   21   VOLUME = 0.3560E+06
 ELEMENT NUMBER   22   VOLUME = 0.3560E+06
```

```
 ELEMENT NUMBER   23     VOLUME = 0.2613E+06
 ELEMENT NUMBER   24     VOLUME = 0.3727E+06
 ELEMENT NUMBER   25     VOLUME = 0.3709E+06
 ELEMENT NUMBER   26     VOLUME = 0.2861E+06
 ELEMENT NUMBER   27     VOLUME = 0.2861E+06
 ELEMENT NUMBER   28     VOLUME = 0.1630E+06
 ELEMENT NUMBER   29     VOLUME = 0.2987E+06
 ELEMENT NUMBER   30     VOLUME = 0.2983E+06
 ELEMENT NUMBER   31     VOLUME = 0.4339E+06
 ELEMENT NUMBER   32     VOLUME = 0.4339E+06
 ELEMENT NUMBER   33     VOLUME = 0.4122E+06
 ELEMENT NUMBER   34     VOLUME = 0.4491E+06
 ELEMENT NUMBER   35     VOLUME = 0.4455E+06
 ELEMENT NUMBER   36     VOLUME = 0.3616E+06
 ELEMENT NUMBER   37     VOLUME = 0.3615E+06
 ELEMENT NUMBER   38     VOLUME = 0.3043E+06
 ELEMENT NUMBER   39     VOLUME = 0.3703E+06
 ELEMENT NUMBER   40     VOLUME = 0.3685E+06
 ELEMENT NUMBER   41     VOLUME = 0.2855E+06
 ELEMENT NUMBER   42     VOLUME = 0.2855E+06
 ELEMENT NUMBER   43     VOLUME = 0.2111E+06
 ELEMENT NUMBER   44     VOLUME = 0.2881E+06
 ELEMENT NUMBER   45     VOLUME = 0.2876E+06
 ELEMENT NUMBER   46     VOLUME = 0.3665E+06
 ELEMENT NUMBER   47     VOLUME = 0.3665E+06
 ELEMENT NUMBER   48     VOLUME = 0.3527E+06
 ELEMENT NUMBER   49     VOLUME = 0.3636E+06
 ELEMENT NUMBER   50     VOLUME = 0.3636E+06
 ELEMENT NUMBER   51     VOLUME = 0.2884E+06
 ELEMENT NUMBER   52     VOLUME = 0.2884E+06
 ELEMENT NUMBER   53     VOLUME = 0.2544E+06
 ELEMENT NUMBER   54     VOLUME = 0.2780E+06
 ELEMENT NUMBER   55     VOLUME = 0.2780E+06
 ELEMENT NUMBER   56     VOLUME = 0.2080E+06
 ELEMENT NUMBER   57     VOLUME = 0.2080E+06
 ELEMENT NUMBER   58     VOLUME = 0.1658E+06
 ELEMENT NUMBER   59     VOLUME = 0.1897E+06
 ELEMENT NUMBER   60     VOLUME = 0.1897E+06


 ******************************** STATIC ANALYSIS ********************************

 ARRAY A STORAGE REQUIRED FOR STATIC ANALYSIS =    49848


      STATIC STEP NUMBER   1
I  ISTPTYP = 1 (GRAVITY STEP)
     ELEMENTS
I    N  NE  NG
I    5   8   3

      STATIC STEP NUMBER   2
I  ISTPTYP = 1 (GRAVITY STEP)
```

```
      ELEMENTS
I     N  NE  NG
I     2   0   0
I     4   7   3

        STATIC STEP NUMBER   3
I   ISTPTYP = 1 (GRAVITY STEP)
      ELEMENTS
I     N  NE  NG
I     1   0   0
I     3   6   3

        STATIC STEP NUMBER   4
I   ISTPTYP = 3 (WATER LEVEL STEP)
I   SELEV = 0.600E+02

        STATIC STEP NUMBER   5
I   ISTPTYP = 3 (WATER LEVEL STEP)
I   SELEV = 0.120E+03

        STATIC STEP NUMBER   6
I   ISTPTYP = 3 (WATER LEVEL STEP)
I   SELEV = 0.180E+03



    ****************************** DYNAMIC ANALYSIS ********************************


        DYNAMIC ANALYSIS PARAMETERS
I   DT =  0.5000E-02
I   NDTGM =   2
I   BINT =  0.5000E-01
I   PINT =  0.5000E+00
I   ALPHA = -0.2000E+00
I   GAMMA =  0.7000E+00
I   BETA =  0.3600E+00
I   A0 =  0.0000E+00
I   A1 =  0.2390E-02
I   NPIC =    1
I   NHIST =   23


        TIME STEP NUMBERS FOR RESPONSE PICTURES
I   IDPIC =    800


        TIME HISTORY RESPONSE QUANTITIES
I   (T HIST NO)  NODEL        NQ
I      (  1)      10 (NODE)    1 (U)
I      (  2)      10 (NODE)    2 (V)
I      (  3)       6 (ELEM)    6 (SIG1 AT UPSF)
I      (  4)       6 (ELEM)    7 (SIG2 AT UPSF)
I      (  5)       6 (ELEM)    8 (TAU12 AT UPSF)
I      (  6)       6 (ELEM)    9 (TAU23 AT UPSF)
```

```
I       (  7)        6 (ELEM)    10 (TAU13 AT UPSF)
I       (  8)        6 (ELEM)    11 (SIG1 AT DNSF)
I       (  9)        6 (ELEM)    12 (SIG2 AT DNSF)
I       ( 10)        6 (ELEM)    13 (TAU12 AT DNSF)
I       ( 11)        6 (ELEM)    14 (TAU23 AT DNSF)
I       ( 12)        6 (ELEM)    15 (TAU13 AT DNSF)
I       ( 13)        6 (ELEM)    16 (OD1 AT UPSF)
I       ( 14)        6 (ELEM)    17 (OD2 AT UPSF)
I       ( 15)        6 (ELEM)    18 (SD12 AT UPSF)
I       ( 16)        6 (ELEM)    19 (SD23 AT UPSF)
I       ( 17)        6 (ELEM)    20 (SD13 AT UPSF)
I       ( 18)        6 (ELEM)    21 (OD1 AT DNSF)
I       ( 19)        6 (ELEM)    22 (OD2 AT DNSF)
I       ( 20)        6 (ELEM)    23 (SD12 AT DNSF)
I       ( 21)        6 (ELEM)    24 (SD23 AT DNSF)
I       ( 22)        6 (ELEM)    25 (SD13 AT DNSF)
I       ( 23)       11 (NODE)    26 (TOT WAT PRES)


I   AXMULT =  0.2474E+02   AYMULT =  0.2474E+02   AZMULT =  0.0000E+00


          GROUND ACCELERATION DATA
I                              X COMPONENT
I    -0.1077E+00 -0.8560E-01 -0.5920E-01 -0.3280E-01 -0.2000E-02  0.2890E-01  0.6540E-01  0.1018E+00  0.1278E+00  0.1538E+00
I     0.1536E+00  0.1534E+00  0.1531E+00  0.1528E+00  0.1751E+00  0.1974E+00  0.2062E+00  0.2151E+00  0.2022E+00  0.1894E+00
I     0.1929E+00  0.1964E+00  0.1864E+00  0.1766E+00  0.1396E+00  0.1026E+00  0.8020E-01  0.5790E-01  0.3860E-01  0.1950E-01
I     0.2690E-01  0.3440E-01  0.4260E-01  0.5090E-01  0.6230E-01  0.7370E-01  0.7200E-01  0.7030E-01  0.4650E-01  0.2270E-01
I     0.4670E-01  0.7060E-01  0.8330E-01  0.9610E-01  0.1087E+00  0.1213E+00  0.1011E+00  0.8090E-01  0.6330E-01  0.4580E-01
I     0.7220E-01  0.9850E-01  0.9680E-01  0.9530E-01  0.9470E-01  0.9410E-01  0.1064E+00  0.1187E+00  0.1326E+00  0.1466E+00
I     0.1498E+00  0.1530E+00  0.1230E+00  0.9300E-01  0.6400E-01  0.3500E-01  0.9900E-02 -0.1510E-01 -0.5330E-01 -0.9160E-01
I    -0.1608E+00 -0.2301E+00 -0.2813E+00 -0.3325E+00 -0.2978E+00 -0.2631E+00 -0.2402E+00 -0.2174E+00 -0.2339E+00 -0.2504E+00
I    -0.2483E+00 -0.2462E+00 -0.2508E+00 -0.2555E+00 -0.2819E+00 -0.3084E+00 -0.2763E+00 -0.2442E+00 -0.1753E+00 -0.1064E+00
I    -0.6520E-01 -0.2400E-01  0.8000E-02  0.4010E-01  0.6080E-01  0.8160E-01  0.8350E-01  0.8530E-01  0.9370E-01  0.1021E+00
I     0.7360E-01  0.4520E-01 -0.3460E-01 -0.1143E+00 -0.1853E+00 -0.2564E+00 -0.2844E+00 -0.3124E+00 -0.2899E+00 -0.2674E+00
I    -0.2352E+00 -0.2029E+00 -0.1353E+00 -0.6760E-01 -0.3100E-02  0.6130E-01  0.7730E-01  0.9340E-01  0.9090E-01  0.8840E-01
I     0.9200E-01  0.9570E-01  0.6680E-01  0.3790E-01  0.8000E-02 -0.2190E-01 -0.1880E-01 -0.1570E-01  0.2900E-02  0.2140E-01
I     0.4240E-01  0.6350E-01  0.6650E-01  0.6950E-01  0.6920E-01  0.6880E-01  0.6840E-01  0.6790E-01  0.6600E-01  0.6420E-01
I     0.6500E-01  0.6570E-01  0.6900E-01  0.7240E-01  0.8070E-01  0.8890E-01  0.8950E-01  0.9020E-01  0.9200E-01  0.9380E-01
I     0.1119E+00  0.1300E+00  0.1479E+00  0.1658E+00  0.1596E+00  0.1533E+00  0.1147E+00  0.7620E-01  0.3000E-01 -0.1620E-01
I    -0.4930E-01 -0.8240E-01 -0.1023E+00 -0.1222E+00 -0.1340E+00 -0.1459E+00 -0.1553E+00 -0.1648E+00 -0.1595E+00 -0.1543E+00
I    -0.1082E+00 -0.6220E-01 -0.1150E-01  0.3920E-01  0.5180E-01  0.6440E-01  0.4990E-01  0.3550E-01  0.1690E-01 -0.1800E-02
I     0.1010E-01  0.2210E-01  0.6020E-01  0.9830E-01  0.1287E+00  0.1591E+00  0.1624E+00  0.1658E+00  0.1690E+00  0.1723E+00
I     0.1553E+00  0.1384E+00  0.9640E-01  0.5430E-01  0.2130E-01 -0.1170E-01 -0.2540E-01 -0.3900E-01 -0.3440E-01 -0.2980E-01
I    -0.2860E-01 -0.2750E-01 -0.1120E-01  0.5200E-02 -0.2900E-02 -0.1090E-01 -0.4240E-01 -0.7390E-01 -0.1035E+00 -0.1332E+00
I    -0.8090E-01 -0.2850E-01  0.1200E-02  0.3080E-01 -0.1700E-02 -0.3430E-01 -0.6320E-01 -0.9210E-01 -0.7330E-01 -0.5450E-01
I    -0.2300E-02  0.4990E-01  0.7260E-01  0.9530E-01  0.8350E-01  0.7170E-01  0.5400E-01  0.3640E-01  0.5900E-02 -0.2450E-01
I    -0.1660E-01 -0.8700E-02 -0.5000E-02 -0.1400E-02  0.3090E-01  0.6330E-01  0.1039E+00  0.1446E+00  0.1067E+00  0.6880E-01
I     0.2260E-01 -0.2350E-01 -0.2330E-01 -0.2310E-01 -0.1960E-01 -0.1610E-01 -0.4430E-01 -0.7240E-01 -0.1075E+00 -0.1425E+00
I    -0.1868E+00 -0.2312E+00 -0.2976E+00 -0.3639E+00 -0.2807E+00 -0.1975E+00  0.6700E-02  0.2110E+00  0.3016E+00  0.3922E+00
I     0.3378E+00  0.2835E+00  0.2356E+00  0.1877E+00  0.1186E+00  0.4950E-01  0.9100E-02 -0.3120E-01 -0.6470E-01 -0.9830E-01
I    -0.1566E+00 -0.2149E+00 -0.1240E+00 -0.3310E-01  0.5130E-01  0.1358E+00  0.6430E-01 -0.7100E-02 -0.4500E-01 -0.8290E-01
I    -0.7770E-01 -0.7240E-01 -0.7910E-01 -0.8580E-01 -0.8890E-01 -0.9200E-01 -0.6400E-01 -0.3600E-01 -0.3330E-01 -0.3070E-01
I    -0.2890E-01 -0.2710E-01 -0.1740E-01 -0.7700E-02  0.9400E-02  0.2650E-01  0.4660E-01  0.6680E-01  0.8180E-01  0.9680E-01
I     0.7760E-01  0.5840E-01 -0.6400E-02 -0.7130E-01 -0.9500E-01 -0.1188E+00 -0.9430E-01 -0.6980E-01 -0.2500E-01  0.1990E-01
I     0.4120E-01  0.6260E-01  0.4620E-01  0.2990E-01  0.4030E-01  0.5080E-01  0.7880E-01  0.1067E+00  0.1244E+00  0.1421E+00
```

I	0.1454E+00	0.1487E+00	0.1398E+00	0.1310E+00	0.1183E+00	0.1057E+00	0.9280E-01	0.7980E-01	0.1022E+00	0.1246E+00	
I	0.1637E+00	0.2029E+00	0.2372E+00	0.2714E+00	0.2876E+00	0.3037E+00	0.2567E+00	0.2099E+00	0.1260E+00	0.4200E-01	
I	-0.1580E-01	-0.7380E-01	-0.1396E+00	-0.2054E+00	-0.2978E+00	-0.3903E+00	-0.4162E+00	-0.4420E+00	-0.3922E+00	-0.3424E+00	
I	-0.2788E+00	-0.2152E+00	-0.1713E+00	-0.1275E+00	-0.1489E+00	-0.1703E+00	-0.2537E+00	-0.3371E+00	-0.3242E+00	-0.3114E+00	
I	-0.2130E+00	-0.1146E+00	-0.4510E-01	0.2430E-01	0.7240E-01	0.1204E+00	0.1884E+00	0.2565E+00	0.3454E+00	0.4343E+00	
I	0.4107E+00	0.3871E+00	0.3450E+00	0.3028E+00	0.2501E+00	0.1974E+00	0.1396E+00	0.8190E-01	-0.3500E-02	-0.8900E-01	
I	-0.5550E-01	-0.2200E-01	0.3640E-01	0.9490E-01	0.9800E-02	-0.7530E-01	-0.1759E+00	-0.2765E+00	-0.2711E+00	-0.2657E+00	
I	-0.1753E+00	-0.8490E-01	-0.1000E-03	0.8460E-01	0.1073E+00	0.1300E+00	0.1028E+00	0.7560E-01	0.7020E-01	0.6470E-01	
I	0.5300E-01	0.4120E-01	-0.1820E-01	-0.7750E-01	-0.1311E+00	-0.1847E+00	-0.1682E+00	-0.1518E+00	-0.5640E-01	0.3900E-01	
I	0.5600E-01	0.7300E-01	0.5960E-01	0.4620E-01	0.5470E-01	0.6320E-01	0.6390E-01	0.6470E-01	0.4910E-01	0.3360E-01	
I	0.2310E-01	0.1270E-01	-0.1580E-01	-0.4420E-01	-0.8560E-01	-0.1270E+00	-0.1781E+00	-0.2291E+00	-0.2053E+00	-0.1816E+00	
I	-0.4750E-01	0.8660E-01	0.1378E+00	0.1889E+00	0.1902E+00	0.1914E+00	0.1988E+00	0.2062E+00	0.1177E+00	0.2920E-01	
I	-0.3780E-01	-0.1048E+00	-0.1249E+00	-0.1449E+00	-0.1975E+00	-0.2501E+00	-0.1932E+00	-0.1364E+00	-0.3810E-01	0.6010E-01	
I	0.4500E-01	0.2990E-01	0.4560E-01	0.6130E-01	0.7470E-01	0.8820E-01	0.8520E-01	0.8220E-01	0.7770E-01	0.7330E-01	
I	0.5930E-01	0.4530E-01	0.2910E-01	0.1300E-01	0.3700E-02	-0.5400E-02	0.1500E-01	0.3560E-01	0.2900E-01	0.2240E-01	
I	-0.2100E-01	-0.6440E-01	-0.7980E-01	-0.9540E-01	-0.9930E-01	-0.1032E+00	-0.1077E+00	-0.1123E+00	-0.8800E-01	-0.6370E-01	
I	-0.4140E-01	-0.1900E-01	0.4360E-01	0.1062E+00	0.1318E+00	0.1574E+00	0.1179E+00	0.7850E-01	0.5840E-01	0.3840E-01	
I	0.2310E-01	0.7900E-02	0.1430E-01	0.2070E-01	0.4480E-01	0.6880E-01	0.4150E-01	0.1410E-01	-0.5070E-01	-0.1156E+00	
I				Y COMPONENT							
I	0.1148E+00	0.1296E+00	0.1093E+00	0.8910E-01	0.5490E-01	0.2070E-01	-0.4400E-02	-0.2940E-01	-0.3600E-01	-0.4250E-01	
I	-0.5320E-01	-0.6390E-01	-0.7800E-01	-0.9220E-01	-0.7690E-01	-0.6160E-01	-0.1970E-01	0.2210E-01	0.7050E-01	0.1190E+00	
I	0.1736E+00	0.2281E+00	0.2381E+00	0.2481E+00	0.2038E+00	0.1596E+00	0.8900E-01	0.1850E-01	-0.4980E-01	-0.1181E+00	
I	-0.1642E+00	-0.2103E+00	-0.2046E+00	-0.1989E+00	-0.1471E+00	-0.9530E-01	-0.3560E-01	0.2390E-01	0.5090E-01	0.7790E-01	
I	0.4710E-01	0.1650E-01	0.7900E-02	-0.7000E-03	-0.7000E-03	-0.7000E-03	-0.2610E-01	-0.5160E-01	-0.9170E-01	-0.1319E+00	
I	-0.1579E+00	-0.1840E+00	-0.1713E+00	-0.1585E+00	-0.1322E+00	-0.1060E+00	-0.5910E-01	-0.1220E-01	0.2730E-01	0.6690E-01	
I	0.8430E-01	0.1016E+00	0.1292E+00	0.1567E+00	0.1381E+00	0.2194E+00	0.2075E+00	0.1957E+00	0.1515E+00	0.1073E+00	
I	0.6800E-01	0.2880E-01	-0.2350E-01	-0.7580E-01	-0.1182E+00	-0.1606E+00	-0.1657E+00	-0.1709E+00	-0.1671E+00	-0.1634E+00	
I	-0.1802E+00	-0.1971E+00	-0.2471E+00	-0.2971E+00	-0.3111E+00	-0.3250E+00	-0.2761E+00	-0.2273E+00	-0.1859E+00	-0.1446E+00	
I	-0.1124E+00	-0.8030E-01	-0.5400E-02	-0.4280E-01	0.3940E-01	0.8440E-01	0.1253E+00	0.1664E+00	0.1706E+00	0.1748E+00	
I	0.1372E+00	0.9970E-01	0.6930E-01	0.3890E-01	0.1990E-01	0.1000E-02	-0.5560E-01	-0.1122E+00	-0.1890E+00	-0.2659E+00	
I	-0.2777E+00	-0.2895E+00	-0.2330E+00	-0.1765E+00	-0.9440E-01	-0.1240E-01	0.3480E-01	0.8190E-01	0.8490E-01	0.8790E-01	
I	0.7990E-01	0.7200E-01	0.6520E-01	0.5860E-01	0.4330E-01	0.2800E-01	0.1220E-01	-0.3700E-02	-0.7700E-02	-0.1180E-01	
I	-0.1440E-01	-0.1710E-01	-0.3240E-01	-0.4770E-01	-0.4890E-01	-0.5010E-01	-0.4590E-01	-0.4170E-01	-0.2330E-01	-0.5000E-02	
I	0.2820E-01	0.6150E-01	0.8050E-01	0.9960E-01	0.9400E-01	0.8830E-01	0.6450E-01	0.4080E-01	0.2350E-01	0.6300E-02	
I	0.1780E-01	0.2930E-01	0.4620E-01	0.6330E-01	0.6440E-01	0.6560E-01	0.4110E-01	0.1670E-01	-0.5400E-02	-0.2760E-01	
I	-0.2880E-01	-0.3010E-01	-0.1650E-01	-0.2900E-02	0.9400E-02	0.2180E-01	0.3160E-01	0.4150E-01	0.1710E-01	-0.7100E-02	
I	-0.4810E-01	-0.8900E-01	-0.1042E+00	-0.1194E+00	-0.1065E+00	-0.9360E-01	-0.3810E-01	0.1740E-01	0.6180E-01	0.1061E+00	
I	0.1109E+00	0.1156E+00	0.1042E+00	0.9280E-01	0.9640E-01	0.1001E+00	0.6670E-01	0.3320E-01	-0.1620E-01	-0.6560E-01	
I	-0.4730E-01	-0.2910E-01	0.1250E-01	0.5420E-01	0.5930E-01	0.6450E-01	0.5360E-01	0.4270E-01	0.3820E-01	0.3360E-01	
I	0.1520E-01	-0.3200E-02	-0.1430E-01	-0.2540E-01	-0.3810E-01	-0.5070E-01	-0.6200E-01	-0.7320E-01	-0.5540E-01	-0.3760E-01	
I	-0.1090E-01	0.1580E-01	0.1740E-01	0.1900E-01	0.8000E-02	-0.2900E-02	-0.1600E-02	-0.4000E-03	0.9500E-02	0.1950E-01	
I	0.6300E-02	-0.6700E-02	-0.2630E-01	-0.4580E-01	-0.5690E-01	-0.6790E-01	-0.6940E-01	-0.7090E-01	-0.1750E-01	0.3580E-01	
I	0.6280E-01	0.8980E-01	0.3440E-01	-0.2090E-01	-0.4720E-01	-0.7350E-01	-0.4380E-01	-0.1410E-01	0.5000E-02	0.2430E-01	
I	0.2780E-01	0.3140E-01	0.2510E-01	0.1880E-01	0.3220E-01	0.4570E-01	0.4370E-01	0.4170E-01	0.1480E-01	-0.1220E-01	
I	-0.5080E-01	-0.8950E-01	-0.1153E+00	-0.1411E+00	-0.1344E+00	-0.1277E+00	-0.5570E-01	0.1630E-01	0.6350E-01	0.1107E+00	
I	0.7860E-01	0.4670E-01	-0.1990E-01	-0.8640E-01	-0.5490E-01	-0.2330E-01	0.1040E-01	0.4410E-01	-0.3700E-02	-0.5170E-01	
I	-0.6740E-01	-0.8320E-01	-0.5520E-01	-0.2720E-01	0.2140E-01	0.6990E-01	0.8180E-01	0.9360E-01	0.4860E-01	0.3600E-02	
I	-0.5060E-01	-0.1049E+00	-0.1300E+00	-0.1551E+00	-0.1283E+00	-0.1016E+00	-0.5390E-01	-0.6100E-02	-0.8000E-03	0.4500E-02	
I	-0.2480E-01	-0.5420E-01	-0.3840E-01	-0.2250E-01	0.2300E-02	0.2710E-01	0.1570E-01	0.4400E-02	0.1420E-01	0.2410E-01	
I	0.3740E-01	0.5070E-01	0.5020E-01	0.4960E-01	0.1540E-01	-0.1880E-01	-0.5310E-01	-0.8740E-01	-0.6650E-01	-0.4560E-01	
I	0.1550E-01	0.7660E-01	0.7490E-01	0.7320E-01	0.3920E-01	0.5200E-02	-0.2200E-01	-0.4940E-01	-0.5410E-01	-0.5890E-01	
I	-0.5470E-01	-0.5060E-01	-0.7300E-01	-0.9540E-01	-0.1211E+00	-0.1468E+00	-0.1545E+00	-0.1623E+00	-0.1413E+00	-0.1204E+00	
I	-0.6690E-01	-0.1330E-01	0.4960E-01	0.1126E+00	0.1266E+00	0.1406E+00	0.1188E+00	0.9710E-01	0.8810E-01	0.7930E-01	
I	0.1119E+00	0.1445E+00	0.1975E+00	0.2506E+00	0.2661E+00	0.2816E+00	0.1813E+00	0.8090E-01	0.1070E-01	-0.5950E-01	
I	-0.1085E+00	-0.1576E+00	-0.2606E+00	-0.3637E+00	-0.4185E+00	-0.4734E+00	-0.4423E+00	-0.4113E+00	-0.3739E+00	-0.3365E+00	
I	-0.2903E+00	-0.2441E+00	-0.1774E+00	-0.1107E+00	-0.2260E-01	0.6550E-01	0.1404E+00	0.2154E+00	0.2921E+00	0.3688E+00	

I	0.3982E+00	0.4276E+00	0.3763E+00	0.3251E+00	0.2108E+00	0.9640E-01	-0.6430E-01	-0.2250E+00	-0.2177E+00	-0.2104E+00	I
I	-0.3470E-01	0.1410E+00	0.1768E+00	0.2127E+00	0.1503E+00	0.8790E-01	0.2450E-01	-0.3890E-01	-0.1092E+00	-0.1795E+00	I
I	-0.1438E+00	-0.1082E+00	-0.3390E-01	0.4030E-01	0.5740E-01	0.7450E-01	0.2290E-01	-0.2860E-01	-0.3630E-01	-0.4400E-01	I
I	0.9800E-02	0.6360E-01	0.9640E-01	0.1293E+00	0.1312E+00	0.1331E+00	0.9980E-01	0.6650E-01	0.5520E-01	0.4390E-01	I
I	0.6300E-02	-0.3140E-01	-0.4670E-01	-0.6200E-01	-0.4080E-01	-0.1970E-01	0.7000E-02	0.3370E-01	0.4310E-01	0.5240E-01	I
I	0.3440E-01	0.1650E-01	0.1350E-01	0.1050E-01	-0.1810E-01	-0.4670E-01	-0.7560E-01	-0.1047E+00	-0.1063E+00	-0.1080E+00	I
I	-0.3140E-01	0.4510E-01	0.9570E-01	0.1464E+00	0.9700E-01	0.4760E-01	0.1370E-01	-0.2010E-01	-0.7400E-02	0.5200E-02	I
I	0.2220E-01	0.3930E-01	0.5320E-01	0.6710E-01	0.4720E-01	0.2730E-01	0.1450E-01	0.1600E-02	-0.1200E-02	-0.4100E-02	I
I	-0.5000E-03	0.3100E-02	0.8600E-02	0.1430E-01	0.3910E-01	0.6400E-01	0.6250E-01	0.6100E-01	0.4330E-01	0.2560E-01	I
I	-0.1820E-01	-0.6210E-01	-0.8520E-01	-0.1082E+00	-0.6710E-01	-0.2600E-01	0.4350E-01	0.1130E+00	0.1551E+00	0.1972E+00	I
I	0.1540E+00	0.1109E+00	0.4100E-01	-0.2880E-01	-0.5630E-01	-0.8390E-01	-0.6940E-01	-0.5490E-01	-0.1400E-02	0.5210E-01	I
I	0.6110E-01	0.7010E-01	0.4540E-01	0.2080E-01	0.1140E-01	0.2100E-02	-0.2280E-01	-0.4770E-01	-0.7730E-01	-0.1068E+00	I
I	-0.6330E-01	-0.1970E-01	0.4810E-01	0.1159E+00	0.1574E+00	0.1989E+00	0.1787E+00	0.1585E+00	0.6450E-01	-0.2950E-01	I
I				Z COMPONENT							I
I	-0.1371E+00	-0.1156E+00	-0.1400E+00	-0.1644E+00	-0.1879E+00	-0.2114E+00	-0.2138E+00	-0.2161E+00	-0.2011E+00	-0.1861E+00	I
I	-0.1705E+00	-0.1550E+00	-0.1381E+00	-0.1211E+00	-0.1112E+00	-0.1013E+00	-0.9910E-01	-0.9680E-01	-0.9640E-01	-0.9590E-01	I
I	-0.9670E-01	-0.9760E-01	-0.1492E+00	-0.2009E+00	-0.2555E+00	-0.3101E+00	-0.3256E+00	-0.3411E+00	-0.3535E+00	-0.3659E+00	I
I	-0.3394E+00	-0.3129E+00	-0.2723E+00	-0.2317E+00	-0.1560E+00	-0.8030E-01	-0.9900E-02	0.6030E-01	0.7280E-01	0.8540E-01	I
I	-0.2200E-01	-0.1293E+00	-0.2031E+00	-0.2769E+00	-0.2546E+00	-0.2323E+00	-0.2717E+00	-0.3112E+00	-0.2915E+00	-0.2718E+00	I
I	-0.2238E+00	-0.1757E+00	-0.1388E+00	-0.1020E+00	-0.7400E-01	-0.4600E-01	-0.9900E-02	0.2630E-01	0.6060E-01	0.9490E-01	I
I	0.1200E+00	0.1450E+00	0.1662E+00	0.1875E+00	0.2265E+00	0.2656E+00	0.2515E+00	0.2375E+00	0.2215E+00	0.2055E+00	I
I	0.2064E+00	0.2073E+00	0.1810E+00	0.1549E+00	0.1626E+00	0.1704E+00	0.1797E+00	0.1890E+00	0.2267E+00	0.2644E+00	I
I	0.3143E+00	0.3641E+00	0.3531E+00	0.3420E+00	0.3471E+00	0.3524E+00	0.3965E+00	0.4407E+00	0.3726E+00	0.3045E+00	I
I	0.2406E+00	0.1768E+00	0.1570E+00	0.1373E+00	0.1270E+00	0.1168E+00	0.1338E+00	0.1509E+00	0.1395E+00	0.1281E+00	I
I	0.9260E-01	0.5720E-01	0.3070E-01	0.4100E-02	0.4010E-01	0.7610E-01	0.8620E-01	0.9640E-01	0.3110E-01	-0.3410E-01	I
I	-0.5840E-01	-0.8270E-01	-0.6070E-01	-0.3870E-01	-0.2290E-01	-0.7100E-02	0.3310E-01	0.7320E-01	0.9870E-01	0.1241E+00	I
I	0.1129E+00	0.1017E+00	0.9470E-01	0.8780E-01	0.2860E-01	-0.3060E-01	-0.7860E-01	-0.1266E+00	-0.1390E+00	-0.1515E+00	I
I	-0.1576E+00	-0.1637E+00	-0.1683E+00	-0.1728E+00	-0.1634E+00	-0.1540E+00	-0.1498E+00	-0.1455E+00	-0.1427E+00	-0.1398E+00	I
I	-0.1296E+00	-0.1195E+00	-0.1139E+00	-0.1082E+00	-0.1183E+00	-0.1283E+00	-0.1468E+00	-0.1654E+00	-0.1690E+00	-0.1726E+00	I
I	-0.1602E+00	-0.1479E+00	-0.1302E+00	-0.1126E+00	-0.9640E-01	-0.8040E-01	-0.7030E-01	-0.6030E-01	-0.5210E-01	-0.4400E-01	I
I	-0.3960E-01	-0.3520E-01	-0.4000E-01	-0.4480E-01	-0.4730E-01	-0.4990E-01	-0.4220E-01	-0.3450E-01	-0.4600E-02	0.4380E-01	I
I	0.8660E-01	0.1294E+00	0.1347E+00	0.1400E+00	0.1342E+00	0.1283E+00	0.1447E+00	0.1611E+00	0.1570E+00	0.1530E+00	I
I	0.9410E-01	0.3540E-01	-0.5600E-01	-0.1475E+00	-0.2209E+00	-0.2944E+00	-0.2839E+00	-0.2734E+00	-0.2080E+00	-0.1426E+00	I
I	-0.7820E-01	-0.1380E-01	0.2710E-01	0.6810E-01	0.8690E-01	0.1058E+00	0.1177E+00	0.1296E+00	0.1494E+00	0.1691E+00	I
I	0.1538E+00	0.1386E+00	0.1253E+00	0.1119E+00	0.1395E+00	0.1670E+00	0.1806E+00	0.1942E+00	0.1738E+00	0.1534E+00	I
I	0.1160E+00	0.7860E-01	-0.2500E-01	-0.1285E+00	-0.2172E+00	-0.3058E+00	-0.2963E+00	-0.2868E+00	-0.2059E+00	-0.1249E+00	I
I	-0.6900E-01	-0.1300E-01	-0.1990E-01	-0.2690E-01	-0.3460E-01	-0.4220E-01	-0.4130E-01	-0.4030E-01	-0.9000E-03	0.4220E-01	I
I	0.8900E-01	0.1360E+00	0.1347E+00	0.1336E+00	0.1269E+00	0.1203E+00	0.1166E+00	0.1129E+00	0.1017E+00	0.9070E-01	I
I	0.9820E-01	0.1058E+00	0.1209E+00	0.1360E+00	0.1532E+00	0.1704E+00	0.1581E+00	0.1457E+00	0.1228E+00	0.1000E+00	I
I	0.6350E-01	0.2710E-01	0.2140E-01	0.1560E-01	0.3260E-01	0.4960E-01	0.3000E-02	-0.4370E-01	-0.9710E-01	-0.1505E+00	I
I	-0.1226E+00	-0.9460E-01	-0.5630E-01	-0.1800E-01	0.3860E-01	0.9530E-01	0.1498E+00	0.2044E+00	0.1924E+00	0.1804E+00	I
I	0.1566E+00	0.1329E+00	0.9700E-01	0.6110E-01	0.8100E-02	-0.4490E-01	-0.4410E-01	-0.4330E-01	0.2770E-01	0.9880E-01	I
I	0.1146E+00	0.1304E+00	0.9060E-01	0.5080E-01	0.5350E-01	0.5630E-01	0.6050E-01	0.6470E-01	0.4220E-01	0.1980E-01	I
I	0.3310E-01	0.4650E-01	0.9630E-01	0.1462E+00	0.1381E+00	0.1302E+00	0.7820E-01	0.2630E-01	0.2360E-01	0.2090E-01	I
I	0.1730E-01	0.1360E-01	-0.3600E-02	-0.2080E-01	-0.2110E-01	-0.2140E-01	-0.5450E-01	-0.8770E-01	-0.1129E+00	-0.1381E+00	I
I	-0.1215E+00	-0.1049E+00	-0.8620E-01	-0.6750E-01	-0.6600E-01	-0.6460E-01	-0.8010E-01	-0.9560E-01	-0.1274E+00	-0.1593E+00	I
I	-0.1833E+00	-0.2074E+00	-0.2119E+00	-0.2164E+00	-0.2076E+00	-0.1988E+00	-0.1732E+00	-0.1477E+00	-0.1071E+00	-0.6640E-01	I
I	-0.4160E-01	-0.1690E-01	-0.1030E-01	-0.3700E-02	-0.5300E-02	-0.7000E-02	-0.2440E-01	-0.4180E-01	-0.5050E-01	-0.5910E-01	I
I	-0.5830E-01	-0.5750E-01	-0.4240E-01	-0.2750E-01	-0.4900E-02	0.1760E-01	0.9070E-01	0.1637E+00	0.1072E+00	0.5070E-01	I
I	0.2900E-02	-0.4480E-01	0.2900E-02	0.5070E-01	0.4500E-01	0.3920E-01	0.1086E+00	0.1781E+00	0.2455E+00	0.3131E+00	I
I	0.3044E+00	0.2959E+00	0.2397E+00	0.1836E+00	0.1528E+00	0.1220E+00	0.1419E+00	0.1619E+00	0.1149E+00	0.6800E-01	I
I	-0.2970E-01	-0.1275E+00	-0.2461E+00	-0.3647E+00	-0.4103E+00	-0.4560E+00	-0.3682E+00	-0.2804E+00	-0.2066E+00	-0.1328E+00	I
I	-0.5560E-01	0.2170E-01	0.4970E-01	0.7770E-01	0.3580E-01	-0.6200E-02	0.7030E-01	0.1467E+00	0.2233E+00	0.2999E+00	I
I	0.2721E+00	0.2444E+00	0.2292E+00	0.2140E+00	0.1570E+00	0.9990E-01	0.5200E-01	0.4100E-02	-0.2180E-01	-0.4780E-01	I
I	-0.4090E-01	-0.3410E-01	-0.3050E-01	-0.2680E-01	0.1250E-01	0.5180E-01	0.6360E-01	0.7540E-01	0.2430E-01	-0.2670E-01	I
I	-0.1304E+00	-0.2342E+00	-0.1966E+00	-0.1591E+00	-0.7160E-01	0.1580E-01	0.4960E-01	0.8360E-01	0.1084E+00	0.1333E+00	I

```
I     0.1505E+00  0.1677E+00  0.1580E+00  0.1483E+00  0.1098E+00  0.7130E-01  0.6410E-01  0.5700E-01  0.1115E+00  0.1661E+00
I     0.1704E+00  0.1747E+00  0.9320E-01  0.1180E-01 -0.7200E-02 -0.2630E-01 -0.4920E-01 -0.7210E-01 -0.8470E-01 -0.9740E-01
I    -0.6300E-01 -0.2860E-01 -0.1600E-01 -0.3500E-02  0.5080E-01  0.1051E+00  0.1597E+00  0.2143E+00  0.1062E+00 -0.1800E-02
I    -0.7610E-01 -0.1505E+00 -0.9750E-01 -0.4450E-01 -0.6580E-01 -0.8730E-01 -0.1068E+00 -0.1265E+00 -0.1613E+00 -0.1960E+00
I    -0.2042E+00 -0.2124E+00 -0.1719E+00 -0.1315E+00 -0.8190E-01 -0.3220E-01  0.2800E-02  0.3790E-01  0.7010E-01  0.1022E+00
I     0.1083E+00  0.1143E+00  0.1460E+00  0.1777E+00  0.1930E+00  0.2083E+00  0.2080E+00  0.2078E+00  0.1451E+00  0.8240E-01
I    -0.7300E-02 -0.9700E-01 -0.2257E+00 -0.3545E+00 -0.4671E+00 -0.5797E+00 -0.5083E+00 -0.4370E+00 -0.3463E+00 -0.2556E+00
I    -0.1995E+00 -0.1436E+00 -0.9430E-01 -0.4510E-01 -0.1180E-01  0.2140E-01  0.1630E-01  0.1140E-01 -0.3000E-03 -0.1200E-01

   GROUND ACCELERATION VALUES (AS SCALED)
    TIME        XACLG        YACLG        ZACLG
  0.0100  -0.2664E+01   0.2840E+01   0.0000E+00
  0.0200  -0.2118E+01   0.3206E+01   0.0000E+00
  0.0300  -0.1465E+01   0.2704E+01   0.0000E+00
  0.0400  -0.8115E+00   0.2204E+01   0.0000E+00
  0.0500  -0.4948E-01   0.1358E+01   0.0000E+00
  0.0600   0.7150E+00   0.5121E+00   0.0000E+00
  0.0700   0.1618E+01  -0.1089E+00   0.0000E+00
  0.0800   0.2519E+01  -0.7274E+00   0.0000E+00
  0.0900   0.3162E+01  -0.8906E+00   0.0000E+00
  0.1000   0.3805E+01  -0.1051E+01   0.0000E+00

        (Output deleted to save space.)

  4.9000   0.9500E+00  -0.2642E+01   0.0000E+00
  4.9100   0.5715E+00  -0.1566E+01   0.0000E+00
  4.9200   0.1954E+00  -0.4874E+00   0.0000E+00
  4.9300   0.3538E+00   0.1190E+01   0.0000E+00
  4.9400   0.5121E+00   0.2867E+01   0.0000E+00
  4.9500   0.1108E+01   0.3894E+01   0.0000E+00
  4.9600   0.1702E+01   0.4921E+01   0.0000E+00
  4.9700   0.1027E+01   0.4421E+01   0.0000E+00
  4.9800   0.3488E+00   0.3921E+01   0.0000E+00
  4.9900  -0.1254E+01   0.1596E+01   0.0000E+00
  5.0000  -0.2860E+01  -0.7298E+00   0.0000E+00

ARRAY A STORAGE REQUIRED FOR DYNAMIC ANALYSIS =    49848
```

Output File on Unit 3

Complete pictures of the dam response that include displacements of the nodes, water pressures on the upstream face, stresses in the elements, and opening and sliding displacements in the elements are output after the static analysis and at NPIC specific times as defined in IDPIC (time step 800 for the sample problem). Following the dynamic analysis, maximum and minimum response pictures are presented. Examination of this file shows that cracking in the dam, as revealed by a nonzero value for OD2, occurs at seven of the 16 locations on either the upstream or downstream faces of the eight elements during the dynamic analysis. The maximum arch compressive stress and contraction joint opening also occur during the dynamic analysis: -236,500 psf (-1830 psi) in element 6 on the upstream face and 0.0359 feet (0.431 inches) in element 6 on the downstream face, respectively.

DISPLACEMENTS AND PRESSURES FROM STATIC ANALYSIS

NODE	U	V	W	THETA	GAMA	TOT WAT PRES
1	-0.7282E-04	-0.2201E-03	-0.5374E-03	-0.3615E-04	-0.4513E-04	0.0000E+00
2	-0.1410E-02	-0.5217E-03	-0.8098E-03	0.4488E-05	-0.2109E-04	-0.3744E+04
3	-0.1167E-01	0.8282E-03	-0.2767E-03	0.3804E-03	-0.4868E-03	0.0000E+00
4	-0.8270E-02	-0.4734E-03	0.1661E-02	-0.1990E-03	-0.5036E-03	-0.3744E+04
5	-0.1489E-02	-0.8143E-03	-0.1334E-02	-0.7216E-04	-0.2531E-04	-0.7488E+04
6	-0.3655E-01	0.4358E-02	0.3439E-02	-0.3233E-03	-0.4113E-03	0.0000E+00
7	-0.2195E-01	0.4506E-03	0.1411E-02	-0.7787E-04	-0.3844E-03	-0.3744E+04
8	-0.8913E-02	-0.9343E-03	0.8443E-03	-0.2281E-03	-0.1792E-03	-0.7488E+04
9	-0.1123E-02	-0.8116E-03	-0.4142E-03	-0.2603E-04	-0.3820E-05	-0.1123E+05
10	-0.4666E-01	0.4685E-02	0.0000E+00	0.2233E-03	0.0000E+00	0.0000E+00
11	-0.3260E-01	0.1690E-02	0.0000E+00	-0.2971E-03	0.0000E+00	-0.3744E+04
12	-0.1491E-01	-0.9350E-03	0.0000E+00	-0.3028E-03	0.0000E+00	-0.7488E+04
13	-0.2416E-03	-0.8026E-03	0.0000E+00	-0.4228E-04	0.0000E+00	-0.1123E+05

STRESSES FROM STATIC ANALYSIS

ELEM	LOC	SIG1	SIG2	TAU12	TAU23	TAU13
1	UPSF	0.0000E+00	-0.1238E+05	0.3153E+03	0.2553E+04	0.0000E+00
1	DNSF	-0.5627E+05	0.4586E+04	0.3200E+04	0.8954E+03	0.3214E+04
2	UPSF	0.0000E+00	0.5995E+04	-0.4913E+04	-0.7904E+04	0.0000E+00
2	DNSF	-0.5303E+05	-0.2293E+05	0.2289E+05	-0.3854E+04	0.5030E+04
3	UPSF	-0.3693E+05	-0.1345E+05	-0.3222E+04	0.1544E+04	0.1565E+04
3	DNSF	-0.2017E+05	0.9947E+04	0.5679E+04	0.4581E+03	0.1292E+04
4	UPSF	-0.1192E+05	-0.6848E+04	-0.8706E+04	-0.1754E+04	0.5708E+04
4	DNSF	-0.2295E+05	-0.6438E+04	0.1586E+05	-0.2621E+04	0.4518E+04
5	UPSF	0.0000E+00	0.1784E+05	-0.2842E+04	-0.9502E+04	0.0000E+00
5	DNSF	-0.2621E+05	-0.3392E+05	0.1873E+05	-0.4740E+04	0.1310E+05
6	UPSF	-0.5537E+05	-0.1690E+05	0.1537E+02	0.2296E+04	0.1052E+04
6	DNSF	-0.2657E+04	0.1264E+05	0.1285E+03	0.1137E+04	0.1516E+03
7	UPSF	-0.4632E+05	-0.1789E+05	-0.4995E+04	-0.1388E+03	0.3308E+04
7	DNSF	0.0000E+00	0.6663E+04	0.3178E+04	-0.1539E+04	0.0000E+00
8	UPSF	-0.1127E+05	0.1859E+05	-0.5163E+04	-0.8870E+04	0.2042E+04
8	DNSF	0.0000E+00	-0.3601E+05	0.2274E+04	-0.6245E+04	0.0000E+00

OPENING AND SLIDING DISPLACEMENTS FROM STATIC ANALYSIS

ELEM	LOC	OD1	OD2	SD12	SD23	SD13
1	UPSF	0.2188E-05	0.0000E+00	0.2890E-03	0.0000E+00	-0.3635E-02
1	DNSF	0.0000E+00	0.0000E+00	-0.3159E-03	0.0000E+00	-0.4918E-02
2	UPSF	0.4099E-02	0.0000E+00	-0.4503E-02	0.0000E+00	0.1911E-02
2	DNSF	0.0000E+00	0.0000E+00	0.7535E-03	0.0000E+00	-0.1719E-02
3	UPSF	0.0000E+00	0.0000E+00	-0.1918E-03	0.0000E+00	-0.1931E-02
3	DNSF	0.0000E+00	0.0000E+00	0.4539E-04	0.0000E+00	-0.2142E-02
4	UPSF	0.0000E+00	0.0000E+00	-0.6987E-03	0.0000E+00	-0.3117E-02
4	DNSF	0.0000E+00	0.0000E+00	0.5118E-03	0.0000E+00	-0.3512E-02
5	UPSF	0.2787E-02	0.0000E+00	-0.2605E-02	0.0000E+00	0.5749E-02
5	DNSF	0.0000E+00	0.0000E+00	0.1153E-02	0.0000E+00	0.6520E-03
6	UPSF	0.0000E+00	0.0000E+00	0.1821E-03	0.0000E+00	-0.3939E-05
6	DNSF	0.0000E+00	0.0000E+00	-0.1673E-03	0.0000E+00	0.3422E-03
7	UPSF	0.0000E+00	0.0000E+00	-0.3862E-03	0.0000E+00	0.5993E-03
7	DNSF	0.1628E-02	0.0000E+00	0.2913E-02	0.0000E+00	0.1409E-02
8	UPSF	0.0000E+00	0.0000E+00	0.0000E+00	0.0000E+00	0.8470E-19
8	DNSF	0.1835E-03	0.0000E+00	0.2085E-02	0.0000E+00	0.4266E-03

DISPLACEMENTS AND PRESSURES AT TIME STEP 800 (TIME = 4.000)

NODE	U	V	W	THETA	GAMA	TOT WAT PRES
1	0.5195E-04	0.1210E-03	-0.4599E-03	-0.4151E-05	0.7199E-05	0.0000E+00
2	-0.1802E-02	-0.2680E-03	-0.6627E-03	-0.1964E-04	-0.4669E-04	-0.3257E+04
3	-0.9742E-01	0.1283E-01	0.4487E-01	-0.5099E-03	0.1405E-02	0.0000E+00
4	-0.4343E-01	0.9882E-02	0.1616E-01	-0.1186E-02	-0.7281E-03	-0.3241E+04
5	-0.2100E-02	-0.3897E-03	-0.1809E-02	-0.7988E-04	-0.6640E-04	-0.6957E+04
6	0.2740E+00	0.5264E-01	-0.4261E-01	0.1025E-01	0.2318E-02	0.0000E+00
7	-0.4281E-01	0.4277E-02	0.8230E-02	0.2966E-03	-0.1227E-03	-0.3514E+04
8	-0.3212E-01	0.8014E-02	0.5413E-02	-0.8249E-03	-0.3443E-03	-0.6854E+04
9	-0.1259E-02	-0.8812E-03	-0.1074E-02	-0.1945E-04	-0.1597E-04	-0.1077E+05
10	0.1311E+00	-0.7565E-03	0.0000E+00	-0.2114E-02	0.0000E+00	0.0000E+00
11	0.4618E-01	0.7828E-01	0.0000E+00	0.5919E-02	0.0000E+00	-0.3822E+04
12	-0.4359E-01	0.3521E-02	0.0000E+00	-0.7057E-03	0.0000E+00	-0.6793E+04
13	-0.9020E-04	-0.8448E-03	0.0000E+00	-0.3671E-04	0.0000E+00	-0.1081E+05

STRESSES AT TIME STEP 800 (TIME = 4.000)

ELEM	LOC	SIG1	SIG2	TAU12	TAU23	TAU13
1	UPSF	-0.2154E+05	-0.3109E+05	-0.1343E+05	0.4530E+04	0.7968E+04
1	DNSF	-0.1239E+05	0.5529E+04	-0.4057E+04	-0.4724E+03	0.1886E+04
2	UPSF	0.0000E+00	0.0000E+00	0.0000E+00	0.0000E+00	0.0000E+00
2	DNSF	-0.9274E+05	-0.5901E+05	0.3541E+05	-0.6324E+05	0.1916E+05
3	UPSF	-0.2924E+05	-0.1013E+05	0.1862E+04	-0.1274E+04	-0.1416E+05
3	DNSF	0.0000E+00	0.0000E+00	0.0000E+00	0.0000E+00	0.0000E+00
4	UPSF	-0.4347E+05	-0.5986E+04	-0.1979E+05	-0.5681E+01	0.9367E+04
4	DNSF	-0.2966E+05	-0.1675E+04	0.5339E+04	-0.2410E+04	0.7262E+04
5	UPSF	0.0000E+00	0.0000E+00	0.0000E+00	0.0000E+00	0.0000E+00
5	DNSF	-0.5711E+05	-0.5875E+05	0.3699E+05	-0.4222E+05	0.2856E+05
6	UPSF	0.0000E+00	-0.5113E+05	0.2388E+04	0.6882E+04	0.0000E+00
6	DNSF	0.0000E+00	0.4694E+05	-0.4992E+04	0.4720E+04	0.0000E+00
7	UPSF	-0.7040E+05	-0.7646E+05	-0.4766E+04	-0.2973E+05	-0.1885E+04
7	DNSF	-0.2017E+04	0.0000E+00	0.5043E+03	0.0000E+00	0.1009E+04
8	UPSF	-0.4414E+05	0.0000E+00	-0.4155E+04	0.0000E+00	0.7907E+04
8	DNSF	-0.1242E+05	-0.6774E+05	0.9755E+04	-0.3827E+05	0.1502E+04

OPENING AND SLIDING DISPLACEMENTS AT TIME STEP 800 (TIME = 4.000)

ELEM	LOC	OD1	OD2	SD12	SD23	SD13
1	UPSF	0.0000E+00	0.0000E+00	-0.4894E-02	0.0000E+00	0.7069E-01
1	DNSF	0.0000E+00	0.0000E+00	-0.5711E-02	0.0000E+00	0.7640E-01
2	UPSF	0.4241E-02	0.1821E-01	-0.2428E-01	-0.3224E-01	0.3582E-01
2	DNSF	0.0000E+00	0.0000E+00	0.2603E-02	0.0000E+00	0.2760E-01
3	UPSF	0.0000E+00	0.0000E+00	-0.8105E-02	0.5497E-01	-0.1604E+00
3	DNSF	0.7364E-02	0.7031E-01	-0.1103E+00	0.4250E-01	-0.1661E+00
4	UPSF	0.0000E+00	0.0000E+00	0.2013E-02	0.0000E+00	-0.3385E-02
4	DNSF	0.0000E+00	0.0000E+00	-0.4930E-02	0.0000E+00	-0.2790E-02
5	UPSF	0.3215E-02	0.1904E-01	-0.2105E-01	-0.2361E-01	0.2700E-01
5	DNSF	0.0000E+00	0.0000E+00	0.1215E-02	0.0000E+00	0.1673E-01
6	UPSF	0.1785E-01	0.0000E+00	0.2189E-02	0.0000E+00	0.4416E-01
6	DNSF	0.1054E-01	0.0000E+00	-0.4576E-02	0.0000E+00	0.4716E-01
7	UPSF	0.0000E+00	0.0000E+00	-0.1129E-01	0.6124E-02	-0.4220E-01
7	DNSF	0.0000E+00	0.8389E-01	-0.8258E-01	-0.2092E-01	-0.4188E-01
8	UPSF	0.0000E+00	0.1485E-01	0.2261E-02	-0.1899E-01	-0.1669E-02
8	DNSF	0.0000E+00	0.0000E+00	0.1842E-02	0.0000E+00	0.3156E-03

MAXIMUM STRESSES FROM STATIC AND DYNAMIC ANALYSIS

ELEM	LOC	SIG1	SIG2	TAU12	TAU23	TAU13
1	UPSF	0.0000E+00	0.2441E+05	0.7597E+04	0.4691E+04	0.7968E+04
1	DNSF	0.0000E+00	0.1950E+05	0.6535E+05	0.2818E+04	0.3124E+05
2	UPSF	0.0000E+00	0.6422E+05	0.1934E+04	0.3123E+04	0.1527E+04
2	DNSF	0.0000E+00	0.8521E+04	0.7706E+05	0.4818E+04	0.3020E+05
3	UPSF	0.0000E+00	0.6422E+05	0.1274E+05	0.1314E+05	0.2091E+05
3	DNSF	0.0000E+00	0.6422E+05	0.3065E+05	0.3087E+04	0.8182E+04
4	UPSF	0.0000E+00	0.4218E+05	0.1221E+05	0.6178E+04	0.1730E+05
4	DNSF	0.0000E+00	0.6158E+05	0.4344E+05	0.3350E+04	0.1266E+05
5	UPSF	0.0000E+00	0.6422E+05	0.6959E+04	0.4847E+04	0.4333E+04
5	DNSF	0.0000E+00	0.2633E+05	0.5682E+05	-0.3922E+03	0.4145E+05
6	UPSF	0.0000E+00	0.7644E+04	0.8334E+04	0.1464E+05	0.2094E+05
6	DNSF	0.0000E+00	0.5884E+05	0.1488E+05	0.4761E+04	0.2690E+04
7	UPSF	0.0000E+00	0.6422E+05	0.1846E+05	0.3650E+05	0.2144E+05
7	DNSF	0.0000E+00	0.6422E+05	0.6749E+04	0.1866E+04	0.1327E+04
8	UPSF	0.0000E+00	0.6422E+05	0.9764E+04	0.5181E+04	0.9108E+04
8	DNSF	0.0000E+00	0.4101E+05	0.1117E+05	-0.2490E+04	0.4896E+04

MINIMUM STRESSES FROM STATIC AND DYNAMIC ANALYSES

ELEM	LOC	SIG1	SIG2	TAU12	TAU23	TAU13
1	UPSF	-0.3608E+05	-0.4064E+05	-0.2503E+05	-0.5603E+04	-0.1426E+05
1	DNSF	-0.2378E+06	-0.4005E+05	-0.7190E+04	-0.3627E+04	-0.6612E+04
2	UPSF	-0.6730E+04	-0.1746E+05	-0.1793E+05	-0.2086E+05	-0.1704E+04
2	DNSF	-0.1939E+06	-0.1118E+06	-0.3668E+04	-0.6839E+05	-0.9874E+04
3	UPSF	-0.7638E+05	-0.5257E+05	-0.4832E+05	-0.9793E+04	-0.1416E+05
3	DNSF	-0.1237E+06	-0.3758E+05	-0.1187E+05	-0.1226E+05	-0.7822E+04
4	UPSF	-0.5486E+05	-0.5967E+05	-0.3448E+05	-0.1052E+05	-0.3406E+04
4	DNSF	-0.9224E+05	-0.4148E+05	-0.1071E+05	-0.7216E+04	-0.4579E+04
5	UPSF	-0.2783E+05	-0.3860E+05	-0.7086E+04	-0.1979E+05	-0.1341E+05
5	DNSF	-0.8565E+05	-0.9637E+05	-0.6606E+04	-0.6666E+05	-0.8205E+04
6	UPSF	-0.2635E+06	-0.9566E+05	-0.2972E+05	-0.2199E+04	-0.2045E+05
6	DNSF	-0.3923E+05	-0.8152E+04	-0.9313E+04	-0.3448E+04	-0.3790E+04
7	UPSF	-0.1645E+06	-0.1243E+06	-0.3002E+05	-0.3591E+05	-0.9956E+04
7	DNSF	-0.1538E+05	-0.6881E+04	-0.4146E+04	-0.5037E+04	-0.4562E+04
8	UPSF	-0.5672E+05	-0.6507E+05	-0.7811E+04	-0.1657E+05	-0.3251E+04
8	DNSF	-0.3021E+05	-0.7432E+05	-0.1263E+05	-0.7393E+05	-0.8404E+04

MAXIMUM OPENING AND SLIDING DISPLACEMENTS FROM STATIC AND DYNAMIC ANALYSES

ELEM	LOC	OD1	OD2	SD12	SD23	SD13
1	UPSF	0.1291E-01	0.0000E+00	0.1220E-02	0.0000E+00	0.7910E-01
1	DNSF	0.8094E-02	0.0000E+00	0.4987E-02	0.0000E+00	0.8036E-01
2	UPSF	0.1227E-01	0.3223E-01	0.1072E-02	0.0000E+00	0.3900E-01
2	DNSF	0.4637E-02	0.0000E+00	0.5731E-02	0.0000E+00	0.3221E-01
3	UPSF	0.1346E-01	0.2079E-01	0.1109E-01	0.1007E+00	-0.1931E-02
3	DNSF	0.1025E-01	0.7329E-01	0.2162E-01	0.1012E+00	-0.2100E-02
4	UPSF	0.3603E-02	0.0000E+00	0.2386E-02	0.0000E+00	0.3399E-02
4	DNSF	0.4105E-02	0.0000E+00	0.5186E-02	0.0000E+00	0.5189E-02
5	UPSF	0.4807E-02	0.3390E-01	0.3588E-02	0.0000E+00	0.4194E-01
5	DNSF	0.5482E-02	0.0000E+00	0.5975E-02	0.0000E+00	0.2901E-01
6	UPSF	0.2429E-01	0.0000E+00	0.2828E-02	0.0000E+00	0.1350E+00
6	DNSF	0.3592E-01	0.0000E+00	0.9435E-02	0.0000E+00	0.1433E+00
7	UPSF	0.2344E-02	0.8349E-02	0.1625E-02	0.6284E-01	0.6662E-03
7	DNSF	0.1208E-01	0.8409E-01	0.6187E-02	0.6482E-01	0.1776E-02

8	UPSF	0.8755E-03	0.2275E-01	0.1046E-01	0.0000E+00	0.3064E-02
8	DNSF	0.8159E-03	0.0000E+00	0.3274E-02	0.0000E+00	0.2460E-02

MINIMUM OPENING AND SLIDING DISPLACEMENTS FROM STATIC AND DYNAMIC ANALYSES

ELEM	LOC	OD1	OD2	SD12	SD23	SD13
1	UPSF	0.0000E+00	0.0000E+00	-0.1810E-01	0.0000E+00	-0.2549E-01
1	DNSF	0.0000E+00	0.0000E+00	-0.6591E-02	0.0000E+00	-0.2466E-01
2	UPSF	0.0000E+00	0.0000E+00	-0.4309E-01	-0.3311E-01	-0.5232E-02
2	DNSF	0.0000E+00	0.0000E+00	-0.3362E-02	0.0000E+00	-0.6006E-02
3	UPSF	0.0000E+00	0.0000E+00	-0.3348E-01	-0.4346E-02	-0.1688E+00
3	DNSF	0.0000E+00	0.0000E+00	-0.1294E+00	-0.4994E-02	-0.1749E+00
4	UPSF	0.0000E+00	0.0000E+00	-0.5708E-02	0.0000E+00	-0.3195E-01
4	DNSF	0.0000E+00	0.0000E+00	-0.9814E-02	0.0000E+00	-0.3440E-01
5	UPSF	0.0000E+00	0.0000E+00	-0.3577E-01	-0.3693E-01	-0.4452E-02
5	DNSF	0.0000E+00	0.0000E+00	-0.6055E-02	0.0000E+00	-0.3669E-02
6	UPSF	0.0000E+00	0.0000E+00	-0.6471E-02	0.0000E+00	-0.1112E+00
6	DNSF	0.0000E+00	0.0000E+00	-0.8537E-02	0.0000E+00	-0.1243E+00
7	UPSF	0.0000E+00	0.0000E+00	-0.2245E-01	-0.1997E-01	-0.4354E-01
7	DNSF	0.0000E+00	0.0000E+00	-0.8337E-01	-0.2739E-01	-0.4634E-01
8	UPSF	0.0000E+00	0.0000E+00	-0.1476E-04	-0.3392E-01	-0.7222E-02
8	DNSF	0.0000E+00	0.0000E+00	-0.3173E-02	0.0000E+00	-0.8590E-02

Log File

This file shows the number of iterations to reach convergence in each load step of the static analysis and in each time step of the dynamic analysis. Only once was the automatic step division capability needed (time step 234). The load steps of the static analysis averaged 17 iterations, and the time steps usually required only a few iterations.

```
  ****************************** STATIC ANALYSIS ********************************

       STATIC STEP NUMBER   1
NPOS =  64  NITER =  7  FMAX = 0.345E+02  ZMAX = 0.727E+03

       STATIC STEP NUMBER   2
NPOS =  64  NITER = 21  FMAX = 0.409E+02  ZMAX = 0.171E+04

       STATIC STEP NUMBER   3
NPOS =  64  NITER = 25  FMAX = 0.268E+02  ZMAX = 0.139E+04

       STATIC STEP NUMBER   4
NPOS =  64  NITER = 23  FMAX = 0.528E+02  ZMAX = 0.170E+04

       STATIC STEP NUMBER   5
NPOS =  64  NITER = 19  FMAX = 0.536E+02  ZMAX = 0.175E+04

       STATIC STEP NUMBER   6
NPOS =  64  NITER =  6  FMAX = 0.616E+02  ZMAX = 0.635E+03

RESTART INFORMATION WRITTEN ON UNIT 9 AFTER STATIC ANALYSIS



  ***************************** DYNAMIC ANALYSIS ********************************

TIME STEP NUMBER     1   (TIME =  0.005)
NPOS = 64  NITER =  2  FMAX=  0.527E+01  ZMAX = 0.174E+03

TIME STEP NUMBER     2   (TIME =  0.010)
NPOS = 64  NITER =  2  FMAX=  0.580E+00  ZMAX = 0.560E+01

TIME STEP NUMBER     3   (TIME =  0.015)
NPOS = 64  NITER =  2  FMAX=  0.137E+01  ZMAX = 0.175E+02

TIME STEP NUMBER     4   (TIME =  0.020)
NPOS = 64  NITER =  2  FMAX=  0.273E+01  ZMAX = 0.395E+02

   (Output deleted to save space.)

TIME STEP NUMBER   232   (TIME =  1.160)
NPOS = 64  NITER =  6  FMAX=  0.239E+01  ZMAX = 0.185E+03

TIME STEP NUMBER   233   (TIME =  1.165)
NPOS = 64  NITER =  6  FMAX=  0.318E+02  ZMAX = 0.892E+03

TIME STEP NUMBER   234   (TIME =  1.170)
NPOS = 16  NITER =  3  FMAX=  0.283E+01  ZMAX = 0.199E+03
NPOS = 64  NITER =  3  FMAX=  0.940E+02  ZMAX = 0.107E+04

TIME STEP NUMBER   235   (TIME =  1.175)
```

```
NPOS = 64  NITER =  7  FMAX=  0.447E+02  ZMAX = 0.136E+04

TIME STEP NUMBER   236   (TIME =  1.180)
NPOS = 64  NITER =  3  FMAX=  0.455E+02  ZMAX = 0.938E+03

TIME STEP NUMBER   237   (TIME =  1.185)
NPOS = 64  NITER = 10  FMAX=  0.240E+02  ZMAX = 0.740E+03

TIME STEP NUMBER   238   (TIME =  1.190)
NPOS = 64  NITER =  5  FMAX=  0.575E+01  ZMAX = 0.166E+03

TIME STEP NUMBER   251   (TIME =  1.255)
NPOS = 64  NITER = 12  FMAX=  0.233E+02  ZMAX = 0.101E+04

TIME STEP NUMBER   252   (TIME =  1.260)
NPOS = 64  NITER =  3  FMAX=  0.196E+01  ZMAX = 0.735E+02

   (Output deleted to save space.)

TIME STEP NUMBER   293   (TIME =  1.465)
NPOS = 64  NITER =  4  FMAX=  0.117E+02  ZMAX = 0.100E+04

TIME STEP NUMBER   294   (TIME =  1.470)
NPOS = 64  NITER =  5  FMAX=  0.297E+01  ZMAX = 0.281E+03

TIME STEP NUMBER   295   (TIME =  1.475)
NPOS = 64  NITER = 18  FMAX=  0.367E+02  ZMAX = 0.133E+04

TIME STEP NUMBER   296   (TIME =  1.480)
NPOS = 64  NITER =  7  FMAX=  0.148E+02  ZMAX = 0.564E+03

TIME STEP NUMBER   297   (TIME =  1.485)
NPOS = 64  NITER =  4  FMAX=  0.341E+01  ZMAX = 0.242E+03

TIME STEP NUMBER   298   (TIME =  1.490)
NPOS = 64  NITER =  4  FMAX=  0.838E+01  ZMAX = 0.540E+03

TIME STEP NUMBER   299   (TIME =  1.495)
NPOS = 64  NITER =  3  FMAX=  0.267E+02  ZMAX = 0.163E+04

TIME STEP NUMBER   300   (TIME =  1.500)
NPOS = 64  NITER = 17  FMAX=  0.359E+02  ZMAX = 0.128E+04

TIME STEP NUMBER   301   (TIME =  1.505)
NPOS = 64  NITER =  8  FMAX=  0.505E+02  ZMAX = 0.179E+04

TIME STEP NUMBER   302   (TIME =  1.510)
NPOS = 64  NITER =  4  FMAX=  0.104E+02  ZMAX = 0.382E+03

   (Output deleted to save space.)

TIME STEP NUMBER   498   (TIME =  2.490)
NPOS = 64  NITER =  3  FMAX=  0.208E+01  ZMAX = 0.580E+02

TIME STEP NUMBER   499   (TIME =  2.495)
NPOS = 64  NITER =  3  FMAX=  0.187E+01  ZMAX = 0.542E+02
```

```
TIME STEP NUMBER   500   (TIME =  2.500)
NPOS = 64  NITER =  3  FMAX=  0.156E+01  ZMAX = 0.473E+02

RESTART INFORMATION WRITTEN ON UNIT 9 AT TIME STEP   500

TIME STEP NUMBER   501   (TIME =  2.505)
NPOS = 64  NITER =  2  FMAX=  0.564E+02  ZMAX = 0.117E+04

TIME STEP NUMBER   502   (TIME =  2.510)
NPOS = 64  NITER =  2  FMAX=  0.754E+02  ZMAX = 0.108E+04

   (Output deleted to save space.)

TIME STEP NUMBER   748   (TIME =  3.740)
NPOS = 64  NITER =  3  FMAX=  0.165E+01  ZMAX = 0.717E+02

TIME STEP NUMBER   749   (TIME =  3.745)
NPOS = 64  NITER =  3  FMAX=  0.142E+01  ZMAX = 0.517E+02

TIME STEP NUMBER   750   (TIME =  3.750)
NPOS = 64  NITER =  3  FMAX=  0.960E+00  ZMAX = 0.299E+02

TIME STEP NUMBER   751   (TIME =  3.755)
NPOS = 64  NITER =  3  FMAX=  0.102E+01  ZMAX = 0.349E+02

TIME STEP NUMBER   752   (TIME =  3.760)
NPOS = 64  NITER =  3  FMAX=  0.100E+01  ZMAX = 0.248E+02

   (Output deleted to save space.)

TIME STEP NUMBER   996   (TIME =  4.980)
NPOS = 64  NITER =  3  FMAX=  0.192E+02  ZMAX = 0.391E+03

TIME STEP NUMBER   997   (TIME =  4.985)
NPOS = 64  NITER =  2  FMAX=  0.131E+03  ZMAX = 0.167E+04

TIME STEP NUMBER   998   (TIME =  4.990)
NPOS = 64  NITER =  2  FMAX=  0.115E+03  ZMAX = 0.973E+03

TIME STEP NUMBER   999   (TIME =  4.995)
NPOS = 64  NITER =  3  FMAX=  0.173E+01  ZMAX = 0.172E+02

TIME STEP NUMBER  1000   (TIME =  5.000)
NPOS = 64  NITER =  5  FMAX=  0.117E+02  ZMAX = 0.498E+03

RESTART INFORMATION WRITTEN ON UNIT 9 AT TIME STEP  1000
```

5. SEISMIC RESPONSE OF A LARGE ARCH DAM

The purpose of this study is to demonstrate some features of the formulation and to document some typical response characteristics of an arch dam. The particular dam considered here has a nearly full reservoir, and its geometry is similar to that of Pacoima Dam located in the San Gabriel Mountains north of Los Angeles. Use of these results to assess the seismic safety of Pacoima Dam must consider that this dam has a spillway tunnel 60 feet below the crest, and so the case analyzed here corresponds to an unlikely simultaneous occurrence of flood and earthquake.

The dam is a 335-foot high arch whose thickness at the crown section varies from 10 feet at the crest to 90 feet at the base. It is analyzed here using the meshes of Figures 17 and 18. In the static analysis each of the six rows of dam elements is added by a construction step, and then the reservoir is filled to within 35 feet of the crest (at the base of the top row of elements) in another five water level steps. The dynamic analysis is conducted at this reservoir condition using a scaled-down version of the ground motions recorded above the left abutment of Pacoima Dam during the 1971 San Fernando earthquake (Figure 19). The same scale factor is applied to all three components of the ground motion to produce a peak acceleration of 0.80g. This peak acceleration occurs in the cross-stream component.

Particulars of the analysis are DT = 0.001 sec, SMINS = 0.0, SMAXS = 0.1, SMIND = 0.0, SMAXD = 0.01, ALPHA = –0.2, GAMMA = 0.70, BETA = 0.36, FTOL = 10 lbs and ZTOL = 200 ft-lbs. The value for DT resulted from a study as that value below which no significant changes occurred in the results. Regarding the tolerances FTOL and ZTOL, although these are smaller than necessary, according to Note H in Section 3.2.3, they do not lead to excessive iterations. Material properties for the dam are EE = 3×10^6 psi, PR = 0.20, WT = 150 lbs/ft^3, TEN = 550 psi, TRF = 0.1 and BINT = 0.05 sec. Keys are omitted for shear components 12 (in-plane shear) and 23 (crack shear) but included for shear component 13 (contraction-joint shear). Friction coefficients are COEF(1) = 0.50 and COEF(2) = 0.75. The shear retention coefficient is ALPS = 0.25. Internal water pressure is included by Option 1 (IPRES=1). For the foundation, EE = 2×10^6 psi and PR = 0.25. For the water, WW = 62.4 lbs/ft^3. Stiffness and mass-proportional damping, computed to give ξ = 5% at frequencies of

4 Hz and 16 Hz, is used for the dam-foundation system. Fundamental frequencies of the dam-foundation system are 4.96 Hz for the stream-direction mode and 4.99 Hz for the cross-stream-direction mode.

The situation defined above is denoted as Case N1 and the corresponding linear case, obtained by removing the contraction joints and restraining cracking, as Case L1. Time histories of various responses are presented in Figure 20. Maximum values of arch and cantilever stresses for the linear analysis, both compressive and tensile, are shown in Figure 21. For the nonlinear analysis, maximum values of arch compressive stress, joint opening, joint sliding (13 component), cantilever tensile stress, crack opening, and crack sliding (23 component) are shown in Figure 22. Figures 21 and 22 were made by post-processing the response pictures from Unit 3. Each value listed in the figures corresponds to an element in the dam mesh and is the largest value from either the upstream or downstream face of the element. A cantilever tension of 0.55 ksi in Figure 22 indicates cracking.

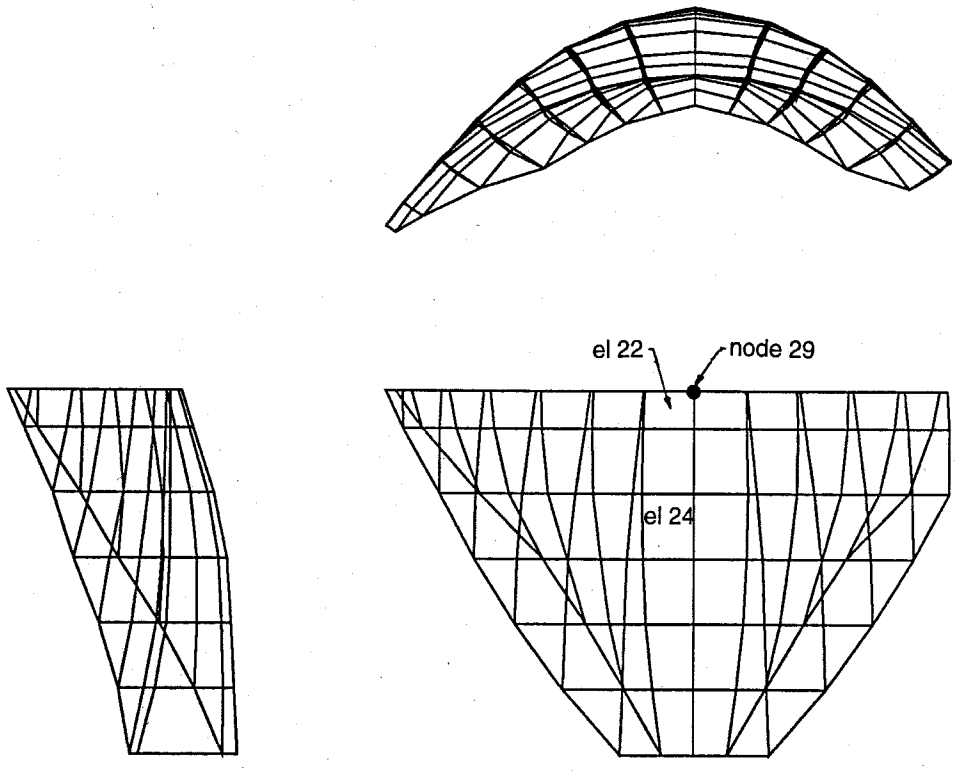

Figure 17. Finite element mesh of dam shown in plan (top), downstream elevation (bottom, right) and cross-stream elevation (bottom, left).

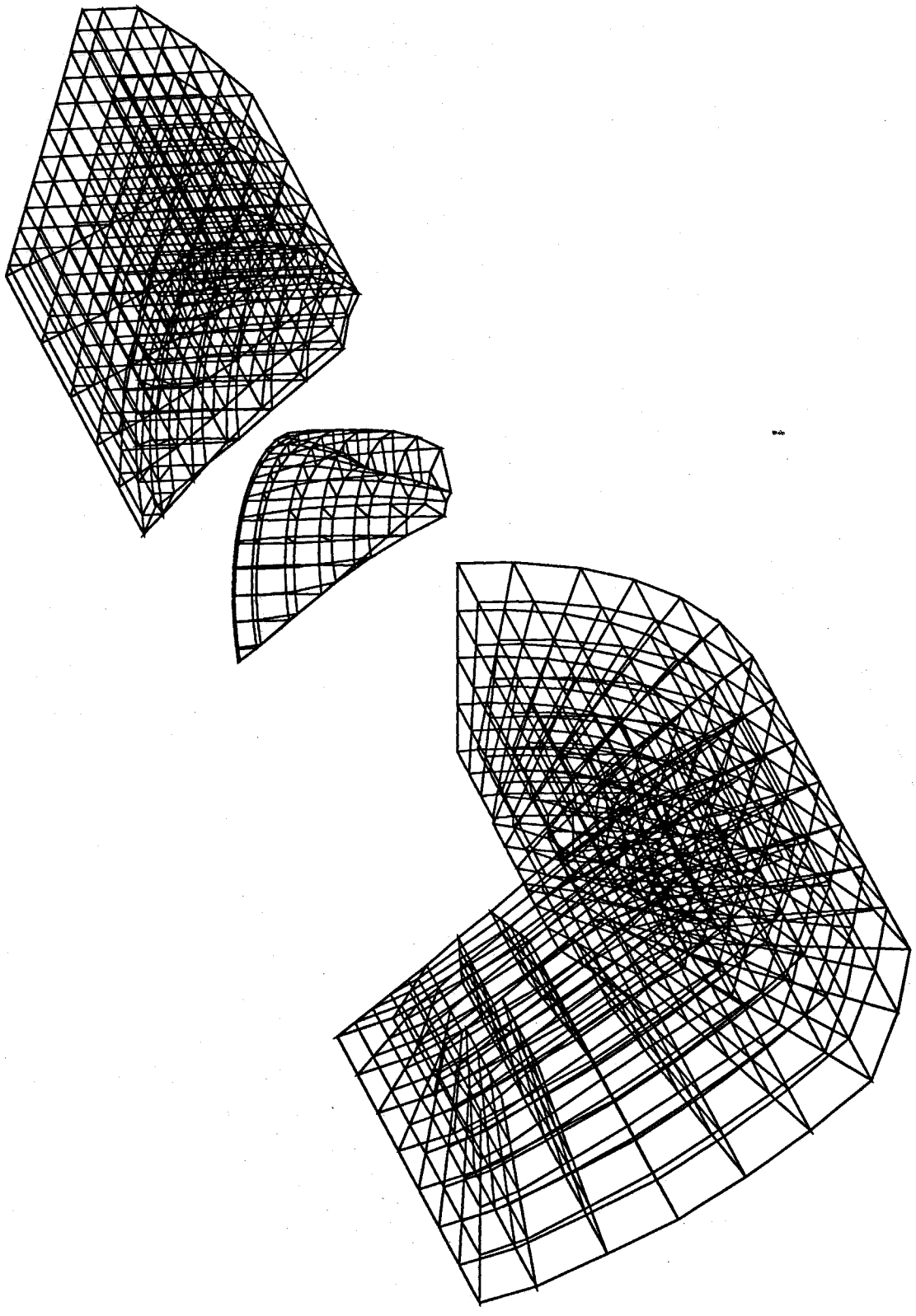

Figure 18. Foundation, dam and water meshes

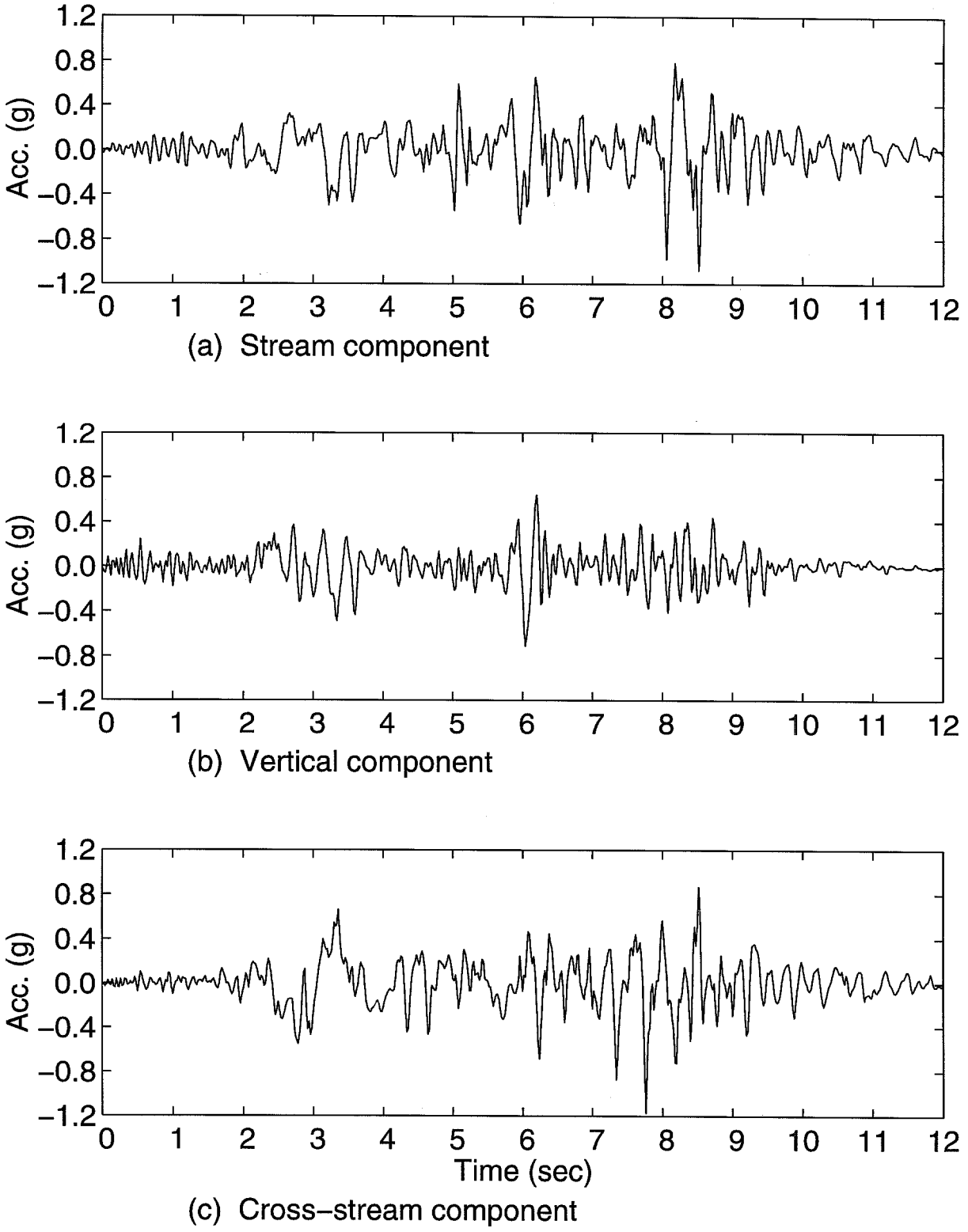

Figure 19. Ground motions recorded above the left abutment of Pacoima Dam during the 1971 San Fernando earthquake.

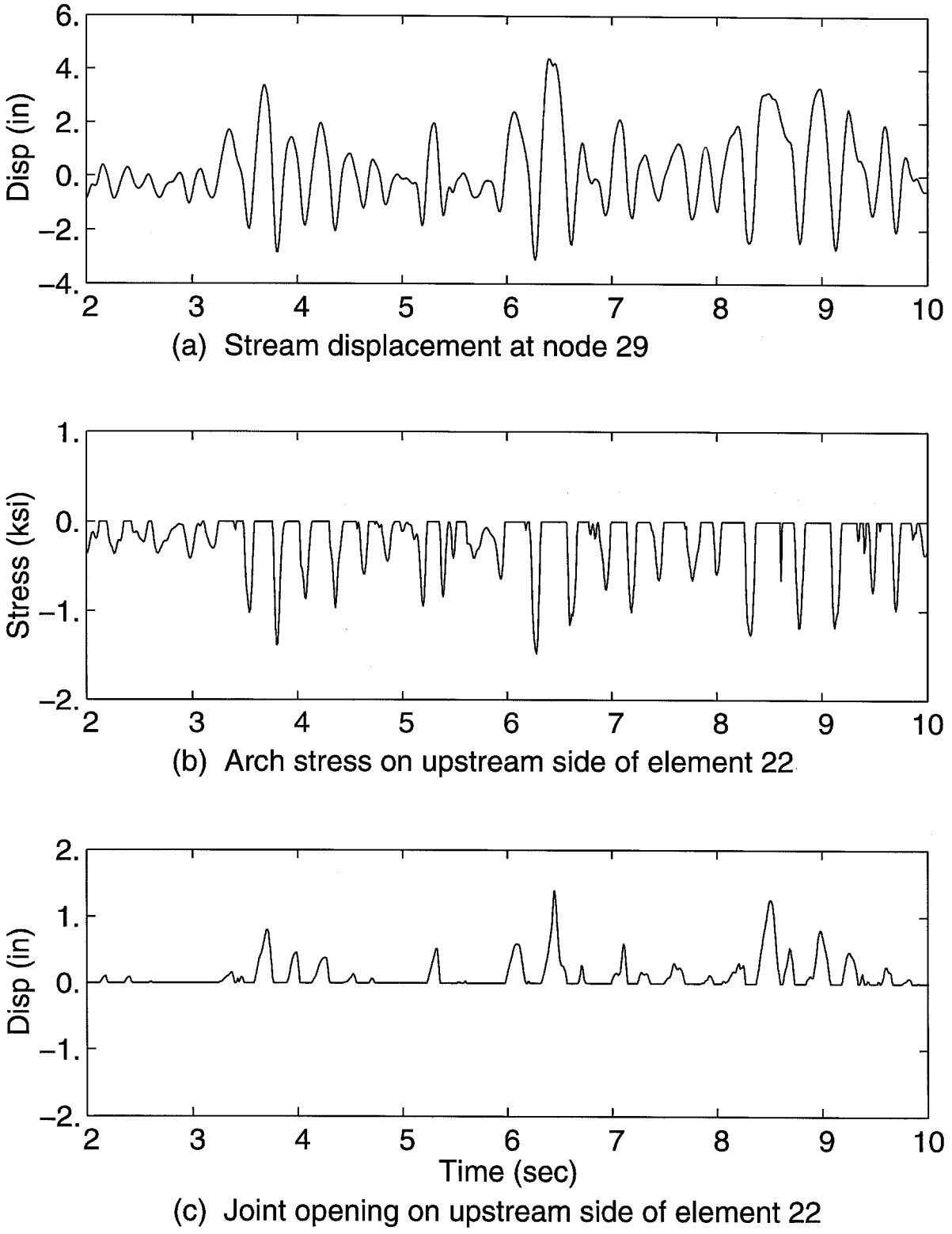

Figure 20. Selected time history responses for Case N1.

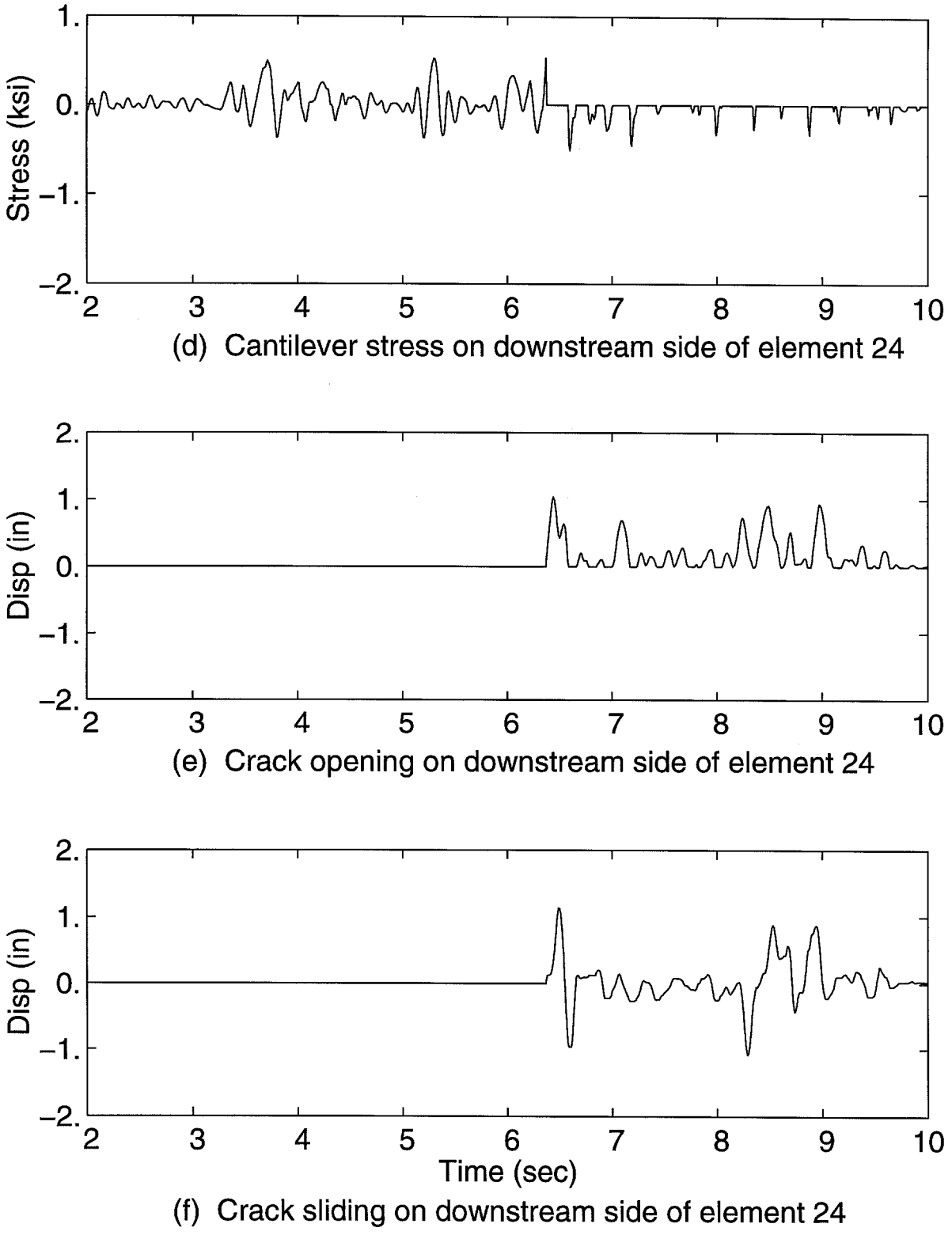

Figure 20. Continued.

```
-0.58 -0.88 -0.96 -0.93 -0.99 -1.27 -1.63 -1.40 -1.25 -1.14 -1.20 -1.13
      -0.93 -1.04 -0.99 -1.04 -0.99 -1.23 -1.11 -0.94 -1.18 -1.05 -0.99
            -0.94 -0.91 -0.87 -0.69 -0.86 -0.83 -0.70 -0.95 -0.81 -0.71
                  -0.79 -0.62 -0.44 -0.56 -0.57 -0.51 -0.66 -0.64
       (a).
                        -0.42 -0.28 -0.30 -0.31 -0.33 -0.48
 Arch compression (ksi)
                              -0.15 -0.10 -0.11 -0.17

 0.34  0.63  0.65  0.61  0.95  0.96  0.99  0.89  0.95  0.99  0.62  1.03
       0.77  0.73  0.65  0.87  0.74  0.68  0.89  0.69  0.68  0.62  0.91
             0.74  0.49  0.74  0.49  0.47  0.62  0.53  0.50  0.54  0.62
                   0.48  0.40  0.35  0.27  0.28  0.37  0.39  0.43
       (b).
                         0.26  0.19  0.13  0.12  0.23  0.29
 Arch tension (ksi)
                               0.11  0.08  0.05  0.13

-0.11 -0.23 -0.28 -0.27 -0.25 -0.31 -0.40 -0.43 -0.34 -0.28 -0.20 -0.14
      -0.45 -0.51 -0.56 -0.48 -0.60 -0.73 -0.77 -0.67 -0.53 -0.40 -0.23
            -0.48 -0.50 -0.53 -0.60 -0.74 -0.68 -0.60 -0.53 -0.44 -0.35
                  -0.50 -0.50 -0.53 -0.63 -0.60 -0.53 -0.42 -0.40
       (c).
                        -0.43 -0.49 -0.54 -0.51 -0.46 -0.36
 Cantilever compression (ksi)
                              -0.37 -0.36 -0.40 -0.35

 0.10  0.19  0.24  0.23  0.20  0.34  0.43  0.36  0.30  0.22  0.16  0.12
       0.40  0.47  0.50  0.40  0.61  0.72  0.65  0.57  0.40  0.39  0.27
             0.49  0.51  0.38  0.51  0.58  0.54  0.49  0.36  0.40  0.32
                   0.40  0.41  0.38  0.40  0.33  0.35  0.30  0.28
       (d).
                         0.37  0.36  0.31  0.24  0.28  0.26
 Cantilever tension (ksi)
                               0.28  0.29  0.29  0.25
```

Figure 21. Distributions of maximum responses for Case L1 linear analysis.

```
-0.58 -0.72 -0.90 -1.06 -1.18 -1.15 -1.47 -1.33 -1.16 -1.37 -1.34 -0.89
      -0.70 -0.90 -1.12 -1.14 -0.97 -1.70 -1.38 -0.92 -1.26 -1.13 -0.85
            -0.91 -1.00 -0.83 -0.81 -1.10 -1.03 -0.70 -0.90 -0.96 -0.81
                  -0.96 -0.79 -0.48 -0.77 -0.76 -0.56 -0.87 -0.91
      (a).                  -0.72 -0.40 -0.43 -0.46 -0.41 -0.64
Arch compression (ksi)            -0.30 -0.15 -0.18 -0.28

0.08  0.13  0.35  0.54  0.40  0.47  1.40  1.23  0.53  0.83  0.47  0.41
      0.18  0.26  0.37  0.77  0.45  0.85  0.79  0.44  1.05  0.47  0.43
            0.30  0.38  0.38  0.16  0.37  0.34  0.24  0.82  0.47  0.39
                  0.53  0.32  0.12  0.14  0.22  0.12  0.48  0.60
      (b).                  0.41  0.09  0.06  0.07  0.12  0.47
Joint opening (in)                0.14  0.05  0.03  0.22

0.00  0.00  0.00  0.00  0.00  0.00  0.00  0.00  0.00  0.00  0.00  0.00
      0.00  0.00  0.00  0.00  0.00  0.00  0.00  0.00  0.00  0.00  0.00
            0.00  0.00  0.00  0.00  0.00  0.00  0.00  0.00  0.00  0.00
                  0.00  0.00  0.00  0.00  0.00  0.00  0.00  0.00
      (c).                  0.00  0.00  0.00  0.00  0.00  0.00
Joint sliding (in)                0.00  0.00  0.00  0.00

0.49  0.23  0.32  0.23  0.45  0.46  0.55  0.55  0.40  0.44  0.31  0.29
      0.28  0.33  0.40  0.47  0.55  0.52  0.49  0.55  0.48  0.26  0.20
            0.23  0.33  0.51  0.55  0.55  0.55  0.55  0.35  0.21  0.32
                  0.35  0.34  0.43  0.53  0.54  0.39  0.20  0.24
      (d).                  0.32  0.32  0.32  0.30  0.21  0.22
Cantilever tension (ksi)          0.30  0.36  0.31  0.26

0.00  0.00  0.00  0.00  0.00  0.00  1.54  1.56  0.00  0.00  0.00  0.00
      0.00  0.00  0.00  0.00  0.27  0.00  0.00  0.26  0.00  0.00  0.00
            0.00  0.00  0.00  0.60  1.04  1.02  0.52  0.00  0.00  0.00
                  0.00  0.00  0.00  0.00  0.00  0.00  0.00  0.00
      (e).                  0.00  0.00  0.00  0.00  0.00  0.00
Crack opening (in)                0.00  0.00  0.00  0.00

0.00  0.00  0.00  0.00  0.00  0.00  1.93  1.91  0.00  0.00  0.00  0.00
      0.00  0.00  0.00  0.00  0.24  0.00  0.00  0.24  0.00  0.00  0.00
            0.00  0.00  0.00 -0.68  1.14  1.05 -0.44  0.00  0.00  0.00
                  0.00  0.00  0.00  0.00  0.00  0.00  0.00  0.00
      (f).                  0.00  0.00  0.00  0.00  0.00  0.00
Crack sliding (in)                0.00  0.00  0.00  0.00
```

Figure 22. Distributions of maximum responses for Case N1 nonlinear analysis.

The size and extent of the tensile stresses from the linear analysis (Figure 21) indicate that considerable joint opening and cracking will occur in the nonlinear analysis. In fact, as shown in Figure 22, cracks occur in 8 elements, and maximum values are 1.40 inches for joint opening, 1.56 inches for crack opening, and 1.93 inches for crack sliding. The maximum compressive stress is -1.70 ksi.

Sixteen other nonlinear analyses were run as listed below (cases N2 through N17).

N2: water free-surface level 215 feet below the crest
N3: dam thickened in its upper portion to 40 feet at the crest
N4: contraction-joint keys (13 component) removed
N5: friction coefficients increased to COEF(1) = 0.75 and COEF(2) = 1.00
N6: internal water pressure omitted (IPRES = 0)
N7: internal water pressure included by Option 2 (IPRES = 2, PINT = 0.5 sec)
N8: ALPS = 0.00
N9: ALPS = 0.50
N10: stiffness-proportional damping only (5% at 4 Hz)
N11: DT = 0.002 sec
N12: DT = 0.005 sec
N13: DT = 0.010 sec
N14: FTOL = 270 lb, ZTOL = 1,350 ft-lb (according to note H)
N15: x and z ground motion components switched
N16: peak ground acceleration scaled to 0.6g
N17: peak ground acceleration scaled to 1.0g

All of these cases are modifications of Case N1 as indicated. Corresponding linear analyses (denoted by an L prefix) for some of these cases were also run. Results are summarized in Tables 1 and 2, and charts of maximum responses simlar to Figures 21 and 22 for Cases L1 and N1 are included for Cases L2, N2, L3, N3, N4, N5, L6, N6, N7, N8, N9, L10, N10, L15, N15, L16, N16, L17 and N17 in Figures 23 to 41, respectively. Note that cases L1, L4, L5, L7, L8, L9 and L14 are identical.

The results in Tables 1 and 2 and in Figures 21 to 41 demonstrate the importance of various parameters. If the extent of cracking is chosen as an indicator of the severity of the damage, then the damage increases with higher water level, absence of keys in the contraction joints, lower value of ALPS and (obviously) stronger ground motion. Results for ALPS = 0 (Case N8) show that the dam elements slide away from the abutments, as indicated by the

larger joint openings there. This tends to overload the central cantilevers and produce more cracking, a tendency that is reduced in Cases N1 and N9 where ALPS is greater than zero.

Sensitivity to the time step DT, as revealed by Cases N1 and N11 to N13, owes to the cracking capability of the nonlinear model. If a change in DT is enough to cause an element previously on the verge of cracking to now crack, then significant differences in the response can result. In the nonlinear analyses, the cracking response did not converge until DT was reduced to 0.002 sec (Case N11), and thus reducing DT to 0.001 sec (Case N1) produced little further change.

In all of the analyses, the computer program shows that the dam survives, even for Case N17 where the response is quite severe. This does not mean that one should allow the dam to be operated with a 300-foot water depth if the 1g earthquake was the ground motion to be considered. Judgment, with consideration of the points in Section 2.5, is required.

All of the analyses were run on a DEC 3000 Model 400 computer with a 100 MIPS processor. The nonlinear analyses each took between 70 and 80 minutes of CPU time except that Cases N11, N12 and N13 with the longer time steps took 42, 25 and 17 minutes, respectively. Increasing the tolerances (Case N14) saved only 2 minutes. Each linear analysis took 13 minutes with DT = 0.001 sec. The value of MTOT required to run this problem was 1.11 million, and most of this was needed for the foundation.

Table 1. Peak stresses in the dam for the linear cases.

Case	Arch compression (ksi)	Arch tension (ksi)	Cantilever compression (ksi)	Cantilever tension (ksi)
L1,L4,L5,L7,L8,L9,L14	-1.63	1.03	-0.77	0.72
L2	-0.88	0.93	-0.46	0.47
L3	-1.33	1.08	-1.05	0.57
L6	-1.63	1.05	-0.78	0.71
L10	-1.15	0.71	-0.53	0.37
L11	-1.63	1.03	-0.77	0.72
L12	-1.63	1.01	-0.75	0.73
L13	-1.59	0.97	-0.76	0.73
L15	-1.89	1.44	-0.86	0.71
L16	-1.26	0.73	-0.60	0.52
L17	-2.01	1.32	-0.95	0.92

Table 2. Peak responses in the dam for the nonlinear cases.

Case	Arch compression (ksi)	Number of elements cracked	Joint opening (in)	Joint sliding (in)	Crack opening (in)	Crack sliding (in)
N1	-1.70	8	1.40	—	1.56	1.93
N2	-1.16	2	1.08	—	0.25	-0.39
N3	-1.43	8	1.71	—	0.76	1.92
N4	-2.27	12	1.36	-4.64	1.24	-1.39
N5	-1.67	8	1.34	—	1.37	1.74
N6	-1.70	9	1.16	—	1.14	-1.42
N7	-1.69	8	1.22	—	0.94	-1.10
N8	-1.71	16	1.71	—	3.56	-5.01
N9	-2.09	7	1.97	—	1.80	3.14
N10	-1.71	4	1.21	—	0.58	0.87
N11	-1.70	8	1.39	—	1.58	1.74
N12	-1.67	9	1.47	—	1.08	1.16
N13	-1.58	12	1.77	—	1.28	-1.21
N14	-1.70	8	1.40	—	1.56	1.93
N15	-1.62	9	1.59	—	1.91	-2.27
N16	-1.36	4	0.90	—	1.07	-1.03
N17	-3.19	17	2.19	—	3.58	-2.66

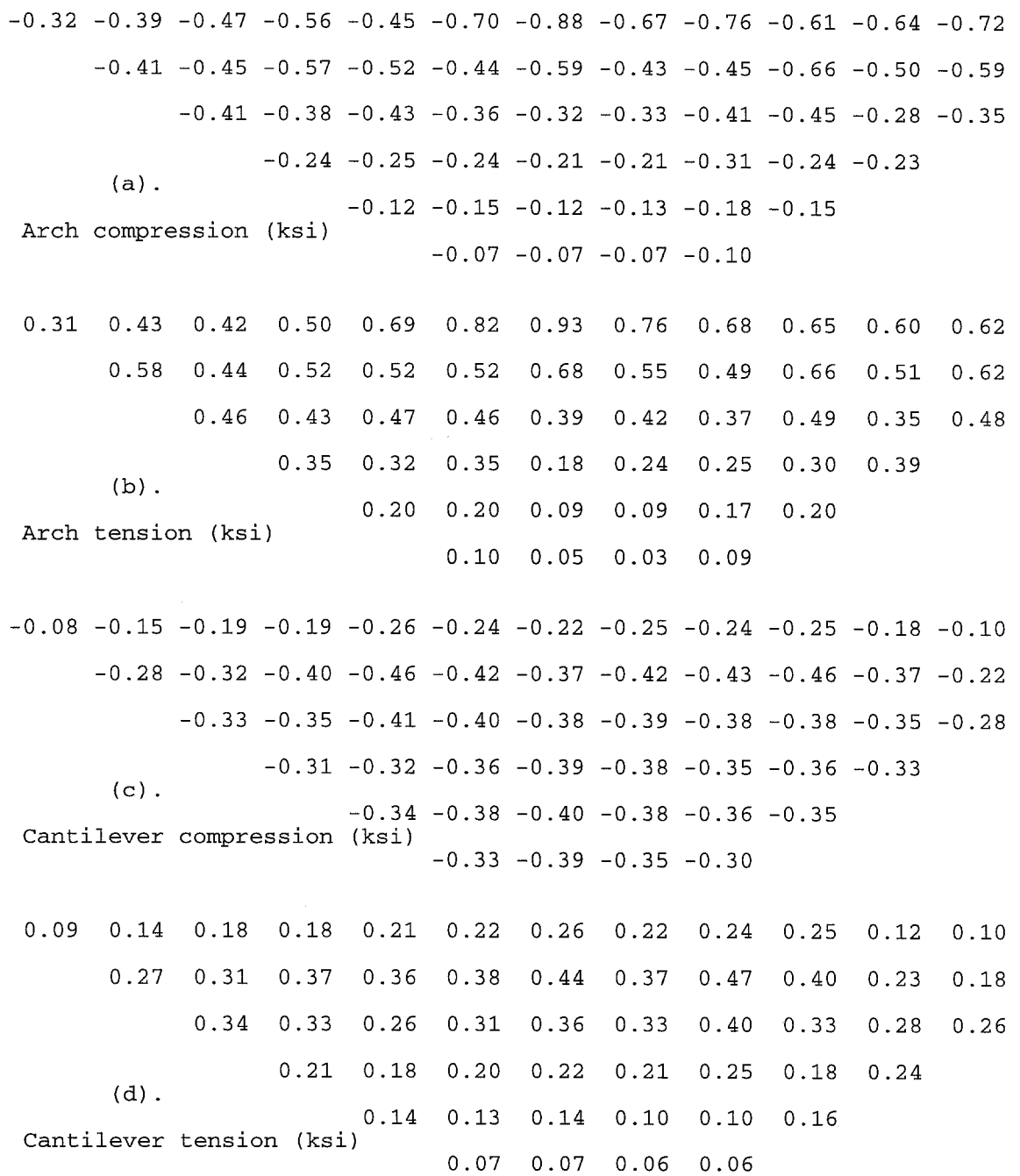

Figure 23. Distributions of maximum responses for Case L2 linear analysis.

```
-0.56 -0.50 -0.73 -0.82 -0.94 -0.93 -1.16 -1.04 -0.92 -0.85 -1.11 -0.77
      -0.46 -0.54 -0.75 -0.77 -0.83 -0.97 -0.82 -0.72 -0.85 -0.83 -0.59
            -0.46 -0.62 -0.55 -0.57 -0.56 -0.54 -0.56 -0.62 -0.48 -0.45
                  -0.61 -0.46 -0.33 -0.41 -0.57 -0.38 -0.39 -0.45
      (a).                  -0.48 -0.27 -0.42 -0.45 -0.33 -0.45
Arch compression (ksi)                -0.28 -0.31 -0.33 -0.21

0.13  0.19  0.46  0.75  0.61  0.47  0.95  1.08  0.61  0.68  0.61  0.54
      0.22  0.35  0.67  0.64  0.41  0.92  0.94  0.47  0.77  0.61  0.43
            0.37  0.57  0.69  0.30  0.73  0.77  0.40  0.87  0.61  0.31
                  0.70  0.68  0.16  0.31  0.46  0.29  0.94  0.64
      (b).                  0.67  0.16  0.13  0.16  0.23  1.06
Joint opening (in)                    0.26  0.03  0.02  0.44

0.00  0.00  0.00  0.00  0.00  0.00  0.00  0.00  0.00  0.00  0.00  0.00
      0.00  0.00  0.00  0.00  0.00  0.00  0.00  0.00  0.00  0.00  0.00
            0.00  0.00  0.00  0.00  0.00  0.00  0.00  0.00  0.00  0.00
                  0.00  0.00  0.00  0.00  0.00  0.00  0.00  0.00
      (c).                  0.00  0.00  0.00  0.00  0.00  0.00
Joint sliding (in)                    0.00  0.00  0.00  0.00

0.20  0.33  0.39  0.28  0.33  0.31  0.34  0.33  0.36  0.22  0.26  0.16
      0.39  0.36  0.32  0.42  0.42  0.55  0.55  0.48  0.33  0.32  0.19
            0.30  0.36  0.42  0.44  0.47  0.40  0.32  0.32  0.26  0.20
                  0.31  0.46  0.41  0.38  0.37  0.34  0.33  0.22
      (d).                  0.39  0.45  0.39  0.36  0.37  0.27
Cantilever tension (ksi)              0.43  0.45  0.45  0.45

0.00  0.00  0.00  0.00  0.00  0.00  0.00  0.00  0.00  0.00  0.00  0.00
      0.00  0.00  0.00  0.00  0.00  0.21  0.25  0.00  0.00  0.00  0.00
            0.00  0.00  0.00  0.00  0.00  0.00  0.00  0.00  0.00  0.00
                  0.00  0.00  0.00  0.00  0.00  0.00  0.00  0.00
      (e).                  0.00  0.00  0.00  0.00  0.00  0.00
Crack opening (in)                    0.00  0.00  0.00  0.00

0.00  0.00  0.00  0.00  0.00  0.00  0.00  0.00  0.00  0.00  0.00  0.00
      0.00  0.00  0.00  0.00  0.00 -0.39 -0.32  0.00  0.00  0.00  0.00
            0.00  0.00  0.00  0.00  0.00  0.00  0.00  0.00  0.00  0.00
                  0.00  0.00  0.00  0.00  0.00  0.00  0.00  0.00
      (f).                  0.00  0.00  0.00  0.00  0.00  0.00
Crack sliding (in)                    0.00  0.00  0.00  0.00
```

Figure 24. Distributions of maximum responses for Case N2 nonlinear analysis.

```
-0.56 -0.79 -0.97 -1.02 -0.91 -1.29 -1.33 -1.24 -1.14 -1.08 -1.02 -1.20
      -0.74 -0.89 -0.85 -0.82 -0.94 -1.02 -0.86 -0.77 -0.99 -0.87 -0.89
            -0.74 -0.69 -0.68 -0.55 -0.70 -0.80 -0.66 -0.78 -0.65 -0.63
                  -0.65 -0.64 -0.45 -0.66 -0.71 -0.46 -0.59 -0.72
       (a).
                        -0.55 -0.37 -0.40 -0.42 -0.32 -0.54
 Arch compression (ksi)
                              -0.22 -0.11 -0.11 -0.19

 0.44  0.61  0.60  0.72  0.79  0.79  0.80  1.08  0.88  0.89  0.81  0.87
       0.73  0.58  0.51  0.64  0.62  0.56  0.74  0.69  0.77  0.69  0.75
             0.61  0.48  0.51  0.43  0.52  0.57  0.50  0.56  0.52  0.54
                   0.52  0.46  0.29  0.40  0.38  0.34  0.42  0.48
       (b).
                         0.34  0.21  0.17  0.16  0.21  0.35
 Arch tension (ksi)
                               0.11  0.07  0.06  0.13

-0.12 -0.12 -0.10 -0.11 -0.11 -0.12 -0.13 -0.14 -0.14 -0.12 -0.12 -0.10
      -0.36 -0.33 -0.38 -0.41 -0.52 -0.61 -0.65 -0.61 -0.50 -0.39 -0.27
            -0.46 -0.50 -0.62 -0.76 -0.95 -1.05 -0.92 -0.67 -0.47 -0.35
                  -0.48 -0.58 -0.67 -0.79 -0.88 -0.73 -0.47 -0.38
       (c).
                        -0.45 -0.55 -0.58 -0.56 -0.51 -0.41
 Cantilever compression (ksi)
                              -0.45 -0.50 -0.52 -0.45

 0.12  0.14  0.07  0.09  0.10  0.09  0.08  0.07  0.08  0.09  0.08  0.05
       0.36  0.34  0.30  0.34  0.41  0.39  0.36  0.38  0.36  0.30  0.19
             0.43  0.38  0.41  0.49  0.55  0.57  0.54  0.43  0.30  0.24
                   0.31  0.31  0.38  0.37  0.42  0.40  0.28  0.24
       (d).
                         0.25  0.25  0.24  0.17  0.20  0.23
 Cantilever tension (ksi)
                               0.22  0.22  0.22  0.20
```

Figure 25. Distributions of maximum responses for Case L3 linear analysis.

```
-0.76 -0.89 -1.10 -1.09 -0.85 -1.22 -1.43 -1.29 -1.00 -1.20 -1.30 -0.85
      -0.81 -0.93 -1.04 -0.85 -1.08 -1.42 -1.21 -0.78 -0.97 -0.98 -0.64
            -0.92 -0.71 -0.59 -0.57 -0.85 -0.88 -0.58 -0.76 -0.73 -0.53
                  -1.03 -0.69 -0.53 -0.71 -0.71 -0.64 -0.76 -0.66
      (a).                  -0.54 -0.35 -0.46 -0.43 -0.42 -0.67
Arch compression (ksi)                -0.29 -0.17 -0.21 -0.29

0.11  0.27  0.73  0.89  0.38  0.84  1.71  1.01  1.17  1.04  1.18  0.80
      0.30  0.75  0.80  0.33  0.41  1.03  0.72  0.96  1.38  1.50  0.60
            0.57  0.54  0.39  0.16  0.32  0.31  0.65  0.93  1.15  0.37
                  0.51  0.31  0.15  0.19  0.16  0.18  0.48  0.62
      (b).                  0.41  0.12  0.08  0.05  0.13  0.88
Joint opening (in)                    0.15  0.04  0.03  0.30

0.00  0.00  0.00  0.00  0.00  0.00  0.00  0.00  0.00  0.00  0.00  0.00
      0.00  0.00  0.00  0.00  0.00  0.00  0.00  0.00  0.00  0.00  0.00
            0.00  0.00  0.00  0.00  0.00  0.00  0.00  0.00  0.00  0.00
                  0.00  0.00  0.00  0.00  0.00  0.00  0.00  0.00
      (c).                  0.00  0.00  0.00  0.00  0.00  0.00
Joint sliding (in)                    0.00  0.00  0.00  0.00

0.22  0.23  0.15  0.18  0.15  0.14  0.21  0.21  0.21  0.17  0.18  0.21
      0.26  0.54  0.42  0.32  0.46  0.32  0.49  0.46  0.39  0.30  0.18
            0.50  0.55  0.55  0.55  0.55  0.55  0.55  0.55  0.33  0.39
                  0.44  0.41  0.54  0.55  0.43  0.38  0.25  0.20
      (d).                  0.34  0.34  0.30  0.34  0.27  0.16
Cantilever tension (ksi)              0.27  0.30  0.21  0.23

0.00  0.00  0.00  0.00  0.00  0.00  0.00  0.00  0.00  0.00  0.00  0.00
      0.00  0.00  0.00  0.00  0.00  0.00  0.00  0.00  0.00  0.00  0.00
            0.00  0.32  0.60  0.75  0.76  0.74  0.66  0.34  0.00  0.00
                  0.00  0.00  0.00  0.16  0.00  0.00  0.00  0.00
      (e).                  0.00  0.00  0.00  0.00  0.00  0.00
Crack opening (in)                    0.00  0.00  0.00  0.00

0.00  0.00  0.00  0.00  0.00  0.00  0.00  0.00  0.00  0.00  0.00  0.00
      0.00  0.00  0.00  0.00  0.00  0.00  0.00  0.00  0.00  0.00  0.00
            0.00 -0.30  0.64  1.03  1.91  1.92  1.19  0.27  0.00  0.00
                  0.00  0.00  0.00  0.16  0.00  0.00  0.00  0.00
      (f).                  0.00  0.00  0.00  0.00  0.00  0.00
Crack sliding (in)                    0.00  0.00  0.00  0.00
```

Figure 26. Distributions of maximum responses for Case N3 nonlinear analysis.

```
-1.19 -0.84 -1.59 -1.34 -0.87 -1.32 -1.83 -2.27 -1.64 -1.23 -1.84 -1.20
      -0.97 -1.57 -1.40 -1.10 -1.37 -1.79 -1.84 -1.18 -1.38 -1.45 -1.05
            -1.69 -1.16 -0.86 -0.74 -1.17 -1.01 -0.84 -0.96 -0.87 -0.80
                  -0.97 -0.65 -0.41 -0.75 -0.61 -0.73 -0.88 -0.79
       (a).
                        -0.48 -0.35 -0.44 -0.43 -0.48 -0.59
 Arch compression (ksi)
                              -0.30 -0.20 -0.17 -0.29

 0.11  0.19  0.52  0.57  0.82  0.76  1.36  1.34  1.23  0.80  0.87  0.46
       0.18  0.89  0.49  0.47  0.36  0.71  0.98  0.38  1.18  0.75  0.39
             1.27  0.42  0.53  0.27  0.47  0.46  0.38  1.17  0.82  0.36
                   0.45  0.24  0.27  0.24  0.26  0.33  0.41  0.47
       (b).
                         0.30  0.06  0.02  0.03  0.09  0.51
 Joint opening (in)
                               0.12  0.03  0.04  0.18

-0.11 -0.49 -1.47 -1.72 -3.06 -4.64 -2.07  2.30  3.89  2.78 -1.65 -0.87
      -0.18 -1.58 -0.81 -1.79 -2.82 -1.39  1.43  2.19 -1.92 -0.93 -0.36
            -1.32  0.62 -0.86 -1.44 -1.38  1.71  1.08 -1.21 -0.52 -0.17
                   0.28 -0.36 -0.47 -0.95  1.10  0.44 -0.28 -0.20
       (c).
                        -0.28 -0.12  0.09  0.10  0.12 -0.27
 Joint sliding (in)
                               0.15 -0.07  0.07 -0.17

 0.35  0.27  0.30  0.55  0.42  0.49  0.37  0.48  0.46  0.42  0.35  0.43
       0.36  0.34  0.42  0.52  0.43  0.41  0.54  0.53  0.53  0.55  0.34
             0.55  0.55  0.55  0.55  0.55  0.55  0.55  0.55  0.51  0.28
                   0.55  0.38  0.54  0.55  0.55  0.53  0.45  0.48
       (d).
                         0.53  0.38  0.40  0.44  0.35  0.42
 Cantilever tension (ksi)
                               0.31  0.25  0.23  0.25

 0.00  0.00  0.00  0.13  0.00  0.00  0.00  0.00  0.00  0.00  0.00  0.00
       0.00  0.00  0.00  0.00  0.00  0.00  0.00  0.00  0.00  0.00  0.00
             0.43  0.32  0.72  1.10  1.24  1.11  1.12  0.43  0.00  0.00
                   0.21  0.00  0.00  0.60  0.58  0.00  0.00  0.00
       (e).
                         0.00  0.00  0.00  0.00  0.00  0.00
 Crack opening (in)
                               0.00  0.00  0.00  0.00

 0.00  0.00  0.00 -0.17  0.00  0.00  0.00  0.00  0.00  0.00  0.00  0.00
       0.00  0.00  0.00  0.00  0.00  0.00  0.00  0.00  0.00  0.00  0.00
             1.13  0.68 -1.16 -1.39  0.91  1.32  1.35 -0.82  0.00  0.00
                  -0.21  0.00  0.00  0.96  0.99  0.00  0.00  0.00
       (f).
                         0.00  0.00  0.00  0.00  0.00  0.00
 Crack sliding (in)
                               0.00  0.00  0.00  0.00
```

Figure 27. Distributions of maximum responses for Case N4 nonlinear analysis.

```
-0.60 -0.76 -0.93 -1.13 -1.24 -1.18 -1.42 -1.28 -1.05 -1.36 -1.30 -0.90
      -0.72 -0.93 -1.10 -1.01 -0.98 -1.67 -1.38 -0.91 -1.12 -1.11 -0.85
            -0.92 -0.99 -0.90 -0.80 -1.13 -1.00 -0.70 -0.90 -0.95 -0.80
                  -0.97 -0.77 -0.49 -0.75 -0.74 -0.53 -0.85 -0.90
      (a).                  -0.68 -0.39 -0.41 -0.46 -0.39 -0.64
Arch compression (ksi)                -0.31 -0.15 -0.17 -0.28

0.11  0.15  0.35  0.59  0.43  0.46  1.34  1.29  0.63  0.94  0.48  0.39
      0.20  0.24  0.40  0.76  0.35  0.81  0.82  0.41  1.09  0.46  0.39
            0.27  0.39  0.40  0.16  0.37  0.34  0.26  0.83  0.46  0.37
                  0.54  0.32  0.15  0.14  0.23  0.11  0.49  0.56
      (b).                  0.43  0.08  0.07  0.07  0.12  0.45
Joint opening (in)                    0.14  0.05  0.03  0.21

0.00  0.00  0.00  0.00  0.00  0.00  0.00  0.00  0.00  0.00  0.00  0.00
      0.00  0.00  0.00  0.00  0.00  0.00  0.00  0.00  0.00  0.00  0.00
            0.00  0.00  0.00  0.00  0.00  0.00  0.00  0.00  0.00  0.00
                  0.00  0.00  0.00  0.00  0.00  0.00  0.00  0.00
      (c).                  0.00  0.00  0.00  0.00  0.00  0.00
Joint sliding (in)                    0.00  0.00  0.00  0.00

0.37  0.24  0.28  0.27  0.44  0.31  0.55  0.55  0.33  0.45  0.26  0.35
      0.26  0.37  0.37  0.49  0.55  0.53  0.51  0.55  0.48  0.26  0.20
            0.25  0.36  0.52  0.55  0.55  0.55  0.55  0.34  0.24  0.29
                  0.37  0.33  0.44  0.52  0.52  0.38  0.20  0.22
      (d).                  0.33  0.32  0.32  0.29  0.21  0.23
Cantilever tension (ksi)              0.30  0.36  0.31  0.26

0.00  0.00  0.00  0.00  0.00  0.00  1.32  1.37  0.00  0.00  0.00  0.00
      0.00  0.00  0.00  0.00  0.23  0.00  0.00  0.21  0.00  0.00  0.00
            0.00  0.00  0.00  0.60  1.08  1.11  0.56  0.00  0.00  0.00
                  0.00  0.00  0.00  0.00  0.00  0.00  0.00  0.00
      (e).                  0.00  0.00  0.00  0.00  0.00  0.00
Crack opening (in)                    0.00  0.00  0.00  0.00

0.00  0.00  0.00  0.00  0.00  0.00  1.74  1.74  0.00  0.00  0.00  0.00
      0.00  0.00  0.00  0.00 -0.19  0.00  0.00  0.25  0.00  0.00  0.00
            0.00  0.00  0.00 -0.77 -1.28  1.10 -0.54  0.00  0.00  0.00
                  0.00  0.00  0.00  0.00  0.00  0.00  0.00  0.00
      (f).                  0.00  0.00  0.00  0.00  0.00  0.00
Crack sliding (in)                    0.00  0.00  0.00  0.00
```

Figure 28. Distributions of maximum responses for Case N5 nonlinear analysis.

```
-0.56 -0.86 -0.94 -0.92 -0.98 -1.26 -1.63 -1.40 -1.25 -1.14 -1.20 -1.11
      -0.92 -1.02 -0.98 -1.05 -0.99 -1.23 -1.11 -0.94 -1.18 -1.04 -0.98
            -0.94 -0.91 -0.88 -0.70 -0.88 -0.85 -0.71 -0.96 -0.81 -0.71
                  -0.81 -0.64 -0.46 -0.59 -0.60 -0.53 -0.68 -0.66
       (a).
                        -0.46 -0.31 -0.34 -0.35 -0.36 -0.51
 Arch compression (ksi)
                              -0.18 -0.14 -0.15 -0.20

 0.36  0.65  0.67  0.62  0.96  0.96  1.00  0.90  0.96  0.99  0.63  1.05
       0.78  0.74  0.65  0.87  0.74  0.68  0.88  0.69  0.68  0.63  0.92
             0.74  0.48  0.73  0.48  0.46  0.60  0.52  0.50  0.53  0.62
                   0.46  0.38  0.33  0.24  0.25  0.35  0.37  0.42
       (b).
                         0.23  0.17  0.09  0.09  0.20  0.26
 Arch tension (ksi)
                               0.08  0.06  0.03  0.10

-0.11 -0.22 -0.28 -0.27 -0.25 -0.31 -0.40 -0.43 -0.33 -0.28 -0.19 -0.14
      -0.45 -0.52 -0.56 -0.49 -0.61 -0.74 -0.78 -0.68 -0.54 -0.41 -0.24
            -0.48 -0.53 -0.56 -0.63 -0.76 -0.71 -0.63 -0.56 -0.45 -0.36
                  -0.51 -0.54 -0.57 -0.67 -0.64 -0.57 -0.46 -0.41
       (c).
                        -0.45 -0.54 -0.59 -0.56 -0.51 -0.41
 Cantilever compression (ksi)
                              -0.39 -0.42 -0.47 -0.41

 0.10  0.19  0.23  0.23  0.20  0.34  0.43  0.37  0.30  0.22  0.16  0.12
       0.40  0.46  0.49  0.39  0.60  0.71  0.64  0.57  0.40  0.39  0.27
             0.48  0.50  0.35  0.48  0.56  0.51  0.46  0.34  0.39  0.32
                   0.36  0.36  0.34  0.36  0.29  0.31  0.26  0.27
       (d).
                         0.32  0.31  0.25  0.19  0.22  0.21
 Cantilever tension (ksi)
                               0.22  0.22  0.23  0.19
```

Figure 29. Distributions of maximum responses for Case L6 linear analysis.

```
-0.52 -0.67 -0.85 -0.96 -1.09 -1.09 -1.39 -1.23 -1.02 -1.27 -1.18 -0.89
      -0.72 -0.83 -1.01 -1.10 -0.95 -1.70 -1.42 -0.90 -1.25 -1.03 -0.83
            -0.90 -0.92 -0.79 -0.72 -1.00 -0.94 -0.75 -0.96 -0.92 -0.77
                  -0.90 -0.76 -0.41 -0.72 -0.74 -0.46 -0.83 -0.86
      (a).                  -0.63 -0.39 -0.42 -0.46 -0.40 -0.63
Arch compression (ksi)                -0.30 -0.15 -0.16 -0.29

0.08  0.13  0.24  0.35  0.35  0.32  1.16  0.97  0.51  0.47  0.43  0.39
      0.20  0.23  0.28  0.37  0.27  0.61  0.60  0.47  0.72  0.45  0.27
            0.26  0.30  0.26  0.12  0.26  0.26  0.19  0.59  0.34  0.23
                  0.36  0.22  0.07  0.09  0.12  0.06  0.31  0.30
      (b).                  0.21  0.03  0.03  0.03  0.04  0.31
Joint opening (in)                    0.05  0.02  0.01  0.07

0.00  0.00  0.00  0.00  0.00  0.00  0.00  0.00  0.00  0.00  0.00  0.00
      0.00  0.00  0.00  0.00  0.00  0.00  0.00  0.00  0.00  0.00  0.00
            0.00  0.00  0.00  0.00  0.00  0.00  0.00  0.00  0.00  0.00
                  0.00  0.00  0.00  0.00  0.00  0.00  0.00  0.00
      (c).                  0.00  0.00  0.00  0.00  0.00  0.00
Joint sliding (in)                    0.00  0.00  0.00  0.00

0.28  0.35  0.30  0.25  0.41  0.40  0.40  0.42  0.34  0.39  0.38  0.29
      0.25  0.30  0.31  0.50  0.55  0.55  0.55  0.55  0.55  0.30  0.23
            0.26  0.28  0.41  0.55  0.55  0.55  0.55  0.32  0.22  0.31
                  0.29  0.27  0.36  0.41  0.41  0.34  0.18  0.17
      (d).                  0.20  0.21  0.22  0.21  0.16  0.14
Cantilever tension (ksi)              0.18  0.24  0.20  0.11

0.00  0.00  0.00  0.00  0.00  0.00  0.00  0.00  0.00  0.00  0.00  0.00
      0.00  0.00  0.00  0.00  0.54  1.14  1.13  0.92  0.43  0.00  0.00
            0.00  0.00  0.00  0.33  0.69  0.67  0.28  0.00  0.00  0.00
                  0.00  0.00  0.00  0.00  0.00  0.00  0.00  0.00
      (e).                  0.00  0.00  0.00  0.00  0.00  0.00
Crack opening (in)                    0.00  0.00  0.00  0.00

0.00  0.00  0.00  0.00  0.00  0.00  0.00  0.00  0.00  0.00  0.00  0.00
      0.00  0.00  0.00  0.00 -0.66 -1.42 -1.24 -0.79 -0.51  0.00  0.00
            0.00  0.00  0.00 -0.65 -1.06 -0.76 -0.33  0.00  0.00  0.00
                  0.00  0.00  0.00  0.00  0.00  0.00  0.00  0.00
      (f).                  0.00  0.00  0.00  0.00  0.00  0.00
Crack sliding (in)                    0.00  0.00  0.00  0.00
```

Figure 30. Distributions of maximum responses for Case N6 nonlinear analysis.

```
-0.60 -0.69 -0.94 -1.12 -1.13 -1.04 -1.34 -1.23 -0.98 -1.31 -1.22 -0.89
      -0.68 -0.91 -1.05 -1.11 -0.91 -1.69 -1.36 -0.89 -1.24 -1.06 -0.83
            -0.90 -0.93 -0.86 -0.76 -1.04 -0.97 -0.68 -0.85 -0.93 -0.77
                  -0.94 -0.73 -0.44 -0.73 -0.68 -0.55 -0.81 -0.85
      (a).                -0.70 -0.37 -0.38 -0.42 -0.39 -0.60
Arch compression (ksi)          -0.28 -0.15 -0.15 -0.26

0.10  0.12  0.29  0.46  0.37  0.46  1.22  0.94  0.48  0.71  0.50  0.37
      0.19  0.23  0.34  0.73  0.43  0.79  0.62  0.40  0.94  0.47  0.38
            0.29  0.36  0.41  0.16  0.28  0.28  0.24  0.69  0.41  0.33
                  0.47  0.28  0.11  0.12  0.17  0.11  0.41  0.58
      (b).                0.37  0.07  0.05  0.04  0.09  0.41
Joint opening (in)              0.12  0.04  0.02  0.16

0.00  0.00  0.00  0.00  0.00  0.00  0.00  0.00  0.00  0.00  0.00  0.00
      0.00  0.00  0.00  0.00  0.00  0.00  0.00  0.00  0.00  0.00  0.00
            0.00  0.00  0.00  0.00  0.00  0.00  0.00  0.00  0.00  0.00
                  0.00  0.00  0.00  0.00  0.00  0.00  0.00  0.00
      (c).                0.00  0.00  0.00  0.00  0.00  0.00
Joint sliding (in)              0.00  0.00  0.00  0.00

0.31  0.27  0.41  0.27  0.32  0.44  0.55  0.49  0.35  0.38  0.28  0.31
      0.27  0.31  0.37  0.44  0.55  0.55  0.53  0.55  0.45  0.27  0.23
            0.24  0.30  0.44  0.55  0.55  0.55  0.55  0.31  0.20  0.32
                  0.35  0.30  0.38  0.48  0.46  0.36  0.19  0.22
      (d).                0.30  0.29  0.27  0.25  0.18  0.21
Cantilever tension (ksi)        0.27  0.33  0.30  0.25

0.00  0.00  0.00  0.00  0.00  0.00  0.17  0.00  0.00  0.00  0.00  0.00
      0.00  0.00  0.00  0.00  0.52  0.49  0.00  0.16  0.00  0.00  0.00
            0.00  0.00  0.00  0.44  0.78  0.94  0.54  0.00  0.00  0.00
                  0.00  0.00  0.00  0.00  0.00  0.00  0.00  0.00
      (e).                0.00  0.00  0.00  0.00  0.00  0.00
Crack opening (in)              0.00  0.00  0.00  0.00

0.00  0.00  0.00  0.00  0.00  0.00  0.16  0.00  0.00  0.00  0.00  0.00
      0.00  0.00  0.00  0.00  0.37  0.49  0.00  0.18  0.00  0.00  0.00
            0.00  0.00  0.00 -0.69 -1.10  0.94 -0.45  0.00  0.00  0.00
                  0.00  0.00  0.00  0.00  0.00  0.00  0.00  0.00
      (f).                0.00  0.00  0.00  0.00  0.00  0.00
Crack sliding (in)              0.00  0.00  0.00  0.00
```

Figure 31. Distributions of maximum responses for Case N7 nonlinear analysis.

```
-1.13 -1.13 -1.20 -1.36 -1.28 -1.11 -1.65 -1.38 -1.71 -1.16 -1.32 -1.19
      -0.96 -1.01 -1.08 -1.01 -1.19 -1.51 -1.24 -0.97 -1.37 -1.06 -0.99
            -1.19 -1.16 -0.90 -1.00 -1.18 -1.01 -0.78 -1.01 -0.99 -0.94
                  -0.91 -0.74 -0.39 -0.68 -0.68 -0.71 -1.00 -0.94
       (a).                 -0.72 -0.40 -0.40 -0.40 -0.44 -0.72
 Arch compression (ksi)                -0.26 -0.22 -0.22 -0.33

 1.08  0.43  0.38  0.45  0.45  0.55  0.82  0.90  0.74  0.73  1.01  1.50
       0.93  0.43  0.53  0.30  0.27  0.59  0.69  0.20  0.57  0.78  1.42
             0.76  0.44  0.21  0.16  0.23  0.19  0.10  0.35  0.56  1.71
                   0.55  0.32  0.18  0.25  0.11  0.11  0.20  1.17
       (b).                 0.48  0.15  0.07  0.06  0.15  0.71
 Joint opening (in)                  0.22  0.05  0.05  0.29

 0.00  0.00  0.00  0.00  0.00  0.00  0.00  0.00  0.00  0.00  0.00  0.00
       0.00  0.00  0.00  0.00  0.00  0.00  0.00  0.00  0.00  0.00  0.00
             0.00  0.00  0.00  0.00  0.00  0.00  0.00  0.00  0.00  0.00
                   0.00  0.00  0.00  0.00  0.00  0.00  0.00  0.00
       (c).                 0.00  0.00  0.00  0.00  0.00  0.00
 Joint sliding (in)                  0.00  0.00  0.00  0.00

 0.55  0.41  0.41  0.37  0.55  0.55  0.55  0.55  0.55  0.55  0.55  0.45
       0.36  0.43  0.47  0.47  0.53  0.45  0.50  0.55  0.55  0.41  0.41
             0.42  0.50  0.55  0.55  0.55  0.55  0.55  0.40  0.32  0.55
                   0.55  0.38  0.38  0.46  0.44  0.38  0.27  0.37
       (d).                 0.43  0.36  0.32  0.31  0.26  0.29
 Cantilever tension (ksi)            0.43  0.42  0.30  0.33

 0.53  0.00  0.00  0.00  0.00  1.38  3.47  3.56  1.64  0.88  0.52  0.00
       0.00  0.00  0.00  0.00  0.00  0.00  0.00  0.47  0.48  0.00  0.00
             0.00  0.00  0.46  1.01  1.55  1.84  0.93  0.00  0.00  0.14
                   0.29  0.00  0.00  0.00  0.00  0.00  0.00  0.00
       (e).                 0.00  0.00  0.00  0.00  0.00  0.00
 Crack opening (in)                  0.00  0.00  0.00  0.00

-0.30  0.00  0.00  0.00  0.00 -2.30 -5.01 -3.71  3.14  2.58  1.02  0.00
       0.00  0.00  0.00  0.00  0.00  0.00  0.00  0.71  0.68  0.00  0.00
             0.00  0.00 -0.56 -1.30 -1.64 -1.00 -0.54  0.00  0.00  0.16
                  -0.11  0.00  0.00  0.00  0.00  0.00  0.00  0.00
       (f).                 0.00  0.00  0.00  0.00  0.00  0.00
 Crack sliding (in)                  0.00  0.00  0.00  0.00
```

Figure 32. Distributions of maximum responses for Case N8 nonlinear analysis.

-0.68	-0.73	-0.79	-1.14	-1.33	-1.40	-2.09	-1.55	-1.45	-1.29	-1.04	-0.95
	-0.72	-0.85	-0.90	-0.86	-0.96	-1.15	-1.12	-1.03	-0.98	-0.97	-0.80
		-0.83	-0.90	-0.96	-0.66	-1.05	-0.92	-0.77	-0.86	-0.80	-0.65
			-0.83	-0.73	-0.42	-0.67	-0.69	-0.45	-0.71	-0.84	
				-0.60	-0.36	-0.40	-0.41	-0.37	-0.53		
					-0.30	-0.17	-0.16	-0.28			

(a). Arch compression (ksi)

0.08	0.12	0.28	0.49	0.69	0.62	1.97	0.99	0.86	0.73	0.37	0.28
	0.20	0.23	0.42	0.53	0.25	0.75	0.41	0.54	0.59	0.40	0.24
		0.33	0.28	0.46	0.20	0.35	0.23	0.17	0.53	0.36	0.21
			0.45	0.34	0.09	0.14	0.16	0.11	0.37	0.30	
				0.30	0.09	0.05	0.04	0.12	0.48		
					0.13	0.05	0.02	0.25			

(b). Joint opening (in)

0.00	0.00	0.00	0.00	0.00	0.00	0.00	0.00	0.00	0.00	0.00	0.00
	0.00	0.00	0.00	0.00	0.00	0.00	0.00	0.00	0.00	0.00	0.00
		0.00	0.00	0.00	0.00	0.00	0.00	0.00	0.00	0.00	0.00
			0.00	0.00	0.00	0.00	0.00	0.00	0.00	0.00	
				0.00	0.00	0.00	0.00	0.00	0.00		
					0.00	0.00	0.00	0.00			

(c). Joint sliding (in)

0.37	0.31	0.41	0.34	0.49	0.51	0.55	0.43	0.46	0.55	0.33	0.48
	0.29	0.29	0.53	0.55	0.55	0.55	0.55	0.55	0.52	0.23	0.19
		0.21	0.36	0.37	0.46	0.43	0.40	0.41	0.42	0.26	0.19
			0.24	0.32	0.34	0.41	0.40	0.33	0.20	0.15	
				0.29	0.35	0.32	0.30	0.26	0.20		
					0.27	0.34	0.30	0.25			

(d). Cantilever tension (ksi)

0.00	0.00	0.00	0.00	0.00	0.00	0.79	0.00	0.00	0.84	0.00	0.00
	0.00	0.00	0.00	0.48	1.30	1.80	1.63	0.96	0.00	0.00	0.00
		0.00	0.00	0.00	0.00	0.00	0.00	0.00	0.00	0.00	0.00
			0.00	0.00	0.00	0.00	0.00	0.00	0.00	0.00	
				0.00	0.00	0.00	0.00	0.00	0.00		
					0.00	0.00	0.00	0.00			

(e). Crack opening (in)

0.00	0.00	0.00	0.00	0.00	0.00	-0.31	0.00	0.00	-0.37	0.00	0.00
	0.00	0.00	0.00	0.71	2.26	3.14	2.11	-1.00	0.00	0.00	0.00
		0.00	0.00	0.00	0.00	0.00	0.00	0.00	0.00	0.00	0.00
			0.00	0.00	0.00	0.00	0.00	0.00	0.00	0.00	
				0.00	0.00	0.00	0.00	0.00	0.00		
					0.00	0.00	0.00	0.00			

(f). Crack sliding (in)

Figure 33. Distributions of maximum responses for Case N9 nonlinear analysis.

```
-0.48 -0.62 -0.77 -0.77 -0.72 -1.02 -1.15 -1.04 -0.90 -0.90 -1.02 -0.80
      -0.64 -0.81 -0.86 -0.81 -0.88 -1.09 -0.93 -0.74 -1.00 -0.93 -0.73
            -0.80 -0.83 -0.71 -0.63 -0.85 -0.69 -0.62 -0.88 -0.72 -0.58
                  -0.75 -0.52 -0.36 -0.55 -0.50 -0.49 -0.66 -0.60
       (a).
                        -0.41 -0.23 -0.30 -0.30 -0.32 -0.46
 Arch compression (ksi)
                              -0.15 -0.09 -0.09 -0.17

 0.26  0.43  0.46  0.44  0.61  0.65  0.71  0.69  0.61  0.53  0.47  0.60
       0.55  0.54  0.43  0.59  0.55  0.46  0.61  0.51  0.46  0.48  0.57
             0.58  0.39  0.49  0.37  0.38  0.38  0.43  0.41  0.41  0.43
                   0.40  0.26  0.24  0.22  0.16  0.31  0.32  0.31
       (b).
                         0.18  0.13  0.09  0.07  0.19  0.23
 Arch tension (ksi)
                               0.08  0.07  0.04  0.10

-0.08 -0.15 -0.16 -0.15 -0.18 -0.21 -0.24 -0.24 -0.19 -0.17 -0.11 -0.08
      -0.27 -0.30 -0.34 -0.33 -0.45 -0.48 -0.44 -0.41 -0.33 -0.23 -0.14
            -0.35 -0.36 -0.37 -0.47 -0.53 -0.47 -0.40 -0.34 -0.31 -0.24
                  -0.43 -0.39 -0.42 -0.49 -0.44 -0.42 -0.33 -0.33
       (c).
                        -0.40 -0.40 -0.43 -0.44 -0.38 -0.29
 Cantilever compression (ksi)
                              -0.35 -0.34 -0.32 -0.32

 0.06  0.13  0.14  0.11  0.13  0.18  0.22  0.18  0.14  0.13  0.08  0.05
       0.23  0.29  0.28  0.26  0.37  0.37  0.31  0.28  0.23  0.18  0.13
             0.35  0.34  0.29  0.35  0.34  0.28  0.25  0.20  0.22  0.18
                   0.28  0.29  0.29  0.27  0.20  0.22  0.19  0.18
       (d).
                         0.27  0.26  0.22  0.16  0.19  0.19
 Cantilever tension (ksi)
                               0.22  0.25  0.18  0.15
```

Figure 34. Distributions of maximum responses for Case L10 linear analysis.

```
-0.52 -0.68 -0.81 -1.18 -1.03 -1.06 -1.55 -1.36 -0.91 -1.10 -1.25 -0.86
      -0.75 -0.85 -1.12 -1.20 -0.89 -1.71 -1.45 -0.88 -1.29 -1.07 -0.82
            -0.87 -0.94 -0.88 -0.75 -0.97 -0.95 -0.64 -0.90 -0.93 -0.75
                  -0.91 -0.73 -0.40 -0.71 -0.68 -0.62 -0.80 -0.83
      (a).                  -0.63 -0.33 -0.39 -0.41 -0.38 -0.59
Arch compression (ksi)            -0.26 -0.20 -0.14 -0.24

0.05  0.09  0.25  0.52  0.26  0.28  1.21  0.91  0.35  0.43  0.49  0.43
      0.14  0.16  0.37  0.66  0.29  0.76  0.63  0.48  0.61  0.45  0.38
            0.27  0.36  0.56  0.18  0.34  0.32  0.39  0.68  0.44  0.32
                  0.47  0.25  0.07  0.10  0.17  0.09  0.44  0.59
      (b).                  0.40  0.05  0.05  0.03  0.07  0.46
Joint opening (in)                0.13  0.04  0.02  0.17

0.00  0.00  0.00  0.00  0.00  0.00  0.00  0.00  0.00  0.00  0.00  0.00
      0.00  0.00  0.00  0.00  0.00  0.00  0.00  0.00  0.00  0.00  0.00
            0.00  0.00  0.00  0.00  0.00  0.00  0.00  0.00  0.00  0.00
                  0.00  0.00  0.00  0.00  0.00  0.00  0.00  0.00
      (c).                  0.00  0.00  0.00  0.00  0.00  0.00
Joint sliding (in)                0.00  0.00  0.00  0.00

0.13  0.17  0.26  0.18  0.19  0.24  0.30  0.31  0.25  0.13  0.18  0.14
      0.28  0.29  0.28  0.32  0.51  0.52  0.52  0.50  0.43  0.18  0.15
            0.21  0.31  0.43  0.55  0.55  0.55  0.55  0.37  0.21  0.15
                  0.35  0.33  0.42  0.46  0.45  0.38  0.18  0.14
      (d).                  0.29  0.30  0.28  0.26  0.20  0.18
Cantilever tension (ksi)          0.27  0.34  0.31  0.24

0.00  0.00  0.00  0.00  0.00  0.00  0.00  0.00  0.00  0.00  0.00  0.00
      0.00  0.00  0.00  0.00  0.00  0.00  0.00  0.00  0.00  0.00  0.00
            0.00  0.00  0.00  0.35  0.58  0.50  0.28  0.00  0.00  0.00
                  0.00  0.00  0.00  0.00  0.00  0.00  0.00  0.00
      (e).                  0.00  0.00  0.00  0.00  0.00  0.00
Crack opening (in)                0.00  0.00  0.00  0.00

0.00  0.00  0.00  0.00  0.00  0.00  0.00  0.00  0.00  0.00  0.00  0.00
      0.00  0.00  0.00  0.00  0.00  0.00  0.00  0.00  0.00  0.00  0.00
            0.00  0.00  0.00 -0.35  0.87 -0.67 -0.27  0.00  0.00  0.00
                  0.00  0.00  0.00  0.00  0.00  0.00  0.00  0.00
      (f).                  0.00  0.00  0.00  0.00  0.00  0.00
Crack sliding (in)                0.00  0.00  0.00  0.00
```

Figure 35. Distributions of maximum responses for Case N10 nonlinear analysis.

```
-0.65 -0.63 -0.93 -1.29 -1.19 -1.18 -1.85 -1.89 -1.24 -1.25 -1.53 -1.11
      -0.79 -0.93 -1.31 -1.29 -0.99 -1.41 -1.47 -0.85 -1.27 -1.37 -0.74
            -0.80 -1.01 -1.02 -0.68 -1.00 -0.85 -0.70 -1.07 -0.92 -0.64
                  -0.82 -0.62 -0.39 -0.58 -0.57 -0.54 -0.74 -0.69
       (a).
                        -0.42 -0.28 -0.28 -0.29 -0.34 -0.45
 Arch compression (ksi)
                              -0.15 -0.10 -0.10 -0.15

 0.47  0.55  0.71  0.87  0.86  1.25  1.44  1.40  1.04  0.90  0.99  0.85
       0.66  0.72  0.87  0.84  0.73  0.96  1.03  0.73  0.85  0.94  0.74
             0.67  0.79  0.73  0.50  0.76  0.75  0.42  0.72  0.78  0.59
                   0.70  0.60  0.26  0.46  0.42  0.31  0.60  0.64
       (b).
                         0.40  0.19  0.17  0.15  0.23  0.41
 Arch tension (ksi)
                               0.12  0.08  0.06  0.12

-0.13 -0.22 -0.23 -0.18 -0.24 -0.36 -0.46 -0.44 -0.26 -0.20 -0.13 -0.12
      -0.36 -0.35 -0.38 -0.52 -0.72 -0.86 -0.81 -0.54 -0.35 -0.32 -0.20
            -0.37 -0.40 -0.52 -0.72 -0.77 -0.76 -0.54 -0.43 -0.33 -0.29
                  -0.41 -0.43 -0.59 -0.64 -0.64 -0.52 -0.38 -0.31
       (c).
                        -0.40 -0.51 -0.60 -0.60 -0.50 -0.36
 Cantilever compression (ksi)
                              -0.43 -0.54 -0.53 -0.41

 0.12  0.20  0.23  0.13  0.22  0.25  0.35  0.34  0.22  0.18  0.09  0.08
       0.35  0.32  0.29  0.44  0.51  0.64  0.64  0.47  0.30  0.19  0.16
             0.36  0.35  0.43  0.50  0.71  0.70  0.50  0.32  0.22  0.22
                   0.28  0.26  0.37  0.59  0.60  0.42  0.23  0.20
       (d).
                         0.32  0.33  0.37  0.39  0.30  0.21
 Cantilever tension (ksi)
                               0.31  0.35  0.28  0.21
```

Figure 36. Distributions of maximum responses for Case L15 linear analysis.

```
-0.48 -0.53 -0.75 -0.98 -1.26 -1.09 -1.62 -1.36 -1.44 -1.55 -0.93 -0.88
      -0.62 -0.74 -0.95 -0.88 -0.96 -1.30 -1.12 -0.98 -0.94 -0.79 -0.72
            -0.87 -0.83 -0.80 -0.73 -1.02 -0.82 -0.85 -0.85 -0.68 -0.60
                  -0.91 -0.62 -0.43 -0.73 -0.62 -0.59 -0.70 -0.72
      (a).                  -0.52 -0.30 -0.33 -0.32 -0.32 -0.46
Arch compression (ksi)                -0.28 -0.22 -0.25 -0.31

0.07  0.17  0.38  0.46  0.40  0.76  1.39  1.59  0.64  0.63  0.50  0.49
      0.24  0.32  0.55  0.44  0.43  0.69  0.43  0.67  0.65  0.39  0.32
            0.38  0.50  0.30  0.18  0.46  0.33  0.22  0.56  0.43  0.29
                  0.56  0.31  0.10  0.14  0.17  0.13  0.45  0.43
      (b).                  0.43  0.12  0.07  0.07  0.10  0.51
Joint opening (in)                    0.21  0.05  0.04  0.29

0.00  0.00  0.00  0.00  0.00  0.00  0.00  0.00  0.00  0.00  0.00  0.00
      0.00  0.00  0.00  0.00  0.00  0.00  0.00  0.00  0.00  0.00  0.00
            0.00  0.00  0.00  0.00  0.00  0.00  0.00  0.00  0.00  0.00
                  0.00  0.00  0.00  0.00  0.00  0.00  0.00  0.00
      (c).                  0.00  0.00  0.00  0.00  0.00  0.00
Joint sliding (in)                    0.00  0.00  0.00  0.00

0.31  0.36  0.36  0.52  0.52  0.43  0.55  0.55  0.48  0.55  0.40  0.43
      0.31  0.37  0.52  0.55  0.55  0.55  0.55  0.55  0.54  0.37  0.23
            0.29  0.39  0.44  0.52  0.53  0.53  0.41  0.41  0.33  0.19
                  0.23  0.36  0.48  0.52  0.55  0.45  0.25  0.21
      (d).                  0.30  0.34  0.34  0.33  0.24  0.20
Cantilever tension (ksi)              0.26  0.28  0.25  0.19

0.00  0.00  0.00  0.00  0.00  0.00  1.28  1.11  0.00  1.03  0.00  0.00
      0.00  0.00  0.00  0.65  1.45  1.80  1.91  1.02  0.00  0.00  0.00
            0.00  0.00  0.00  0.00  0.00  0.00  0.00  0.00  0.00  0.00
                  0.00  0.00  0.00  0.00  0.13  0.00  0.00  0.00
      (e).                  0.00  0.00  0.00  0.00  0.00  0.00
Crack opening (in)                    0.00  0.00  0.00  0.00

0.00  0.00  0.00  0.00  0.00  0.00 -0.98 -1.06  0.00 -0.51  0.00  0.00
      0.00  0.00  0.00  0.53  1.41  1.86 -2.27 -1.19  0.00  0.00  0.00
            0.00  0.00  0.00  0.00  0.00  0.00  0.00  0.00  0.00  0.00
                  0.00  0.00  0.00  0.00  0.08  0.00  0.00  0.00
      (f).                  0.00  0.00  0.00  0.00  0.00  0.00
Crack sliding (in)                    0.00  0.00  0.00  0.00
```

Figure 37. Distributions of maximum responses for Case N15 nonlinear analysis.

-0.46 -0.69 -0.75 -0.73 -0.76 -0.98 -1.26 -1.08 -0.97 -0.88 -0.94 -0.89
-0.72 -0.81 -0.78 -0.81 -0.78 -0.97 -0.88 -0.74 -0.92 -0.82 -0.77
-0.74 -0.73 -0.69 -0.55 -0.70 -0.68 -0.55 -0.75 -0.65 -0.57
-0.64 -0.50 -0.35 -0.47 -0.47 -0.41 -0.53 -0.52
(a).
-0.35 -0.23 -0.26 -0.27 -0.27 -0.39
Arch compression (ksi)
-0.13 -0.09 -0.09 -0.14

0.23 0.45 0.46 0.43 0.69 0.69 0.71 0.64 0.69 0.72 0.43 0.73
0.56 0.51 0.45 0.62 0.52 0.46 0.61 0.49 0.48 0.43 0.65
0.52 0.32 0.51 0.34 0.30 0.41 0.37 0.34 0.36 0.43
0.32 0.26 0.23 0.16 0.16 0.25 0.25 0.28
(b).
0.16 0.12 0.07 0.06 0.15 0.19
Arch tension (ksi)
0.07 0.06 0.04 0.09

-0.08 -0.18 -0.21 -0.21 -0.20 -0.23 -0.31 -0.33 -0.26 -0.22 -0.16 -0.11
-0.34 -0.38 -0.44 -0.38 -0.47 -0.57 -0.60 -0.52 -0.42 -0.32 -0.18
-0.37 -0.39 -0.42 -0.47 -0.58 -0.54 -0.47 -0.42 -0.34 -0.27
-0.40 -0.39 -0.42 -0.50 -0.48 -0.42 -0.34 -0.32
(c).
-0.35 -0.39 -0.43 -0.41 -0.37 -0.28
Cantilever compression (ksi)
-0.32 -0.31 -0.32 -0.29

0.08 0.15 0.18 0.18 0.15 0.25 0.31 0.27 0.22 0.17 0.12 0.09
0.30 0.35 0.37 0.29 0.44 0.52 0.46 0.41 0.30 0.29 0.20
0.35 0.37 0.26 0.36 0.41 0.38 0.34 0.25 0.29 0.23
0.29 0.29 0.26 0.27 0.21 0.24 0.21 0.19
(d).
0.27 0.25 0.20 0.15 0.19 0.18
Cantilever tension (ksi)
0.20 0.20 0.21 0.18

Figure 38. Distributions of maximum responses for Case L16 linear analysis.

```
-0.59 -0.54 -0.69 -0.74 -1.00 -1.17 -1.36 -1.10 -0.93 -0.83 -0.94 -0.84
      -0.53 -0.67 -0.73 -0.70 -0.66 -1.02 -0.84 -0.69 -0.80 -0.83 -0.64
            -0.69 -0.72 -0.62 -0.55 -0.81 -0.78 -0.56 -0.71 -0.69 -0.58
                  -0.75 -0.59 -0.33 -0.58 -0.61 -0.39 -0.61 -0.66
      (a).                  -0.49 -0.28 -0.35 -0.36 -0.29 -0.52
Arch compression (ksi)                -0.23 -0.11 -0.13 -0.24

0.06  0.08  0.13  0.23  0.40  0.31  0.90  0.48  0.32  0.23  0.37  0.23
      0.16  0.15  0.23  0.35  0.16  0.35  0.24  0.22  0.27  0.38  0.19
            0.21  0.21  0.18  0.10  0.14  0.13  0.10  0.29  0.28  0.18
                  0.21  0.14  0.07  0.04  0.04  0.07  0.21  0.23
      (b).                  0.21  0.05  0.03  0.02  0.08  0.25
Joint opening (in)                    0.08  0.02  0.02  0.15

0.00  0.00  0.00  0.00  0.00  0.00  0.00  0.00  0.00  0.00  0.00  0.00
      0.00  0.00  0.00  0.00  0.00  0.00  0.00  0.00  0.00  0.00  0.00
            0.00  0.00  0.00  0.00  0.00  0.00  0.00  0.00  0.00  0.00
                  0.00  0.00  0.00  0.00  0.00  0.00  0.00  0.00
      (c).                  0.00  0.00  0.00  0.00  0.00  0.00
Joint sliding (in)                    0.00  0.00  0.00  0.00

0.16  0.29  0.34  0.20  0.33  0.36  0.30  0.34  0.37  0.33  0.20  0.14
      0.25  0.29  0.27  0.37  0.55  0.55  0.55  0.55  0.34  0.17  0.11
            0.23  0.24  0.30  0.43  0.49  0.52  0.47  0.23  0.15  0.13
                  0.19  0.20  0.27  0.31  0.32  0.26  0.12  0.12
      (d).                  0.19  0.22  0.18  0.19  0.15  0.13
Cantilever tension (ksi)              0.20  0.25  0.21  0.14

0.00  0.00  0.00  0.00  0.00  0.00  0.00  0.00  0.00  0.00  0.00  0.00
      0.00  0.00  0.00  0.00  0.57  1.07  0.88  0.43  0.00  0.00  0.00
            0.00  0.00  0.00  0.00  0.00  0.00  0.00  0.00  0.00  0.00
                  0.00  0.00  0.00  0.00  0.00  0.00  0.00  0.00
      (e).                  0.00  0.00  0.00  0.00  0.00  0.00
Crack opening (in)                    0.00  0.00  0.00  0.00

0.00  0.00  0.00  0.00  0.00  0.00  0.00  0.00  0.00  0.00  0.00  0.00
      0.00  0.00  0.00  0.00 -0.55 -1.03  0.67  0.43  0.00  0.00  0.00
            0.00  0.00  0.00  0.00  0.00  0.00  0.00  0.00  0.00  0.00
                  0.00  0.00  0.00  0.00  0.00  0.00  0.00  0.00
      (f).                  0.00  0.00  0.00  0.00  0.00  0.00
Crack sliding (in)                    0.00  0.00  0.00  0.00
```

Figure 39. Distributions of maximum responses for Case N16 nonlinear analysis.

```
-0.69 -1.08 -1.16 -1.13 -1.21 -1.56 -2.01 -1.72 -1.54 -1.41 -1.47 -1.38
      -1.15 -1.26 -1.20 -1.27 -1.20 -1.48 -1.34 -1.13 -1.45 -1.27 -1.20
            -1.14 -1.10 -1.04 -0.82 -1.02 -0.98 -0.85 -1.15 -0.96 -0.86
                  -0.95 -0.73 -0.52 -0.66 -0.67 -0.61 -0.78 -0.75
       (a).
                        -0.50 -0.33 -0.35 -0.36 -0.40 -0.57
 Arch compression (ksi)
                              -0.18 -0.12 -0.13 -0.21

 0.45  0.81  0.85  0.80  1.21  1.22  1.27  1.14  1.22  1.26  0.82  1.32
       0.98  0.95  0.85  1.12  0.97  0.91  1.16  0.90  0.89  0.82  1.17
             0.95  0.65  0.97  0.64  0.64  0.83  0.69  0.67  0.72  0.81
                   0.64  0.54  0.46  0.38  0.39  0.49  0.52  0.58
       (b).
                         0.36  0.26  0.19  0.19  0.31  0.40
 Arch tension (ksi)
                               0.15  0.09  0.06  0.17

-0.14 -0.27 -0.35 -0.33 -0.31 -0.39 -0.50 -0.54 -0.41 -0.34 -0.24 -0.18
      -0.56 -0.64 -0.68 -0.58 -0.73 -0.90 -0.95 -0.82 -0.65 -0.48 -0.29
            -0.59 -0.61 -0.65 -0.73 -0.89 -0.82 -0.73 -0.65 -0.54 -0.43
                  -0.60 -0.60 -0.64 -0.75 -0.72 -0.63 -0.51 -0.48
       (c).
                        -0.50 -0.59 -0.64 -0.60 -0.56 -0.44
 Cantilever compression (ksi)
                              -0.42 -0.43 -0.49 -0.43

 0.13  0.24  0.29  0.29  0.25  0.43  0.54  0.46  0.38  0.28  0.20  0.16
       0.50  0.58  0.62  0.50  0.77  0.92  0.83  0.74  0.51  0.49  0.34
             0.63  0.65  0.49  0.66  0.75  0.70  0.63  0.47  0.51  0.42
                   0.50  0.52  0.50  0.53  0.44  0.46  0.40  0.37
       (d).
                         0.47  0.47  0.42  0.34  0.37  0.33
 Cantilever tension (ksi)
                               0.36  0.37  0.38  0.32
```

Figure 40. Distributions of maximum responses for Case L17 linear analysis.

```
-0.92 -0.94 -1.32 -1.69 -1.47 -1.93 -3.19 -1.63 -2.16 -1.79 -1.83 -1.20
      -0.88 -1.17 -1.44 -1.23 -1.10 -1.78 -1.38 -1.42 -1.44 -1.42 -0.81
            -1.02 -1.05 -1.26 -0.92 -1.62 -1.50 -1.06 -1.32 -0.98 -0.79
                  -0.91 -0.86 -0.49 -0.88 -0.85 -0.73 -0.98 -0.80
      (a).                  -0.84 -0.44 -0.47 -0.44 -0.55 -0.69
Arch compression (ksi)            -0.40 -0.27 -0.21 -0.49

0.14  0.22  0.65  0.73  0.83  0.84  2.19  1.14  1.21  1.60  0.73  0.51
      0.31  0.44  0.60  0.81  0.32  0.99  1.19  0.43  1.14  0.65  0.45
            0.48  0.48  0.75  0.37  0.59  0.68  0.38  1.20  0.65  0.40
                  0.66  0.60  0.18  0.17  0.15  0.13  0.67  0.61
      (b).                  0.61  0.11  0.08  0.11  0.13  0.66
Joint opening (in)                0.22  0.06  0.06  0.29

0.00  0.00  0.00  0.00  0.00  0.00  0.00  0.00  0.00  0.00  0.00  0.00
      0.00  0.00  0.00  0.00  0.00  0.00  0.00  0.00  0.00  0.00  0.00
            0.00  0.00  0.00  0.00  0.00  0.00  0.00  0.00  0.00  0.00
                  0.00  0.00  0.00  0.00  0.00  0.00  0.00  0.00
      (c).                  0.00  0.00  0.00  0.00  0.00  0.00
Joint sliding (in)                0.00  0.00  0.00  0.00

0.54  0.46  0.50  0.55  0.47  0.55  0.46  0.52  0.55  0.55  0.54  0.34
      0.46  0.42  0.55  0.55  0.55  0.55  0.55  0.55  0.52  0.44  0.36
            0.42  0.40  0.38  0.51  0.55  0.55  0.55  0.46  0.37  0.35
                  0.40  0.49  0.55  0.55  0.55  0.55  0.35  0.31
      (d).                  0.41  0.33  0.42  0.45  0.32  0.20
Cantilever tension (ksi)          0.29  0.34  0.29  0.21

0.00  0.00  0.00  0.63  0.00  0.56  0.00  0.00  1.97  1.56  0.00  0.00
      0.00  0.00  1.01  2.40  2.62  3.58  3.35  1.38  0.00  0.00  0.00
            0.00  0.00  0.00  0.00  0.83  1.26  0.48  0.00  0.00  0.00
                  0.00  0.00  0.00  0.54  0.79  0.64  0.43  0.00  0.00
      (e).                  0.00  0.00  0.00  0.00  0.00  0.00
Crack opening (in)                0.00  0.00  0.00  0.00

0.00  0.00  0.00  0.43  0.00  0.33  0.00  0.00 -1.51 -1.15  0.00  0.00
      0.00  0.00 -0.58 -0.87 -2.12 -2.66 -2.45 -1.13  0.00  0.00  0.00
            0.00  0.00  0.00  0.00  0.83  1.26  0.65  0.00  0.00  0.00
                  0.00  0.00  0.00  0.27  0.58  0.55  0.32  0.00  0.00
      (f).                  0.00  0.00  0.00  0.00  0.00  0.00
Crack sliding (in)                0.00  0.00  0.00  0.00
```

Figure 41. Distributions of maximum responses for Case N17 nonlinear analysis.

6. REFERENCES

1a. G. L. Fenves, S. Mojtahedi and R. B. Reimer, "ADAP-88: A Computer Program for Nonlinear Earthquake Analysis of Concrete Arch Dams," Report No. UCB/EERC 89/12, Earthquake Engineering Research Center, University of California at Berkeley, November 1989.

1b. G. L. Fenves, S. Mojtahedi and R. B. Reimer, "Parameter Study of Joint Opening Effects on Earthquake Response of Arch Dams," Report No. UCB/EERC-89/12, Earthquake Engineering Research Center, University of California at Berkeley, April 1992.

2. M. J. Dowling, "Nonlinear Seismic Analysis of Arch Dams," Report No. EERL 87-03, Earthquake Engineering Research Laboratory, Caltech, Pasadena, CA, 1987.

3. K.-L. Fok, J. F. Hall and A. K. Chopra, "EACD-3D: A Computer Program for Three-Dimensional Earthquake Analysis of Concrete Dams," Report No. UCB/EERC 86/09, Earthquake Engineering Research Center, University of California at Berkeley, July 1986.

4. K. J. Bathe, **Finite Element Procedures in Engineering Analysis**, Prentice-Hall, 1982.

5. D. D. Adams and W. L. Wood, "Comparison of Hilber-Hughes-Taylor and Bossak 'α-methods' for the Numerical Integration of Vibration Equations," *International Journal for Numerical Methods in Engineering*, Vol. 19, No. 5, 1983.

6. California Division of Mines and Geology, "CSMIP Strong-Motion Records from the Northridge, California Earthquake of January 17, 1994," Report OSMS 94-07.

7. P. S. Nowak, "Effect of Nonuniform Seismic Input on Arch Dams," Report No. EERL 88-03, Earthquake Engineering Research Laboratory, Caltech, Pasadena, CA, 1988.

8. Z. H. Duron, "Experimental and Finite Element Studies of a Large Arch Dam," Report No. EERL 87-02, Earthquake Engineering Research Laboratory, Caltech, Pasadena, CA, 1987.

9. J. F. Hall, "The Dynamic and Earthquake Behavior of Concrete Dams: Review of Experimental Behavior and Observational Evidence," *Soil Dynamics and Earthquake Engineering*, Vol. 7, No. 2, April 1988.

10. Earthquake Engineering Research Institute, "Northridge Earthquake Reconnaissance Report Volume 1," *Earthquake Spectra*, Supplement C to Volume 11, April 1995.